

RECENT DEVELOPMENTS IN CLASSICAL DENSITY FUNCTIONAL THEORY

JAMES F. LUTSKO

*Center for Nonlinear Phenomena and Complex Systems CP 231, Université
Libre de Bruxelles, 1050 Brussels, Belgium*

CONTENTS

- I. Introduction
- II. Fundamentals
 - A. Statistical Mechanical Preliminaries
 - B. Foundations of DFT
 - C. Integration of Functional Equations
 - D. Expression for the Ideal Gas Contribution to the Free Energy Function
 - E. A Simple Example: The Small Cavity
 - F. Exact General Expression for the Excess Part of the Free Energy Functional
 - G. Correlation Functions
 - H. Parameterized Profiles and Gradient Expansions
- III. DFT Models based on the Liquid State
 - A. A Preview of DFT: The Square Gradient Model
 - B. A Survey of Models
 - 1. Models based on Perturbation Theory about the Uniform Liquid State
 - 2. Nonlocal Theories
 - C. Some Applications
 - 1. Freezing of Hard Spheres
 - 2. Liquid-Solid Interface
 - 3. Properties of the Bulk Liquid State
- IV. Fundamental Measure Theory for Hard Spheres
 - A. Motivation
 - 1. Hard Rods
 - 2. Generalization to Higher Dimensions
 - B. Rosenfeld's FMT
 - C. Refinement of FMT
 - D. Dimensional Reduction and the Tarazona Functional
 - E. The White-Bear Functional
 - F. Calculating the Densities
 - G. Further Developments and Open Questions

- V. Beyond Hard Spheres
 - A. Treatment of the Tail Contribution: Perturbative Theories
 - B. Approaches Based on PDF
 - C. Mean-Field Theories
- VI. Extensions away from Equilibrium
 - A. Dynamical DFT
 - 1. Some ideas from Kinetic Theory
 - 2. A Simple Kinetic-Theory Approach
 - 3. Brownian Dynamics
 - 4. A Note on Interpretation
 - 5. Applications of DDFT
 - B. Energy Surface Methods and the Problem of Nucleation
- VII. Conclusions
- Acknowledgments
- Appendix A: DFT for hard rods
- Appendix B: FMT Two-Body Term
- Appendix C: Proof of the Wall theorem for the VdW model
- References

I. INTRODUCTION

The central question in equilibrium statistical mechanics is the calculation of various physical quantities—pressure, magnetization, charge distribution, and so on—from the known many-body distribution function. The technical difficulty lies in first formulating the macroscopic quantity as the average of some quantity and then performing the calculation. The first task is often straightforward. In most cases, the second task can be cast as an average over the one- or two-body distributions that result from integrating the original N -body distribution over $N-1$ or $N-2$ of the coordinates. In equilibrium, the velocity distribution is always Maxwellian and therefore trivial, so the real work concerns the configurational part of the averages. The configurational part of the one-body distribution is precisely the same as the average local (number) density, while that of the two-body distribution is closely related to the pair distribution function. As explained below, the pair-distribution function can itself be viewed as the one-body distribution in a system subject to a particular external potential, so that it follows that a large part of equilibrium statistical mechanics is solved by a general method to obtain the one-body distribution—or, equivalently, the local density—of systems subject to arbitrary external fields. This is the rationale behind Density Functional Theory (DFT), which aims to provide just such a method.

The modern approach to DFT can be traced back to the work of van der Waals on the free energy of fluids made inhomogeneous by gravity [1, 2]. Consider a system confined to a volume V in which the local density is $\rho(\mathbf{r})$ and the average density is $\bar{\rho} = \int_V \rho(\mathbf{r}) d\mathbf{r}$. Naively, one might imagine that if the free energy per unit

volume in a bulk fluid, for which $\rho(\mathbf{r}) = \bar{\rho}$, is $f(\bar{\rho})$, so that the total free energy $F = Vf(\bar{\rho})$, then the free energy of the inhomogeneous fluid is $F = \int_V f(\rho(\mathbf{r})) d\mathbf{r}$. However, as discussed by van der Waals, a small volume of fluid bounded on one side by fluid at a lower density and on the other side by fluid at a higher density will feel a force due to the different numbers of interactions between it and the neighboring volumes. Thus, the free energy must contain terms taking this into account and a simple analysis of the forces leads to squared-gradient terms, thus giving the well-known squared-gradient model, which is still widely used today. Similar ideas were rediscovered in the form of Ginzburg–Landau theory [3] and in the work of Cahn and Hilliard [4] on planar interfaces.

However, DFT is more than just the idea that the free energy can be expressed as a functional of a set of order parameters. The formal development of DFT begins with the theorem of Mermin that, for a given temperature and chemical potential, an external field will give rise to a unique equilibrium density distribution and that this profile will minimize a particular functional [5]. The uniqueness of the external field/density distribution mapping means that the field can be eliminated in favor of the density so that the functional determining the density has only a trivial dependence on the field. Once the field-independent, nontrivial part of that functional is known, *all* problems involving external fields can in principle be solved.

The required functional can furthermore be expressed, exactly, as an infinite series constructed from the correlation functions of a bulk homogeneous fluid. Since liquid-state theory gives models for those functions, the earliest approaches to DFT involved trying to use the lowest terms from that series as an approximate model. This led to the first DFT of freezing by Ramakrishnan and Yussouff [6] as well as to the work by Saam and Ebner on the properties of nonuniform fluids such as the liquid–vapor interface [7, 8]. Many other theories followed, all based on the idea of using knowledge of bulk liquids to model the DFT functional for more complex systems.

At about the same time that this early work was beginning, in the mid-1970s, Percus gave the exact DFT for one-dimensional hard rods [9]. Of course, attempts were quickly made to generalize these results to higher dimension with limited success. However, in the 1990s, Rosenfeld formulated Fundamental Measure Theory (FMT) as a generalization of the old Scaled Particle Theory [10–12] and it was soon recognized that this was best thought of in terms of a generalization of Percus' results. FMT represented a departure from other methods in that it does not explicitly depend on some sort of mapping to an effective liquid. As discussed below, it has many attractive features and is currently considered the best approximate DFT for hard-sphere systems.

Implicit in all of this is the fact that hard-core systems are much better understood than are more realistic particles with attractive interactions. However, as is the case in liquid-state theory, the hard-core system is a useful first approximation and attractive interactions can be treated in a perturbative or

mean-field fashion. This represents the state of the art in most calculations. On this basis, the use of DFT has exploded so that today, new papers based on DFT are published in numerous journals every month.

Over the course of the development of the history, many important reviews have been written. The 1979 review by Evans [13] helped to unify and define the subject, and his 1992 review [14] is an excellent summary of the state of DFT at that time, including a very interesting discussion of the history of DFT and the interplay between the classical and quantum theories. Important overviews have also been written by Baus and Lutsko [15] and Löwen [16]. An excellent review stressing applications is given by Wu [17]. The point of the present chapter is to describe DFT in its current form. The next section gives the formal theory. It seems appropriate to emphasize this because it is important to understand the limitations of the theory as well as its use. Section III presents a review of liquid-based DFT models. While FMT is viewed as the most accurate model for hard-core systems, it is also more complicated than the earlier theories and computationally more demanding. Thus, it is still quite common to see even the simplest DFT models used (e.g., in the study of three-body contributions to freezing [18] and of glasses [19]) while, for example, the Modified Weighted Density Approximation (discussed below) is also still frequently used [20]. The next section is devoted to explaining the development of FMT starting with the exact results of Percus, the SPT-inspired FMT of Rosenfeld followed by the important idea of dimensional reduction and culminating in the very accurate functionals currently in use. Notwithstanding its successes, FMT is not perfect and the section concludes with a discussion of open questions and problematic issues. Section V addresses the problem of attractive interactions and gives some representative calculations for simple fluids. Section VI is devoted to attempts to use DFT to understand dynamical phenomena, the so-called Dynamical Density Functional Theory and Energy Surface methods. The chapter ends with a short summary.

II. FUNDAMENTALS

A. Statistical Mechanical Preliminaries

Since the local density is the fundamental unknown, DFT is formulated in the grand canonical ensemble with the temperature T and the chemical potential μ as fixed parameters. Consider a classical, conservative system of N particles having coordinates and velocities, \mathbf{q}_i and \mathbf{p}_i respectively. The dynamics are governed by a Hamiltonian $\hat{H}_N = \hat{K}_N + \hat{V}_N + \hat{U}_N$, where the kinetic energy is

$$\hat{K}_N = \sum_{i=1}^N p_i^2 / 2m_i \quad (1)$$

The potential is an arbitrary function of the coordinates, $\hat{V}_N = V(\mathbf{q}_1, \dots, \mathbf{q}_N)$ and the energy of interaction with the external field is

$$\hat{U}_N = \sum_{i=1}^N \phi(\mathbf{q}_i) \quad (2)$$

In the following, a caret will indicate a microscopic quantity having an instantaneous value calculated from the particle positions and momenta. The equilibrium distribution, f , giving the probability density that the system consists of N particles with positions $\mathbf{q}^N \equiv \mathbf{q}_1, \dots, \mathbf{q}_N$ and momenta $\mathbf{p}^N \equiv \mathbf{p}_1, \dots, \mathbf{p}_N$ is

$$f(\mathbf{q}^N, \mathbf{p}^N, N; [\phi]) = \frac{1}{\Xi[\phi] N! h^{DN}} \exp(-\beta(\hat{H}_N - \mu N)) \quad (3)$$

where the inverse temperature is $\beta = 1/k_B T$, k_B is Boltzmann's constant and h is Planck's constant. The notation $[\phi]$ on the left-hand side indicates a *functional* dependence. The grand potential, Ω , and the grand partition function, Ξ , are

$$\Xi[\phi] = \exp(-\beta\Omega[\phi]) = \sum_{N=0}^{\infty} \frac{1}{N! h^{DN}} \int \exp(-\beta(\hat{H}_N - \mu N)) d\mathbf{p}^N d\mathbf{q}^N \quad (4)$$

where $d\mathbf{q}^N = d\mathbf{q}_1 \dots d\mathbf{q}_N$, and so on.

The local number density simply counts the number of particles in a given volume and so its microscopic expression is

$$\hat{\rho}(\mathbf{r}) = \sum_{i=1}^N \delta(r - \mathbf{q}_i) \quad (5)$$

Note that we use the traditional notation even though in other contexts the symbol ρ more commonly refers to the mass density. For single-component systems, this is unimportant but care must be exercised when the particles have different masses. The contribution of the external field to the Hamiltonian can be written as

$$\hat{U}_N = \int \phi(\mathbf{r}) \hat{\rho}(\mathbf{r}) d\mathbf{r} \quad (6)$$

Hence, it immediately follows that

$$\begin{aligned} \frac{\delta\Omega[\phi]}{\delta\phi(\mathbf{r})} &= \Xi^{-1} \sum_{N=0}^{\infty} \frac{1}{N! h^{DN}} \exp(\beta\mu N) \int \hat{\rho}^N(\mathbf{r}) \exp(-\beta\hat{H}_N) d\mathbf{p}^N d\mathbf{q}^N \\ &= -\langle \hat{\rho}(\mathbf{r}) \rangle \\ &\equiv -\rho(\mathbf{r}; [\phi]) \end{aligned} \quad (7)$$

where $\langle \dots \rangle_\phi$ denotes an average in the grand canonical ensemble with field ϕ and the last line defines the average local equilibrium density, $\rho(\mathbf{r}; [\phi])$. From its definition, it is easy to see that $\rho(\mathbf{r}; [\phi])$ is the probability to find a particle at position \mathbf{r} . A second functional derivative gives

$$\begin{aligned} \frac{\delta^2 \Omega[\phi]}{\delta \phi(\mathbf{r}_1) \delta \beta \phi(\mathbf{r}_2)} &= - \frac{\delta \rho(\mathbf{r}_1; [\phi])}{\delta \beta \phi(\mathbf{r}_2)} \\ &= \langle \hat{\rho}(\mathbf{r}_1) \hat{\rho}(\mathbf{r}_2) \rangle - \langle \hat{\rho}(\mathbf{r}_1) \rangle \langle \hat{\rho}(\mathbf{r}_2) \rangle \\ &= \rho(\mathbf{r}_1) \delta(\mathbf{r}_1 - \mathbf{r}_2) + \rho(\mathbf{r}_1) \rho(\mathbf{r}_2) h(\mathbf{r}_1, \mathbf{r}_2; [\phi]) \end{aligned} \quad (8)$$

where the structure function $h(\mathbf{r}_1, \mathbf{r}_2; [\phi]) = g(\mathbf{r}_1, \mathbf{r}_2; [\phi]) - 1$ and $g(\mathbf{r}_1, \mathbf{r}_2; [\phi])$ is the usual pair distribution function (PDF) [21].

B. Foundations of DFT

Density Functional Theory is based on a fundamental theorem first given by Mermin [5] stating that the grand potential of an electron gas in the presence of a one-body potential is a unique functional of the local density. The theorem is a finite temperature generalization of the Hohenberg–Kohn theorem which applies to zero-temperature systems and underlies the Density Functional Theory approach to *ab initio* quantum mechanical calculations. It is in these theorems that the two, now very different, disciplines called ‘‘Density Functional Theory’’ find their common roots. In keeping with the focus of this chapter, the proof given here will follow that found in Evans [13] and Hansen and McDonald [21] which are specific to a classical system.

The result is obtained in two steps: First, we form a functional over the space of distributions and show that the equilibrium distribution minimizes it. Second, this is used to show that two different external fields must give different local densities. This means there is a one-to-one relation between fields and densities so that the field can be eliminated in favor of the density, thus giving a functional of the density which is minimized by the equilibrium distribution.

Consider the space of distribution functions that are purely functionals of the applied external field as defined in Eq. (3). For brevity, these will here be denoted $f_N[\phi]$ with all other arguments being suppressed. Consider the functional

$$\Lambda[\phi; \phi_0] \equiv k_B T \sum_{N=0}^{\infty} \int (\ln(f_N[\phi]/f_N[\phi_0]) - \ln \Xi[\phi_0]) f_N[\phi] d\mathbf{p}^N d\mathbf{q}^N \quad (9)$$

and note that $\Lambda[\phi_0; \phi_0] = -k_B T \ln \Xi[\phi_0]$, which is just $\Omega[\phi_0]$, the grand potential, so that

$$\Lambda[\phi; \phi_0] = \Lambda[\phi_0; \phi_0] + k_B T \sum_{N=0}^{\infty} \int f_N[\phi] \ln(f_N[\phi]/f_N[\phi_0]) d\mathbf{p}^N d\mathbf{q}^N \quad (10)$$

Using the fact that $x \ln x \geq x - 1$ with equality only for $x = 1$, one has that

$$\begin{aligned}
 & \sum_{N=0}^{\infty} \int f_N[\phi] \ln(f_N[\phi]/f_N[\phi_0]) d\mathbf{p}^N d\mathbf{q}^N \\
 &= \sum_{N=0}^{\infty} \int f_N[\phi_0] \frac{f_N[\phi]}{f_N[\phi_0]} \ln(f_N[\phi]/f_N[\phi_0]) d\mathbf{p}^N d\mathbf{q}^N \\
 &\geq \sum_{N=0}^{\infty} \int f_N[\phi_0] \left(\frac{f_N[\phi]}{f_N[\phi_0]} - 1 \right) d\mathbf{p}^N d\mathbf{q}^N \\
 &= 0
 \end{aligned} \tag{11}$$

hence $\Lambda[\phi; \phi_0] \geq \Lambda[\phi_0; \phi_0]$ with equality only if the two functions are equal at all points. This completes the first step of the proof.

Next, suppose that $\phi \neq \phi_0$ and use the derived inequality and the explicit form of the distribution to find

$$\begin{aligned}
 \Lambda[\phi_0; \phi_0] < \Lambda[\phi; \phi_0] &= \sum_{N=0}^{\infty} \int (\hat{U}_N[\phi_0] - \hat{U}_N[\phi] - k_B T \ln \Xi[\phi]) f_N[\phi] d\mathbf{p}^N d\mathbf{q}^N \\
 &= \int d\mathbf{r} (\phi_0(\mathbf{r}) - \phi(\mathbf{r})) \sum_{N=0}^{\infty} \int \hat{\rho}(\mathbf{r}) f_N[\phi] d\mathbf{p}^N d\mathbf{q}^N - k_B T \ln \Xi[\phi] \\
 &= \Omega[\phi] + \int (\phi_0(\mathbf{r}) - \phi(\mathbf{r})) \rho(\mathbf{r}; [\phi]) d\mathbf{r} \\
 &= \Lambda[\phi; \phi] + \int (\phi_0(\mathbf{r}) - \phi(\mathbf{r})) \rho(\mathbf{r}; [\phi]) d\mathbf{r}
 \end{aligned} \tag{12}$$

Reversing the roles of ϕ and ϕ_0 gives

$$\Lambda[\phi; \phi] < \Lambda[\phi_0; \phi_0] + \int (\phi(\mathbf{r}) - \phi_0(\mathbf{r})) \rho(\mathbf{r}; [\phi_0]) d\mathbf{r} \tag{13}$$

If $\rho(\mathbf{r}; [\phi_0]) = \rho(\mathbf{r}; [\phi])$, then these two inequalities imply

$$\Lambda[\phi_0; \phi_0] - \Lambda[\phi; \phi] < \int (\phi_0(\mathbf{r}) - \phi(\mathbf{r})) \rho(\mathbf{r}; [\phi]) d\mathbf{r} < \Lambda[\phi_0; \phi_0] - \Lambda[\phi; \phi] \tag{14}$$

which is a contradiction. Hence, different fields cannot generate the same average local density.

The conclusion is that there is a unique local density for a given external field and vice versa so that there is an invertible functional relation between average equilibrium density for a given field, $\rho(\mathbf{r}; [\phi]) \Leftrightarrow \phi(\mathbf{r}; [\rho])$. Since two equilibrium distributions, $f_N[\phi]$ and $f_N[\phi']$, differ only in the explicit form of the external field and its implicit effect on the partition function, the distribution is a functional of the field and, hence, of the local density. We can therefore interpret the functional Λ in this way by writing

$$\Lambda[\phi; \phi_0] = \Lambda[\phi[\rho]; \phi_0] = \Omega[\rho; \phi_0] \tag{15}$$

where

$$\rho(\mathbf{r}; [\phi]) = \sum_{N=0}^{\infty} \int \hat{\rho}(\mathbf{r}) f(\mathbf{q}^N, \mathbf{p}^N, N; [\phi]) d\mathbf{q}^N d\mathbf{p}^N \quad (16)$$

is the density corresponding to the field ϕ . Note that we use the notation Ω for this functional as well as for the grand partition function. This is justified by the fact that the functional chain rule implies that since $\Lambda[\phi; \phi_0]$ is minimized by the field $\phi = \phi_0$, so also $\Omega[\rho; \phi_0]$ is minimized by the equilibrium average density function, $\rho(\mathbf{r}) = \rho(\mathbf{r}; [\phi_0])$, corresponding to ϕ_0 ,

$$\left. \frac{\delta \Omega[\rho; \phi_0]}{\delta \rho} \right|_{\rho(\mathbf{r})=\rho(\mathbf{r}; [\phi_0])} = 0 \quad (17)$$

and $\Omega[\rho(\mathbf{r}; [\phi_0]); \phi_0] = \Omega$. Finally, it is convenient to separate out the part of $\Omega[\rho; \phi_0]$ which is independent of ϕ_0 and μ by defining

$$\Omega[\rho; \phi_0] = F[\rho] + \int \rho(\mathbf{r})(\phi_0(\mathbf{r}) - \mu) d\mathbf{r} \quad (18)$$

where

$$F[\rho] = \sum_{N=0}^{\infty} \int (\hat{K}_N + \hat{U}_N + k_B T \ln(N! h^{DN}) + k_B T \ln f[\phi[\rho]]) f[\phi[\rho]] d\mathbf{p}^N d\mathbf{q}^N \quad (19)$$

has no explicit dependence on the field ϕ and, hence, *is unique for a given interaction potential*. This is the key conceptual point underlying classical density functional theory: The free energy functional $F[\rho]$ is independent of the applied field, and therefore the same model can be used for any external field. Once this functional is known, the average density for any given external field is calculated from the Euler–Lagrange equation

$$0 = \frac{\delta \Omega[\rho; \phi]}{\delta \rho(\mathbf{r})} \Rightarrow \frac{\delta F[\rho]}{\delta \rho(\mathbf{r})} = \mu - \phi(\mathbf{r}). \quad (20)$$

This equation plays a central role in DFT: Given an external field and a model free energy functional, it can be solved to give the equilibrium density. Conversely, it defines the dependence of the field on the equilibrium density, $\phi(\mathbf{r}; \rho)$. Finally, given some independent determination of $\phi(\mathbf{r}; \rho)$, it can be integrated to give $F[\rho]$ as in the case of the ideal gas below.

Once the equilibrium profile is known, let us call it $\rho_0(\mathbf{r})$, the grand potential is given by $\Omega = \Omega[\rho_0; \phi]$. However, since ρ_0 is the solution to the Euler–Lagrange equation, the field dependence can be eliminated by noting that

$$\int \rho_0(\mathbf{r})(\mu - \phi(\mathbf{r})) d\mathbf{r} = \int \rho_0(\mathbf{r}) \left\{ \frac{\delta F[\rho]}{\delta \rho(\mathbf{r})} \right\}_{\rho(\mathbf{r})=\rho_0(\mathbf{r})} d\mathbf{r} \quad (21)$$

If we abuse the notation somewhat and write

$$\left\{ \frac{\delta F[\rho]}{\delta \rho(\mathbf{r})} \right\}_{\rho(\mathbf{r})=\rho_0(\mathbf{r})} = \frac{\delta F[\rho_0]}{\delta \rho_0(\mathbf{r})} \quad (22)$$

then the grand potential becomes

$$\Omega = F[\rho_0] - \int \rho_0(\mathbf{r}) \frac{\delta F[\rho_0]}{\delta \rho_0(\mathbf{r})} d\mathbf{r} \quad (23)$$

These expressions should be interpreted with care because they are only valid when $\rho_0(\mathbf{r})$ is a solution of the Euler–Lagrange equation.

C. Integration of Functional Equations

There are two common circumstances in DFT in which the need arises to integrate functional differential equations. The first is the case of exactly solvable systems where one typically calculates the partition function for an arbitrary field, $\phi(\mathbf{r})$, differentiates with respect to the field to get the local density $\rho(\mathbf{r}; [\phi])$ and then inverts this relation to get the field as a functional of the density, $\phi(\mathbf{r}; [\rho])$. Then, integrating the Euler–Lagrange equation, Eq. (20), gives the key functional $F[\rho]$. The other circumstance is described in more detail later, but it has to do with the construction of approximate free energy functionals.

In either case, we recall that the equation

$$\frac{\delta F[\rho]}{\delta \rho(\mathbf{r}_1)} = c(\mathbf{r}_1; [\rho]) \quad (24)$$

where the right-hand side is some known functional, is integrable if and only if [22]

$$\frac{\delta c(\mathbf{r}_1; [\rho])}{\delta \rho(\mathbf{r}_2)} = \frac{\delta c(\mathbf{r}_2; [\rho])}{\delta \rho(\mathbf{r}_1)} \quad (25)$$

In this case, we can choose any two functions in density space, $\rho_0(\mathbf{r})$ and $\rho_1(\mathbf{r})$, and integrate between them along some path $\rho(\mathbf{r}; \lambda)$ where $\rho(\mathbf{r}; 0) = \rho_0(\mathbf{r})$ and $\rho(\mathbf{r}; 1) = \rho_1(\mathbf{r})$, giving

$$F[\rho_1] - F[\rho_0] = \int_0^1 d\lambda \int d\mathbf{r} \frac{\partial \rho(\mathbf{r}; \lambda)}{\partial \lambda} c(\mathbf{r}; [\rho]) \quad (26)$$

and the result is independent of the chosen path. In practice, the linear path $\rho(\mathbf{r}; \lambda) = \rho_0(\mathbf{r}) + \lambda(\rho_1(\mathbf{r}) - \rho_0(\mathbf{r}))$ is often used.

D. Expression for the Ideal Gas Contribution to the Free Energy Function

The final ingredient needed to make DFT useful is a way to relate the various functionals defined in the last subsection to physically meaningful quantities. In a system with no interactions, $\phi = 0$, one has

$$\begin{aligned}\Xi[\phi] &= \exp(-\beta\Omega[\phi]) = \sum_{N=0}^{\infty} \frac{1}{N!h^{DN}} (2\pi k_B T)^{-DN/2} \left(\int \exp(-\beta(\phi(\mathbf{q})-\mu)) d\mathbf{q} \right)^N \\ &= \exp\left(\Lambda^{-D} \int \exp(-\beta(\phi(\mathbf{q})-\mu)) d\mathbf{q} \right)\end{aligned}\quad (27)$$

where $\Lambda = h/\sqrt{2m\pi k_B T}$ is the thermal wavelength. The average density is thus

$$\rho(\mathbf{r}; [\phi]) = \frac{\delta\Omega[\phi]}{\delta\phi(\mathbf{r})} = \Lambda^{-D} \exp(-\beta(\phi(\mathbf{r})-\mu)) \quad (28)$$

Denoting the ideal gas free energy functional by $F_{\text{id}}[\rho]$ and substituting into the Euler–Lagrange equation, Eq. (20), gives

$$\frac{\delta F_{\text{id}}[\rho]}{\delta\rho(\mathbf{r})} = \mu - \phi(\mathbf{r}; [\rho]) = k_B T \ln \Lambda^D \rho(\mathbf{r}) \quad (29)$$

which is integrated to give the explicit, exact result

$$\begin{aligned}\beta F_{\text{id}}[\rho] &= \int_0^1 d\lambda \int d\mathbf{r} \rho(\mathbf{r}) \ln \Lambda^D \lambda \rho(\mathbf{r}) \\ &= \int (\rho(\mathbf{r}) \ln \Lambda^D \rho(\mathbf{r}) - \rho(\mathbf{r})) d\mathbf{r}\end{aligned}\quad (30)$$

For interacting systems, the ideal-gas contribution is usually treated exactly, so one can write $F[\rho] = F_{\text{id}}[\rho] + F_{\text{ex}}[\rho]$ where the second term on the right is called the excess free energy functional. Thus, Euler–Lagrange equation becomes

$$k_B T \ln \rho(\mathbf{r}) + \frac{\delta F_{\text{ex}}[\rho]}{\delta\rho(\mathbf{r})} = \mu - \phi(\mathbf{r}) \quad (31)$$

A common method of solving this equation numerically is to write it in the form

$$\rho(\mathbf{r}) = \exp\left(\beta\mu - \beta\phi(\mathbf{r}) - \frac{\delta\beta F_{\text{ex}}[\rho]}{\delta\rho(\mathbf{r})} \right) \quad (32)$$

and to iterate by making an initial guess at $\rho(\mathbf{r})$, using this to evaluate the right-hand side and thus giving a new $\rho(\mathbf{r})$ and so forth. Mixing between the iterations can be useful.

E. A Simple Example: The Small Cavity

An exactly solvable model that plays an important role later is that of a hard sphere in a small cavity. Specifically, consider fields that are infinite outside some

specified region, V , but are still considered to be arbitrary within V . If V is so small that the maximum number of hard spheres that can occupy it is one, then the partition function is just

$$\begin{aligned}\Xi[\phi] &= \exp(-\beta\Omega[\phi]) = \sum_{N=0}^{\infty} \frac{1}{N!h^{DN}} (2\pi k_B T)^{-DN/2} \left(\int \exp(-\beta(\phi(\mathbf{q})-\mu)) d\mathbf{q} \right)^N \\ &= 1 + \Lambda^{-D} \int_V \exp(-\beta(\phi(\mathbf{q})-\mu)) d\mathbf{q}\end{aligned}\quad (33)$$

Hence, the relation between the equilibrium density and the field is simply

$$\rho(\mathbf{r}) = -k_B T \frac{\delta \ln \Xi[\phi]}{\delta \phi(\mathbf{r})} = \frac{\Lambda^{-D} \exp(-\beta(\phi(\mathbf{r})-\mu))}{1 + \Lambda^{-D} \int_V \exp(-\beta(\phi(\mathbf{q})-\mu)) d\mathbf{q}} \quad (34)$$

Integrating this and rearranging gives

$$\Lambda^{-D} \int_V \exp(-\beta(\phi(\mathbf{q})-\mu)) d\mathbf{q} = \frac{\langle N \rangle}{1 - \langle N \rangle}, \quad \langle N \rangle = \int_V \rho(\mathbf{r}) d\mathbf{q} \quad (35)$$

The Euler-Lagrange equation then becomes

$$\frac{\delta \beta F[\rho]}{\delta \rho(\mathbf{r})} = \beta(\mu - \phi(\mathbf{r})) = \ln \frac{\Lambda^D \rho(\mathbf{r})}{1 - \langle N \rangle} \quad (36)$$

so

$$\begin{aligned}\beta F[\rho] &= \int_0^1 d\lambda \int d\mathbf{r} \rho(\mathbf{r}) \ln \frac{\Lambda^D \lambda \rho(\mathbf{r})}{1 - \lambda \langle N \rangle} \\ &= \int d\mathbf{r} \rho(\mathbf{r}) \ln \Lambda^D \rho(\mathbf{r}) + (1 - \langle N \rangle) (\ln(1 - \langle N \rangle)) \\ &= \beta F_{\text{id}}[\rho] + (1 - \langle N \rangle) (\ln(1 - \langle N \rangle)) + \langle N \rangle\end{aligned}\quad (37)$$

Note that this result is quite generally independent of the details of the size and shape of the cavity and only depends on the condition that the cavity cannot hold more than one hard sphere.

F. Exact General Expression for the Excess Part of the Free Energy Functional

Recall the relation

$$-\frac{\delta \rho(\mathbf{r}_1; [\phi])}{\delta \beta \phi(\mathbf{r}_2)} = \rho(\mathbf{r}_1) \delta(\mathbf{r}_1 - \mathbf{r}_2) + \rho(\mathbf{r}_1) \rho(\mathbf{r}_2) h(\mathbf{r}_1, \mathbf{r}_2) \quad (38)$$

derived above (see Eq. 8). Let us write the inverse relation as

$$\frac{\delta \beta \phi(\mathbf{r}_2; [\rho])}{\delta \rho(\mathbf{r}_1)} = -\frac{1}{\rho(\mathbf{r}_1)} \delta(\mathbf{r}_1 - \mathbf{r}_2) + \Gamma(\mathbf{r}_1, \mathbf{r}_2; [\rho]) \quad (39)$$

where we must clarify the nature of $\Gamma(\mathbf{r}_1, \mathbf{r}_2)$. Substituting these into the functional chain rule,

$$\delta(\mathbf{r}_1 - \mathbf{r}_3) = \int \frac{\delta\rho(\mathbf{r}_1; [\phi])}{\delta\beta\phi(\mathbf{r}_2)} \frac{\delta\beta\phi(\mathbf{r}_2; [\rho])}{\delta\rho(\mathbf{r}_3)} d\mathbf{r}_2$$

gives the relation

$$h(\mathbf{r}_1, \mathbf{r}_3) = \Gamma(\mathbf{r}_1, \mathbf{r}_3; [\rho]) + \int h(\mathbf{r}_1, \mathbf{r}_2)\rho(\mathbf{r}_2)\Gamma(\mathbf{r}_2, \mathbf{r}_3; [\rho])d\mathbf{r}_2 \quad (40)$$

This is recognized as the Ornstein–Zernike equation for an inhomogeneous system [21] so that we can identify the unknown function Γ as the (two-body) direct correlation function (DCF), $\Gamma(\mathbf{r}_2, \mathbf{r}_3) = c_2(\mathbf{r}_2, \mathbf{r}_3; [\rho])$.

The excess part of the free energy can be understood by taking advantage of the fact that it is independent of the applied field. In particular, in the case of the equilibrium field, $\phi(\mathbf{r}) = \phi(\mathbf{r}; [\rho])$, a functional differentiation of the Euler–Lagrange equation, Eq. (20), gives

$$\begin{aligned} \frac{\delta^2\beta F_{\text{ex}}[\rho]}{\delta\rho(\mathbf{r}_1)\delta\rho(\mathbf{r}_2)} &= -\frac{1}{\rho(\mathbf{r}_1)}\delta(\mathbf{r}_1 - \mathbf{r}_2) - \frac{\delta\beta\phi(\mathbf{r}_1; [\rho])}{\delta\rho(\mathbf{r}_2)} \\ &= -c_2(\mathbf{r}_1, \mathbf{r}_2; [\rho]) \end{aligned} \quad (41)$$

This result is very important and deserves to be highlighted: The functional $F_{\text{ex}}[\rho]$ is a general functional of its argument, ρ , independent of the applied field. We have derived its form by assuming a particular field—namely, the equilibrium field $\phi[\rho]$. However, having determined it for this field, it is the same for all other fields as well. This therefore completes the specification of the general functional $\Omega[\rho; \phi_0]$.

This result can be used to give an expression for the exact excess free energy functional. Since Eq. (41) is an exact relation and since the two-body DCF is an exact derivative, it can be integrated through density space to give an exact relation between the excess free energy functional for the density $\rho_0(\mathbf{r})$ and that for the density, $\rho_1(\mathbf{r})$. If one forms a path between these two density profiles parameterized by some scalar such as $\rho_\lambda(\mathbf{r}) = (1 - \lambda)\rho_0(\mathbf{r}) + \lambda\rho_1(\mathbf{r})$, then the result is

$$\begin{aligned} \beta F_{\text{ex}}[\rho_1] &= \beta F_{\text{ex}}[\rho_0] + \int_0^1 d\lambda \int d\mathbf{r}_1 \left[\frac{\delta\beta F_{\text{ex}}[\rho_\lambda(\mathbf{r}_1)]}{\delta\rho_\lambda(\mathbf{r}_1)} \right]_{\rho_0} \frac{\partial\rho_\lambda(\mathbf{r}_1)}{\partial\lambda} \\ &\quad - \int_0^1 d\lambda \int_0^1 d\lambda' \int d\mathbf{r}_1 d\mathbf{r}_2 c_2(\mathbf{r}_1, \mathbf{r}_2; [\rho_{\lambda'}]) \frac{\partial\rho_{\lambda'}(\mathbf{r}_1)}{\partial\lambda'} \frac{\partial\rho_{\lambda'}(\mathbf{r}_2)}{\partial\lambda'} \end{aligned} \quad (42)$$

Note that this is independent of the parameterization chosen. From the equivalence of fields and densities, there will be some field that generates the density profile $\rho_0(\mathbf{r})$ at the given chemical potential. Calling this field $\phi(\mathbf{r}_1; [\rho_0])$, the

Euler–Lagrange equation can be used, giving

$$\begin{aligned} \beta F_{\text{ex}}[\rho_1] &= \beta F_{\text{ex}}[\rho_0] + \int d\mathbf{r}_1 [\beta\mu - \ln \rho_0(\mathbf{r}_1) - \beta\phi(\mathbf{r}_1; [\rho_0])](\rho_1(\mathbf{r}_1) - \rho_0(\mathbf{r}_1)) \\ &\quad - \int_0^1 d\lambda \int_0^\lambda d\lambda' \int d\mathbf{r}_1 d\mathbf{r}_2 c_2(\mathbf{r}_1, \mathbf{r}_2; [\rho_{\lambda'}]) \frac{\partial \rho_{\lambda'}(\mathbf{r}_1)}{\partial \lambda'} \frac{\partial \rho_{\lambda'}(\mathbf{r}_2)}{\partial \lambda'} \end{aligned} \quad (43)$$

Specializing to the case that the reference state is a liquid, $\rho_0(\mathbf{r}) = \bar{\rho}_0$, the field $\beta\phi(\mathbf{r}_1; [\rho_0])$ will be a constant such that $\mu - \phi(\mathbf{r}_1; [\rho_0])$ will be chemical potential that generates $\bar{\rho}_0$ which, though an abuse of notation, we will denote as $\mu(\bar{\rho}_0)$. This should not be confused with the applied chemical potential μ , which is an external parameter in the grand canonical ensemble. Then, taking the linear parameterization through density space, the excess functional is

$$\begin{aligned} \frac{1}{V} \beta F_{\text{ex}}[\rho_1] &= \beta f_{\text{ex}}(\bar{\rho}_0) + \frac{\partial \beta f_{\text{ex}}(\bar{\rho}_0)}{\partial \bar{\rho}_0} (\bar{\rho}_1 - \bar{\rho}_0) \\ &\quad - \frac{1}{V} \int_0^1 d\lambda \int_0^\lambda d\lambda' \int d\mathbf{r}_1 d\mathbf{r}_2 c_2(\mathbf{r}_1, \mathbf{r}_2; [(1 - \lambda')\rho_0 + \lambda'\rho_1]) \\ &\quad \times (\rho_1(\mathbf{r}_1) - \bar{\rho}_0)(\rho_1(\mathbf{r}_2) - \bar{\rho}_0) \end{aligned} \quad (44)$$

This is still not useful because it involves the unknown two-body direct correlation function for an arbitrary density distribution. The idea underlying many DFT models is that, at least in the liquid state, the DCF is relatively simple in structure compared to other properties such as the pair distribution function. For example, the PDF in a dense simple fluid has a slowly decaying oscillatory structure describing successive shells of neighbors, whereas, for example, in the hard-sphere fluid, the DCF is well-approximated as a monotonic cubic function vanishing outside the hard core. Hence, it was hoped that relatively crude approximations to the DCF might be adequate.

One way to implement this intuition is to perform a functional Taylor expansion of the DCF about another reference liquid density,

$$\begin{aligned} c_2(\mathbf{r}_1, \mathbf{r}_2; [\rho_\lambda]) &= c_2(\mathbf{r}_{12}; \bar{\rho}(\lambda)) \\ &\quad + \sum_{n=3}^{\infty} \frac{1}{(n-2)!} \int d\mathbf{r}_3 \dots d\mathbf{r}_N c_n(\mathbf{r}_3, \dots, \mathbf{r}_N; \bar{\rho}(\lambda)) \\ &\quad (\rho_\lambda(\mathbf{r}_3) - \bar{\rho}(\lambda)) \dots (\rho_\lambda(\mathbf{r}_N) - \bar{\rho}(\lambda)) \end{aligned} \quad (45)$$

where the right-hand side is written using the higher-order direct correlation functions for the liquid,

$$c_N(\mathbf{r}_3, \dots, \mathbf{r}_N; \bar{\rho}) = \left. \frac{\delta^{N-2} c_2(\mathbf{r}_1, \mathbf{r}_2; [\rho])}{\delta \rho(\mathbf{r}_3) \dots \delta \rho(\mathbf{r}_N)} \right|_{\rho(\mathbf{r})=\bar{\rho}} \quad (46)$$

Equations (44) and (45) give an exact expression of the excess free energy functional in terms of the properties of a uniform fluid. It is independent of the path taken through density space so that one can choose, for example, $\rho_\lambda(\mathbf{r}) = \lambda\rho(\mathbf{r})$ and it is also exact for all choices of $\bar{\rho}_0$ and $\bar{\rho}(\lambda)$. In principle, this gives a method to describe *nonuniform* systems, even solids, based only on knowledge of the uniform fluid. Unfortunately, little is known about the higher-order direct correlation functions so that in practice, only the first three terms of the expansion are used. A simple approximation consists of truncation of the higher-order terms and the choice $\bar{\rho}(\lambda) = \bar{\rho}_0$, giving

$$\begin{aligned} \frac{1}{V}\beta F_{\text{ex}}[\rho_1] &\simeq \beta f_{\text{ex}}(\bar{\rho}_0) + \frac{\partial \beta f_{\text{ex}}(\bar{\rho}_0)}{\partial \rho_0}(\bar{\rho}_1 - \bar{\rho}_0) \\ &\quad - \frac{1}{2V} \int d\mathbf{r}_1 d\mathbf{r}_2 c_2(r_{12}; \bar{\rho}_0)(\rho_1(\mathbf{r}_1) - \bar{\rho}_0)(\rho_1(\mathbf{r}_2) - \bar{\rho}_0) \end{aligned} \quad (47)$$

However, this is not really satisfactory because it is inconsistent when the target system is itself the uniform fluid, that is, $\rho_1(\mathbf{r}) = \bar{\rho}_1$. To remedy this, one should take $\bar{\rho}_0 = \bar{\rho}_1$, which is the oldest and simplest approximate DFT, first studied by Ramakrishnan and Yussouff [6]:

$$\frac{1}{V}\beta F_{\text{ex}}[\rho_1] - \frac{1}{V}\beta F_{\text{ex}}(\bar{\rho}_1) \simeq -\frac{1}{2V} \int d\mathbf{r}_1 d\mathbf{r}_2 c_2(\mathbf{r}_{12}; \bar{\rho}_0)(\rho_1(\mathbf{r}_1) - \bar{\rho}_1)(\rho_1(\mathbf{r}_2) + \bar{\rho}_1) \quad (48)$$

This approximation, which involves only knowledge of the DCF in the liquid, is still a standard starting point for calculations in which simplicity is favored over accuracy.

G. Correlation Functions

Given the free energy functional $F[\rho]$, the entire hierarchy of direct correlation functions follows immediately by functional differentiation. In many cases, however, it is more useful to have the pair distribution function, $g(\mathbf{r}_1, \mathbf{r}_2; \mu, [\phi])$, giving the probability to find a particle at position \mathbf{r}_2 given that their is one at position \mathbf{r}_1 . One method is to use the Ornstein–Zernike equation for inhomogeneous fluids [see Eq. (40)]. However, as pointed out by Percus [23, 24], DFT provides another method of obtaining the PDF which can be easier to implement in practice. Suppose the system interacts via a two-body potential, $v(\mathbf{r}_1, \mathbf{r}_2)$, and is subject to an external potential $\phi(\mathbf{r})$. The two-body distribution $\rho(\mathbf{r}_1, \mathbf{r}_2; \mu, [\phi])$ is the probability to find one particle at position \mathbf{r}_1 and another at position \mathbf{r}_2 . It is related to the PDF by $\rho(\mathbf{r}_1, \mathbf{r}_2; \mu, [\phi]) = \rho(\mathbf{r}_1; \mu, [\phi]) \times \rho(\mathbf{r}_2; \mu, [\phi])g(\mathbf{r}_1, \mathbf{r}_2; \mu, [\phi])$. Since the one-body density is the probability to find a particle at a given position, it follows that $\rho(\mathbf{r}_1, \mathbf{r}_2; \mu, [\phi])/\rho(\mathbf{r}_1; \mu, [\phi]) = \rho(\mathbf{r}_2; \mu, [\phi])g(\mathbf{r}_1, \mathbf{r}_2; \mu, [\phi])$ is the conditional distribution giving the probability

to find a particle at position \mathbf{r}_2 given that there is one at position \mathbf{r}_1 . Conceptually, this is identical to the probability to find a particle at position \mathbf{r}_2 in a system with a particle fixed at position \mathbf{r}_1 . A fixed particle is equivalent to an external field acting on the rest of the system, so another way to interpret this is that $\rho(\mathbf{r}_2; \mu, [\phi]) \times g(\mathbf{r}_1, \mathbf{r}_2; \mu, [\phi])$ is the same as the density profile in a system with the same external field *plus* the field $v(\mathbf{r}_1, \mathbf{r}_2)$,

$$\rho(\mathbf{r}_2; \mu, [\phi])g(\mathbf{r}_1, \mathbf{r}_2; \mu, [\phi]) = \rho(\mathbf{r}_2; \mu, [\phi'_{r_1}]) \quad (49)$$

where

$$\phi'_{r_1} = \phi'(\mathbf{r}) + v(\mathbf{r}_1, \mathbf{r}). \quad (50)$$

Using the Euler–Lagrange equation, Eq. (32), this can be written as

$$\begin{aligned} & \rho(\mathbf{r}_2; \mu, [\phi])g(\mathbf{r}_1, \mathbf{r}_2; \mu, [\phi]) \\ &= \exp\left(\beta\mu - \beta\phi(\mathbf{r}_2) - \beta v(\mathbf{r}_1, \mathbf{r}_2) - \frac{\delta\beta F_{\text{ex}}[n]}{\delta n(\mathbf{r}_2)} \Big|_{n(\mathbf{r})=\rho(\mathbf{r}; \mu, [\phi'_{r_1}])}\right) \end{aligned} \quad (51)$$

Thus, by solving the DFT with the field ϕ'_{r_1} , one obtains the PDF for the system with field ϕ . In particular, if $\phi = 0$, one finds that the PDF of the bulk fluid is given by

$$\bar{\rho}(\mu)g(\mathbf{r}_1, \mathbf{r}_2; \mu) = \exp\left(\beta\mu - \beta v(\mathbf{r}_1, \mathbf{r}_2) - \frac{\delta\beta F_{\text{ex}}[n]}{\delta n(\mathbf{r}_2)} \Big|_{n(\mathbf{r})=\rho(\mathbf{r}; \mu, [\phi'_{r_1}])}\right) \quad (52)$$

These relations are often used in practical calculations to get the PDF from a DFT calculation. Furthermore, since the same DFT allows one to calculate both the PDF and the DCF and since they are related via the Ornstein–Zernike relation, this gives a method to check the self-consistency of model calculations analogous to the comparison of the virial and compressibility routes to the equation of state in liquid-state theory.

H. Parameterized Profiles and Gradient Expansions

In a typical application of DFT, given some approximation to the free energy functional, the Euler–Lagrange equations are solved to get the equilibrium density profile and, from this, the free energy is calculated. Since the density profile is a function, this procedure involves discretization and can become computationally very expensive. In many cases, one is able to make a reasonable guess as to the general properties of the density profile and can therefore propose an analytic form that is expected to closely approximate the exact result. For example, in the case of a planar interface in which the density is uniform except in one direction,

a hyperbolic tangent is a natural choice:

$$\rho(z; \bar{\rho}_{-\infty}, \bar{\rho}_{\infty}, z_0, a) = \bar{\rho}_{-\infty} + (\bar{\rho}_{\infty} - \bar{\rho}_{-\infty}) \frac{\exp(a(z - z_0))}{\exp(a(z - z_0)) + \exp(-a(z - z_0))} \quad (53)$$

so that there are four parameters: the densities at $z = \pm\infty$, the location of the interface, z_0 , and the inverse width, a . A similar form, with the Cartesian coordinate z replaced by the radial coordinate r , might be used to describe a spherical cluster (droplet or bubble in a liquid–vapor system). A very important parameterization used in many calculations of solids is to approximate the density as a sum of Gaussians centered at the lattice sites:

$$\rho(\mathbf{r}; \alpha, x, \bar{\rho}_{\text{latt}}) = x \sum_{n=0}^{\infty} \left(\frac{\alpha}{\pi}\right)^{3/2} \exp(-\alpha(\mathbf{r} - \mathbf{R}_n)^2) \quad (54)$$

where the sum is over lattice vectors, \mathbf{R}_n , the magnitudes of which depend on the lattice density $\bar{\rho}_{\text{latt}}$, where α controls the width of the Gaussians and $0 < x \leq 1$ is the occupancy that allows for the possibility that not all lattice sites are occupied. This is actually a very flexible parameterization, as can be seen when it is written in Fourier space as

$$\rho(\mathbf{r}; \alpha, x, \bar{\rho}_{\text{latt}}) = x \bar{\rho}_{\text{latt}} \sum_{n=0}^{\infty} \exp(i\mathbf{K}_n \cdot \mathbf{r}) \exp(-K_n^2/4\alpha) \quad (55)$$

where the sum is now over all reciprocal lattice vectors, \mathbf{K}_n . In this form, it is clear that $\lim_{\alpha \rightarrow 0} \rho(\mathbf{r}; \alpha, x, \bar{\rho}_{\text{latt}}) = x \bar{\rho}_{\text{latt}}$, which is the uniform fluid limit. Hence, the Gaussian approximation can be used to approximate both liquid-like and solid-like systems and, most importantly, the transition from one to another. Note that with this parameterization, the calculation of the ideal contribution to the free energy is not trivial. If the lattice parameter is denoted a , then for $\alpha a^2 \ll 1$, asymptotic expressions are available [25], but these are not very useful. For $\alpha a^2 \gg 1$, a simple calculation [25] gives $F_{\text{id}}[\rho] \simeq \frac{3}{2} \ln(\alpha \Lambda^2/\pi) - \frac{5}{2}$, which becomes essentially exact for $\alpha a^2 > 100$. At intermediate values, the calculation must be performed numerically. The accuracy of the Gaussian parameterization has been checked in several studies, and it seems to always be a very good first approximation [26–28].

Denote an arbitrary parameterized profile as $\rho(\mathbf{r}; \Gamma)$, where $\Gamma = \{\Gamma_i\}_{i=1}^n$ represents a set of n parameters. If there is a set of parameters so that $\rho(\mathbf{r}; \Gamma)$ is the exact equilibrium functional, then

$$\frac{\partial \Omega[\rho; \phi_0]}{\partial \Gamma_i} = \int \frac{\delta \Omega[\rho; \phi_0]}{\delta \rho(\mathbf{r}; \Gamma)} \frac{\partial \rho(\mathbf{r}; \Gamma)}{\partial \Gamma_i} d\mathbf{r} = 0 \quad (56)$$

so

$$\frac{\partial F[\rho]}{\partial \Gamma_i} = \int \frac{\partial \rho(\mathbf{r}; \Gamma)}{\partial \Gamma_i} (\mu - \phi(\mathbf{r})) d\mathbf{r} \quad (57)$$

If the only effect of the field is to confine the system to a volume V , then this becomes

$$\frac{\partial F[\rho]}{\partial \Gamma_i} = \mu \frac{\partial \bar{\rho}(\Gamma)}{\partial \Gamma_i} V, \quad \bar{\rho}(\Gamma) V \equiv \int \rho(\mathbf{r}; \Gamma) d\mathbf{r} \quad (58)$$

which is the key equation that serves to fix the parameters in practical calculations.

In some cases, a simple parameterization of this form is insufficient. For example, to describe a liquid–solid interface, one would might use the Gaussian parameterization but with values of the average density and of α that vary as one moves from the liquid region to the solid region. There is no difficulty in extending the discussion of parameterized profiles to this case, but even with the parameterization the calculations can be quite expensive. If the variation of the parameters is expected to be slow relative to the atomic and interfacial length scales, then one might imagine performing a gradient expansion of the free energy. There are actually two versions of the gradient expansion in use [29] and both are based on a parameterization of the density appropriate for liquid–solid interfaces. The first is due to Evans [13] and refined by Oxtoby and Haymet [30, 31]. Imagine that we have some parameterization, $\rho(\mathbf{r}; \Gamma(\mathbf{r}))$, and calculate the (Helmholtz) free energy difference between this system and that of a uniform fluid at second order in perturbation theory [see Eq. (48)],

$$\begin{aligned} \beta F[\rho] - \beta F(\bar{\rho}_0) &\simeq \beta F_{\text{id}}[\rho] - \beta F_{\text{id}}(\bar{\rho}_0) \\ &\quad - \frac{1}{2V} \int d\mathbf{r}_1 d\mathbf{r}_2 c_2(r_{12}; \bar{\rho}_0) (\rho(\mathbf{r}_1; \Gamma(\mathbf{r}_1)) - \bar{\rho})(\rho(\mathbf{r}_2; \Gamma(\mathbf{r}_2)) - \bar{\rho}) \\ &= \beta \int \Delta f(\rho(\mathbf{r}; \Gamma(\mathbf{r})); \bar{\rho}_0) d\mathbf{r}_1 - \frac{1}{2V} \int d\mathbf{r}_1 d\mathbf{r}_2 c_2(\mathbf{r}_{12}; \bar{\rho}_0) \\ &\quad \times (\rho(\mathbf{r}_1; \Gamma(\mathbf{r}_1)) - \bar{\rho})(\rho(\mathbf{r}_2; \Gamma(\mathbf{r}_2)) - \rho(\mathbf{r}_2; \Gamma(\mathbf{r}_1))) \end{aligned} \quad (59)$$

where the second line uses the uniform free energy difference per unit volume,

$$\Delta f(\rho; \bar{\rho}_0) = \frac{1}{V} F(\rho) - \frac{1}{V} F(\bar{\rho}_0) \quad (60)$$

Thus, the first term looks like a local free energy contribution while the second depends on $\rho_1(\mathbf{r}_2; \Gamma(\mathbf{r}_2)) - \rho_1(\mathbf{r}_2; \Gamma(\mathbf{r}_1))$, which can then be expanded in gradients

of $\Gamma(\mathbf{r})$. Further development of this model depends on an explicit choice for the parameterization,

$$\rho(\mathbf{r}; \Gamma(\mathbf{r})) = \rho_0 \left(1 + \Gamma_0(\mathbf{r}) + \sum_{n=1} \exp(i\mathbf{K}_n \cdot \mathbf{r}) \Gamma_n(\mathbf{r}) \right) \quad (61)$$

The result, truncated at second order in the gradient expansion, is

$$\beta F[\rho] - \beta F[\bar{\rho}_0] \simeq \beta \int \left\{ \Delta f(\rho(r; \Gamma(\mathbf{r})); \bar{\rho}_0) + \frac{1}{2} \sum_{i,j=1}^D \sum_{a,b=1}^N K_{ij}^{ab} \frac{\partial \Gamma_a(\mathbf{r})}{\partial r_i} \frac{\partial \Gamma_b(\mathbf{r})}{\partial r_j} \right\} d\mathbf{r} \quad (62)$$

with

$$K_{ij}^{ab} = \delta_{ab} \frac{1}{2} \rho_0^2 \int \exp(i\mathbf{K}_a \cdot \mathbf{r}) r_i r_j c_2(r; \bar{\rho}_0) d\mathbf{r} \quad (63)$$

and can be found in the cited papers. One feature of this model is that the local free energy term still involves $\rho(\mathbf{r}; \Gamma(\mathbf{r}))$, so that the long-wavelength and short-wavelength variations of the density are not completely separated.

An alternative expansion was given by Löwen, Beyer, and Wagner [32, 33] and further developed by Lutsko [29]. The idea is that space is divided into Wigner–Seitz cells centered on the lattice sites. Within each cell, the free energy is functionally Taylor-expanded about the value of the density parameters at the center of the cell; and the result, which will depend on terms like $\Gamma(\mathbf{r}) - \Gamma(\mathbf{R}_n)$, is again expanded in gradients of the parameters. It turns out that if the gradient expansion is truncated at second order, this automatically truncates the functional expansion at second order as well. At this point, the free energy has the gradient form, but is written as a sum over Wigner–Seitz cells. The transition to a continuum description is subtle and requires the further neglect of contributions of higher order in the gradients of the density parameters. The final result is

$$\beta F[\rho] \simeq \beta \int \left\{ \frac{1}{V} \beta \tilde{F}(\Gamma(\mathbf{r})) + \frac{1}{2} \sum_{i,j=1}^D \sum_{a,b=1}^N K_{ij}^{ab}(\Gamma(\mathbf{r})) \frac{\partial \Gamma_a(\mathbf{r})}{\partial r_i} \frac{\partial \Gamma_b(\mathbf{r})}{\partial r_j} \right\} d\mathbf{r} \quad (64)$$

where

$$\begin{aligned} \tilde{F}(\Gamma) &= \beta F[\rho_\Gamma] \\ K_{ij}^{ab}(\Gamma) &= \frac{1}{2V} \int r_{12,i} r_{12,j} c_2(\mathbf{r}_1, \mathbf{r}_2; [\rho_\Gamma]) \frac{\partial \rho(\mathbf{r}_1; \Gamma)}{\partial \Gamma_a} \frac{\partial \rho(\mathbf{r}_2; \Gamma)}{\partial \Gamma_b} d\mathbf{r}_1 d\mathbf{r}_2 \end{aligned} \quad (65)$$

and the notation $F[\rho_\Gamma]$ indicates the functional $F[\rho]$ evaluated with the function $\rho(\mathbf{r}; \Gamma)$ —that is, for fixed values of Γ . This result is more general and more complex

than the previous one. The DCF occurring here is that for the system with uniform density parameters, not the uniform fluid as in the previous case. It also does not depend on any particular parameterization of the density. In fact, if one makes the approximation $c_2(\mathbf{r}_1, \mathbf{r}_2; [\rho_\Gamma]) \sim c_2(r_{12}; \bar{\rho}_0)$ and uses the Haymet–Oxtoby parameterization for the density, then the coefficients $K_{ij}^{ab}(\Gamma)$ become the same in both theories.

One important aspect of both theories is that the expression for the coefficient K_{ij}^{ab} will only be finite if the DCF is short-ranged (or goes to zero sufficiently quickly so that the second moment exists). In fact, the derivations implicitly assume that analogous higher-order terms also exist so that in general the interactions should be short-ranged. This is not a problem if the potential is truncated, as is typically the case when comparing to simulation, or if the free energy is separated into a short-ranged and a long-ranged contribution, as is discussed in more detail below, and the gradient expansion only applied to the short-ranged part. A final comment is that the use of gradient expansions has been questioned in general on the grounds that they treat correlations too crudely [34]. This criticism seems more apropos of the first form of the gradient model where one is using a very crude model for the DCF function (namely that of a uniform liquid). In the more sophisticated model, no such assumption is made and, in fact, the truncation of the functional Taylor expansion at second order is an exact consequence of the truncation of the gradient expansion at second order, thus suggesting that this criticism may carry less weight.

III. DFT MODELS BASED ON THE LIQUID STATE

A. A Preview of DFT: The Square Gradient Model

The previous section dealt with the theoretical basis for DFT without giving much indication as to how it could be used in practice. Toward this end, we observe that some knowledge is available for the liquid state. If there is no applied field, then there is no source of spatial anisotropy and the average density must be a constant, $\rho(\mathbf{r}) = \bar{\rho}$. (Note that we often speak of solids in the absence of fields and these are not translationally invariant; however, there must actually be a field that serves to fix the position and orientation of the crystal lattice: Averaging over all translations and rotations of the lattice would give a uniform density. We assume it is enough that such a field act at the boundaries of the system and that its effect is negligible in the thermodynamic limit.) Rather than having no field at all, we will assume the system is in a container, which means that the field is zero in the interior region and infinite outside this region. Again, we assume that the interior can be made so large that the surface effects of the container are negligible. Then, if the available volume is V , the grand potential is $\frac{1}{V}\Omega = \Lambda[\bar{\rho}; \phi[\bar{\rho}] = 0] = \bar{\rho} \ln \Lambda^D \bar{\rho} - \bar{\rho} + \frac{1}{V} F_{\text{ex}}[\bar{\rho}] - \mu \bar{\rho}$; hence, it follows that

$\frac{1}{V}F_{\text{ex}}[\bar{\rho}]$ is the excess Helmholtz free energy for a uniform liquid which will be denoted as $f_{\text{ex}}(\bar{\rho})$. Whenever necessary, it is assumed in DFT that this function as well as other properties of the uniform liquid such as its two-body DCF, $c_2(\mathbf{r}_1, \mathbf{r}_2; [\bar{\rho}]) = c_2(r_{12}; \bar{\rho})$, the pair distribution function, and so on, are known or knowable from liquid-state theory (thermodynamic perturbation theory or integral equation theories, see, for example, Ref. 21).

It might seem that one could make a simple DFT model based on the (known) free energy function of the liquid by postulating that

$$F_{\text{ex}}[\rho] \simeq \int f_{\text{ex}}(\rho(\mathbf{r}))d\mathbf{r} \quad (66)$$

which is known as the ‘‘local density approximation.’’ However, a moment’s thought shows that this is too simple. For example, in the case of a planar liquid–vapor interface, the grand potential of the liquid and vapor are the same (by definition of coexistence). Since the coexisting phases are minima of the grand potential, the free energy for densities between that of the liquid and vapor must be larger, thus implying that the density functional is minimized by a system with an infinitely thin interface, which is a very crude and not very useful approximation. This defect can be corrected, as first discussed by van der Waals himself [1, 2], by realizing that gradients of the density must be energetically costly since a small volume in the system with neighboring volumes having different densities will necessarily feel a net force. Calculating the forces in the limit of slowly varying densities leads to the well-known ‘‘square-gradient approximation’’ [1, 2],

$$F_{\text{ex}}[\rho] \simeq \int \left[f_{\text{ex}}(\rho(\mathbf{r})) + \frac{1}{2}g(\nabla\rho(\mathbf{r}))^2 \right] d\mathbf{r} \quad (67)$$

The parameter g is, at this point, unknown and is often treated phenomenologically. As discussed above, it can be calculated from knowledge of the DCF. To give a flavor of the types of calculations performed using DFT, we can use this model to calculate the structure of the liquid–vapor interface. Let the densities of the coexisting liquid and vapor at some given temperature and chemical potential be $\bar{\rho}_l$ and $\bar{\rho}_v$, respectively. Then, for a planar interface we expect the density to depend only on one coordinate, say the z -coordinate, and to take the values $\rho(\infty) = \bar{\rho}_l$ and $\rho(-\infty) = \bar{\rho}_v$. The Euler–Lagrange equation becomes

$$\frac{df(\rho(z))}{d\rho(z)} - g \frac{d^2\rho(z)}{dz^2} = \mu \quad (68)$$

where $f(\rho) = \rho \ln \rho - \rho + f_{\text{ex}}(\rho)$. Multiplying through by $d\rho(z)/dz$ and integrating under the assumption that the derivatives vanish at large $|z|$ gives

$$f(\rho(z)) - \frac{1}{2}g \left(\frac{d\rho(z)}{dz} \right)^2 - \mu\rho(z) = f(\bar{\rho}_v) - \mu\bar{\rho}_v \equiv \omega(\bar{\rho}_v; \mu) \quad (69)$$

This equation can be solved by quadratures and, given an analytic form of $f_{ex}(\rho)$, the profile determined numerically. The excess free energy per unit area, the surface free energy γ which is often assumed to be the same as the surface tension, can then be calculated from

$$\gamma = \int_{-\infty}^{\infty} \left(f(\rho(z)) + \frac{1}{2} g \left(\frac{d\rho(z)}{dz} \right)^2 - \mu\rho(z) - \omega(\bar{\rho}_v; \mu) \right) dz \quad (70)$$

If the profile is monotonic, one can solve Eq. (69) for $d\rho/dz$ and write this as

$$\gamma = \sqrt{2g} \int_{\bar{\rho}_v}^{\bar{\rho}_l} \sqrt{f(\rho) - \mu\rho - \omega(\bar{\rho}_v; \mu)} dn \quad (71)$$

so that the surface free energy can be determined by a simple integration without even solving for the profile.

B. A Survey of Models

One of the applications that motivated the development of early DFT models was the description of freezing and particularly the description of hard-sphere freezing. It was always recognized that if good models could be created for hard-spheres, then realistic potentials with long-ranged attractive interactions could, at worst, be treated perturbatively (an assumption justified by the extension of thermodynamic perturbation theory to the solid state [35]). At best, a successful model for hard-spheres would be immediately generalizable to simple fluids and beyond. The strategy that dominated much of the early work was to try to somehow use information about the uniform liquid to construct a functional applicable to nonuniform systems, particularly the solid that in this context is viewed as a highly nonuniform liquid. In the remainder of this section, a variety of models based on this approach is reviewed and their successes and shortcomings are pointed out. A more thorough discussion of these developments can be found in Evans [13].

1. Models Based on Perturbation Theory about the Uniform Liquid State

a. The Ramakrishnan–Yussouff/Haymet–Oxtoby Theory. Perhaps the earliest successful DFT of freezing was that due to Ramakrishnan and Yussouff [6] and further developed by Haymet and Oxtoby [30]. It is based on the truncation of the perturbative expansion, Eqs. (44) and (45), with the simplest choices $\bar{\rho}_0 = \bar{\rho}(\lambda) = \bar{\rho}_1$ giving

$$\frac{1}{V} \beta F_{ex}[\rho_1] = \beta f_{ex}(\bar{\rho}_0) - \frac{1}{2V} \int d\mathbf{r}_1 d\mathbf{r}_2 c_2(r_{12}; \bar{\rho}_0) (\rho_1(\mathbf{r}_1) - \bar{\rho}_0) (\rho_1(\mathbf{r}_2) - \bar{\rho}_0) + \dots \quad (72)$$

Higher-order terms are not written as practical calculations are usually, but not always, done after truncating the expansion at second order. The suspicion

that higher-order terms were not negligible, particularly the work of Curtin [36] indicating that the series converges slowly, if at all, led to a desire for “nonperturbative” alternatives to this simple theory. Nevertheless, it is still frequently used as a simplest first approximation.

b. The Effective Liquid Theory. Baus and Colot [37] proposed what was termed a “nonperturbative” theory, meaning it was not based on perturbation about a liquid with the same density as the inhomogeneous system (usually a solid, in this context). It can, however, still be viewed as a perturbative theory based on Eqs. (44, 45) with $\bar{\rho}_0 = \bar{\rho}_1$. The idea was that the unknown DCF be approximated by that of the liquid at a density, $\bar{\rho}_{\text{ELA}}$ for which the first peak of the structure factor of the liquid occurs at the smallest reciprocal lattice vector of the solid (thus, in some sense matching the structure of the liquid and solid). This is equivalent to taking $\bar{\rho}(\lambda) = \bar{\rho}_{\text{ELA}}$ in Eqs. (44)–(45) giving

$$\frac{1}{V}\beta F_{\text{ex}}[\rho_1] = \beta f_{\text{ex}}(\bar{\rho}_1) - \frac{1}{2V} \int d\mathbf{r}_1 d\mathbf{r}_2 c_2(\mathbf{r}_{12}; \bar{\rho}_{\text{ELA}}) (\rho_1(\mathbf{r}_1) - \bar{\rho}_1) (\rho_1(\mathbf{r}_2) - \bar{\rho}_1) + \dots \quad (73)$$

which is the ELA result.

c. The Self-Consistent Effective Liquid Theory. Proposed by Baus [38], this theory involved an actual integration though density space. First, the initial reference is taken to be zero, $\bar{\rho}_0 = 0$, and then the choice $\bar{\rho}(\lambda) = \lambda \bar{\rho}_{\text{SCELA}}$ is made giving

$$\begin{aligned} \frac{1}{V}\beta F_{\text{ex}}[\rho_1] &= -\frac{1}{V} \int_0^1 d\lambda \int_0^\lambda d\lambda' \int d\mathbf{r}_1 d\mathbf{r}_2 c_2(r_{12}; \lambda' \bar{\rho}_{\text{SCELA}}) \rho_1(\mathbf{r}_1) \rho_1(\mathbf{r}_2) + \dots \\ &= -\frac{1}{V} \int_0^1 d\lambda \int d\mathbf{r}_1 d\mathbf{r}_2 (1-\lambda) c_2(r_{12}; \lambda \bar{\rho}_{\text{SCELA}}) \rho_1(\mathbf{r}_1) \rho_1(\mathbf{r}_2) + \dots \end{aligned} \quad (74)$$

where the second line follows from an integration by parts. The density $\bar{\rho}_{\text{SCELA}}$ is chosen to satisfy the self-consistency requirement that the excess free energy per atom be the same in the solid as in the reference system,

$$\psi_{\text{ex}}(\bar{\rho}_{\text{SCELA}}) \equiv \frac{1}{\bar{\rho}_{\text{SCELA}}} f_{\text{ex}}(\bar{\rho}_{\text{SCELA}}) = \frac{1}{\rho_1 V} F_{\text{ex}}[\rho_1] \quad (75)$$

The idea is that there is always some liquid density for which this equation—the thermodynamic mapping—holds true. Similarly, there is always some liquid density for which Eq. (74) holds true, the so-called structural mapping. The SCELA results from a demand for self-consistency in the sense of equating the structural mapping and the thermodynamic mapping.

d. Generalized Effective Liquid Theory. A further development of this idea was proposed by Lutsko and Baus [25, 39]. It extends the idea of the SCELA by requiring self-consistency for all densities along the integration path in the hope that this would suppress the contribution of higher order terms. The result is

$$\frac{1}{V}\beta F_{\text{ex}}[\rho_1] = -\frac{1}{V}\int_0^1 d\lambda \int d\mathbf{r}_1 d\mathbf{r}_2 (1-\lambda)c_2(r_{12}; \bar{\rho}_{\text{GELA}}(\lambda))\rho_1(\mathbf{r}_1)\rho_1(\mathbf{r}_2) + \dots \quad (76)$$

with

$$\begin{aligned} \beta\psi_{\text{ex}}(\bar{\rho}_{\text{GELA}}(\alpha)) &= \frac{1}{\alpha\rho_1 V}\beta F_{\text{ex}}[\alpha\rho_1] \\ &= -\frac{1}{\alpha\bar{\rho}_1 V}\int_0^1 d\lambda \int_0^\lambda d\lambda' \int d\mathbf{r}_1 d\mathbf{r}_2 c_2(\mathbf{r}_{12}; \bar{\rho}_{\text{GELA}}(\alpha\lambda')) \\ &\quad \times \alpha\rho_1(\mathbf{r}_1)\alpha\rho_1(\mathbf{r}_2) + \dots \\ &= -\frac{1}{\alpha\bar{\rho}_1 V}\int_0^\alpha d\gamma \int_0^\alpha d\lambda' \int d\mathbf{r}_1 d\mathbf{r}_2 c_2(\mathbf{r}_{12}; \bar{\rho}_{\text{GELA}}(\gamma')) \\ &\quad \times \rho_1(\mathbf{r}_1)\rho_1(\mathbf{r}_2) + \dots \end{aligned} \quad (77)$$

Notice that when truncated at second order, this can be converted into a differential equation for $\bar{\rho}_{\text{GELA}}(\alpha)$ [25],

$$\frac{\partial^2}{\partial\alpha^2}\alpha\beta\psi_{\text{ex}}(\bar{\rho}_{\text{GELA}}(\alpha)) = -\frac{1}{\bar{\rho}_1 V}\int d\mathbf{r}_1 d\mathbf{r}_2 c_2(r_{12}; \bar{\rho}_{\text{GELA}}(\alpha))\rho_1(\mathbf{r}_1)\rho_1(\mathbf{r}_2) \quad (78)$$

e. Modified Weighted Density Approximation. The Weighted Density Approximation (WDA) of Curtin and Ashcroft [40] will be described separately below. The goal was to try to construct a density functional having the property that it reproduces the DCF of the liquid in the uniform limit,

$$c_2(r_{12}; \bar{\rho}) = -\lim_{\rho(\mathbf{r}) \rightarrow \bar{\rho}} \frac{\delta^2 \beta F^{(\text{WDA})}[\rho]}{\delta\rho(\mathbf{r}_1)\delta\rho(\mathbf{r}_2)} \quad (79)$$

The Modified Weighted Density Approximation of Denton and Ashcroft is a simplified form of the same idea [41]. It is derived by introducing an effective liquid ansatz,

$$\frac{1}{\bar{\rho}V}F_{\text{ex}}[\rho] = \psi_{\text{ex}}(\bar{\rho}_{\text{MWDA}}[\rho]) \quad (80)$$

and writing the MWDA density as a weighted average,

$$\bar{\rho}_{\text{MWDA}}[\rho] = \frac{1}{\bar{\rho}V}\int w(r_{12}; \bar{\rho}_{\text{MWDA}}[\rho])\rho(\mathbf{r}_1)\rho(\mathbf{r}_2)d\mathbf{r}_1 d\mathbf{r}_2 \quad (81)$$

and demanding that the weighting function be normalized. Demanding that the theory reproduce a given DCF, $c_2(r_{12}; \bar{\rho})$, in the bulk limit is enough to uniquely determine the weight function as

$$w(r_{12}; \bar{\rho}) = \frac{-1}{2\beta\psi'(\bar{\rho})} \left(c_2(r_{12}; \bar{\rho}) + \frac{1}{V} \bar{\rho} \beta \psi''(\bar{\rho}) \right) \quad (82)$$

Then the effective density is determined from

$$\begin{aligned} & 2\bar{\rho}_{\text{MWDA}}\beta\psi'(\bar{\rho}_{\text{MWDA}}) + \bar{\rho}_1\bar{\rho}_{\text{MWDA}}\beta\psi''(\bar{\rho}_{\text{MWDA}}) \\ &= -\frac{1}{\bar{\rho}V} \int c_2(r_{12}; \bar{\rho}_{\text{MWDA}}) \rho(\mathbf{r}_1) \rho(\mathbf{r}_2) d\mathbf{r}_1 d\mathbf{r}_2 \end{aligned} \quad (83)$$

This is equivalent to a perturbative theory, Eqs. (44) and (45), truncated at second order with $\bar{\rho}(\lambda) = \bar{\rho}_{\text{MWDA}}$ and $\bar{\rho}_0$ determined from

$$\begin{aligned} \bar{\rho}\psi_{\text{ex}}(\bar{\rho}_0) + (\bar{\rho} - \bar{\rho}_0)\bar{\rho}_0\psi'_{\text{ex}}(\bar{\rho}_0) &= \bar{\rho}\psi_{\text{ex}}(\bar{\rho}_{\text{MWDA}}) \\ &\quad - (\bar{\rho}\bar{\rho}_{\text{MWDA}} - 2\bar{\rho}_0\bar{\rho} + \bar{\rho}_0^2)\psi'_{\text{ex}}(\bar{\rho}_{\text{MWDA}}) \\ &\quad - \frac{1}{2}(\bar{\rho} - \bar{\rho}_0)^2\bar{\rho}_{\text{MWDA}}\psi''_{\text{ex}}(\bar{\rho}_{\text{MWDA}}) \end{aligned} \quad (84)$$

2. Nonlocal Theories

a. Simple Position-Dependent Effective Liquid. In the simple truncated perturbation theory, one effectively replaces the DCF of the inhomogeneous system by that of a fluid at some specified density. For bulk properties, this might suffice, even for the bulk solid, but it obviously runs into conceptual difficulties when applied to more complex systems. For example, what single value of the reference density should be chosen to approximate correlations in a liquid–vapor interface or vapor–solid interface? For a liquid–vapor system, far from the interface one knows what the DCF should be (since the DCF in the bulk is required as input for most of the DFTs discussed here). This suggests the use of a position-dependent reference density. Since the DCF is a two-point function that is symmetric in its arguments, some care must be taken in introducing such an approximation. Two simple possibilities are

$$c_2(\mathbf{r}_1, \mathbf{r}_2; [\rho]) \simeq c_2 \left(r_{12}; \frac{\rho(\mathbf{r}_1) + \rho(\mathbf{r}_2)}{2} \right) \quad (85)$$

and

$$c_2(\mathbf{r}_1, \mathbf{r}_2; [\rho]) \simeq \frac{1}{2} (c_2(r_{12}; \rho(\mathbf{r}_1)) + c_2(r_{12}; \rho(\mathbf{r}_2))) \quad (86)$$

Substituting the first into the exact expression, Eq. (44), gives, after some rearrangement,

$$\begin{aligned} \beta F_{\text{ex}}[\rho] \simeq & \int d\mathbf{r} \beta f_{\text{ex}}(\rho(\mathbf{r})) \\ & + \frac{1}{4} \int_V d\mathbf{r}_1 d\mathbf{r}_2 (\rho(\mathbf{r}_1) - \rho(\mathbf{r}_2))^2 \bar{c}_2 \left(r_{12}; \frac{\rho(\mathbf{r}_1) + \rho(\mathbf{r}_2)}{2}, \bar{\rho}_0 \right) \\ & - \frac{1}{2} \int_V d\mathbf{r}_1 d\mathbf{r}_2 \left[\left(\frac{\rho(\mathbf{r}_1) + \rho(\mathbf{r}_2)}{2} - \bar{\rho}_0 \right)^2 \bar{c}_2 \left(r_{12}; \frac{\rho(\mathbf{r}_1) + \rho(\mathbf{r}_2)}{2}, \bar{\rho}_0 \right) \right. \\ & \quad \left. - (\rho(\mathbf{r}_1) - \bar{\rho}_0)^2 \bar{c}_2(r_{12}; \rho(\mathbf{r}_1), \bar{\rho}_0) \right] \end{aligned} \quad (87)$$

for the first approximation, where

$$\bar{c}_2(r; \rho, \bar{\rho}_0) \equiv 2 \int_0^1 \int_0^\lambda c_2(r; \bar{\rho}_0 + \lambda'(\rho - \bar{\rho}_0)) d\lambda' d\lambda \quad (88)$$

The second approximation gives a somewhat simpler result,

$$\begin{aligned} \beta F_{\text{ex}}[\rho] = & \int d\mathbf{r} f_{\text{ex}}(\rho(\mathbf{r})) \\ & + \frac{1}{2} \int_V (\rho(\mathbf{r}_1) - \bar{\rho}_0)(\rho(\mathbf{r}_1) - \rho(\mathbf{r}_2)) \bar{c}_2(r_{12}; \rho(\mathbf{r}_1), \bar{\rho}_0) d\mathbf{r}_2 d\mathbf{r}_1 \end{aligned} \quad (89)$$

which has the intuitively appealing form of a local effective liquid approximation plus a contribution that depends on density gradients. It is straightforward to show that an expansion in the inhomogeneity—that is, in powers of $(\rho(\mathbf{r}_1) - \rho(\mathbf{r}_2))$ —gives [42]

$$\begin{aligned} \beta F_{\text{ex}}[\rho] = & \int d\mathbf{r} f(\rho(\mathbf{r})) + \frac{1}{4} \int_V (\rho(\mathbf{r}_1) - \rho(\mathbf{r}_2))^2 \\ & \times \left[2 \int_0^1 \lambda c_2 \left(r_{12}; \bar{\rho}_0 + \lambda \left(\frac{\rho(\mathbf{r}_1) + \rho(\mathbf{r}_2)}{2} - \bar{\rho}_0 \right) \right) d\lambda \right] d\mathbf{r}_1 d\mathbf{r}_2 + \dots \end{aligned} \quad (90)$$

and further expanding the integrand about $\lambda = 1$ gives, to lowest order,

$$\begin{aligned} \beta F_{\text{ex}}[\rho] = & \int d\mathbf{r} f(\rho(\mathbf{r})) \\ & + \frac{1}{4} \int_V (\rho(\mathbf{r}_1) - \rho(\mathbf{r}_2))^2 c_2 \left(r_{12}; \frac{\rho(\mathbf{r}_1) + \rho(\mathbf{r}_2)}{2} \right) d\mathbf{r}_1 d\mathbf{r}_2 + \dots \end{aligned} \quad (91)$$

which is the well-known form used by Saam and Ebner in some of the earliest DFT calculations [7, 8].

b. Weighted Density Approximation of Curtin and Ashcroft. One criticism of many of the models discussed so far is that they are formally inconsistent. They require as input the DCF of the bulk liquid, but the second functional derivative of the model excess free energy functional does not, in the uniform limit, give the input function $c_2(r_{12}; \rho)$. The Weighted Density Approximation of Curtin and Ashcroft [40] was specifically designed to solve this problem. They begin by writing the exact expression for the excess free energy functional, Eq. (44), with $\bar{\rho}_0 = 0$ as

$$F_{\text{ex}}[\rho] = \int \Psi_{\text{ex}}(\mathbf{r}; [\rho]) \rho(\mathbf{r}) d\mathbf{r} \quad (92)$$

where

$$\Psi_{\text{ex}}(\mathbf{r}; [\rho]) = - \int_0^1 d\lambda \int_0^\lambda d\lambda' \int d\mathbf{r}_2 c_2(\mathbf{r}_1, \mathbf{r}_2; [\lambda' \rho_1]) \rho_1(\mathbf{r}_2)$$

They then introduce a *local* effective liquid approximation

$$\Psi_{\text{ex}}(\mathbf{r}; [\rho]) = \psi_{\text{ex}}(\rho_{\text{WDA}}(\mathbf{r}; [\rho])) \quad (93)$$

where we recall that $\psi(\bar{\rho}) = \frac{1}{\bar{\rho}V} F(\bar{\rho})$ is the free energy per atom and $\psi_{\text{ex}}(\bar{\rho})$ is the excess contribution. The local effective density is expressed in terms of a weighted-density ansatz,

$$\rho_{\text{WDA}}(\mathbf{r}_1; [\rho]) = \int w(\mathbf{r}_1 - \mathbf{r}_2; \rho_{\text{WDA}}(\mathbf{r}_1; [\rho])) \rho(\mathbf{r}_2) d\mathbf{r}_2 \quad (94)$$

The weighting function is fixed by demanding that it is normalized, $\int w(\mathbf{r}; \bar{\rho}) d\mathbf{r} = 1$, and that the ansatz be consistent with the (known) DCF in the liquid state,

$$c_2(r_{12}; \bar{\rho}) = - \lim_{\rho(\mathbf{r}) \rightarrow \bar{\rho}} \frac{\delta^2 \beta F_{\text{ex}}[\rho]}{\delta \rho(\mathbf{r}_1) \delta \rho(\mathbf{r}_2)} \quad (95)$$

leading to [40] $w(\mathbf{r}; \bar{\rho}) = w(r; \bar{\rho})$ and an integrodifferential equation for $w(r; \bar{\rho})$. Taking the Fourier transform,

$$\tilde{w}(k; \bar{\rho}) = \int \exp(i\mathbf{k} \cdot \mathbf{r}) w(r; \bar{\rho}) d\mathbf{r} \quad (96)$$

the weighting function is determined from

$$\begin{aligned} k_B T \tilde{c}_2(k; \bar{\rho}) &= -2 \frac{\partial \psi_{\text{ex}}(\bar{\rho})}{\partial \bar{\rho}} \tilde{w}(k; \bar{\rho}) - \bar{\rho} \frac{\partial^2 \psi_{\text{ex}}(\bar{\rho})}{\partial \bar{\rho}^2} \tilde{w}^2(k; \bar{\rho}) \\ &\quad - 2\bar{\rho} \frac{\partial \psi_{\text{ex}}(\bar{\rho})}{\partial \rho} \tilde{w}(k; \bar{\rho}) \frac{\partial \tilde{w}(k; \bar{\rho})}{\partial \bar{\rho}} \end{aligned} \quad (97)$$

The WDA is therefore computationally more complex than the simpler effective liquid theories because it involves a different effective liquid for each wave vector.

c. Tarazona's Weighted Density Theory. A similar theory was constructed by Tarazona [43] for the specific case of hard spheres. However, rather than enforce the exact relation between the excess free energy functional and the DCF, a simpler approximation was employed. The structure of the theory is the same as that of the WDA, but the determination of the weighting function is different. It is expanded as a series,

$$w(\mathbf{r}; \rho) = w_0(r) + w_1(r)\rho + w_2(r)\rho^2 \quad (98)$$

and the first two functions, $w_0(r)$ and $w_1(r)$, are determined by requiring agreement with the first two terms of the virial expansion of the DCF. The final function is fit so as to give a reasonable reproduction of the Percus–Yevick DCF at higher densities.

C. Some Applications

1. Freezing of Hard Spheres

The equilibrium density distribution under action of a given external potential ϕ_0 , fixed chemical potential μ and inverse temperature β is that which minimizes the free energy functional $\Omega[\rho; \phi_0]$. In the language of DFT, different phases correspond to different density distributions. Two phases with densities $\rho_1(\mathbf{r})$ and $\rho_2(\mathbf{r})$ can coexist when they simultaneously minimize this functional—that is, when they both satisfy the Euler–Lagrange equation and when $\Omega[\rho_1; \phi_0] = \Omega[\rho_2; \phi_0]$. Since they satisfy they minimize the free energy functional, its value at those density distributions is the grand-canonical free energy, $\Omega[\rho_1; \phi_0] = \Omega$. Since the grand potential is proportional to the pressure, $\Omega = -PV$, this implies the usual thermodynamic condition of equal pressures. The Euler–Lagrange equation,

$$\frac{\delta F[\rho_1]}{\delta \rho_1(\mathbf{r})} = \mu - \phi_0(\mathbf{r}) = \frac{\delta F[\rho_2]}{\delta \rho_2(\mathbf{r})} \quad (99)$$

generalizes the usual condition of equal chemical potentials. Thus, in the grand ensemble used in DFT, two-phase coexistence is in principle determined by adjusting the parameter μ , determining the resultant densities $\rho_1(\mathbf{r})$ and $\rho_2(\mathbf{r})$ and evaluating $\Omega[\rho_1; \phi_0]$ and $\Omega[\rho_2; \phi_0]$ until a value of μ is found for which $\Omega[\rho_1; \phi_0] = \Omega[\rho_2; \phi_0]$. For uniform phases, say liquid and vapor, with a field that only acts to confine the system to a large but finite volume, this reduces to the usual conditions:

$$\begin{aligned} \frac{\partial f(\bar{\rho}_1)}{\partial \bar{\rho}_1} &= \mu = \frac{\partial f(\bar{\rho}_2)}{\partial \bar{\rho}_2} \\ f(\bar{\rho}_1) - \mu &= f(\bar{\rho}_2) - \mu \end{aligned} \quad (100)$$

Solids are most often modeled by using the Gaussian parameterization of the density [see Eqs. (54) and (55) and the accompanying discussion]. In this case, the parameters are the number density of lattice sites, $\bar{\rho}_{\text{latt}}$ (or, equivalently, the lattice constant a), the Gaussian parameter α , and the occupancy x ; or, equivalently, the average density is $\bar{\rho} = x\bar{\rho}_{\text{latt}}$. Assuming no field except for at the boundaries of the (large) volume, the Euler–Lagrange equations for the uniform solid are

$$\begin{aligned}\frac{\partial F[\rho]}{\partial \bar{\rho}_{\text{latt}}} &= \mu x \\ \frac{\partial F[\rho]}{\partial x} &= \mu \bar{\rho}_{\text{latt}} \\ \frac{\partial F[\rho]}{\partial \alpha} &= 0\end{aligned}\tag{101}$$

In fact, in many calculations, the occupancy is held fixed to $x = 1$ since one expects values very close to this in equilibrium solids. In this case, the second of these equations is dropped.

All of the theories discussed above give reasonable results for hard-sphere freezing. Obviously, the quality of the numerical predications depends on the quality of the liquid-state data that all of these theories require (i.e., the DCF of the liquid). The Percus–Yevick DCF is very good at low densities but inaccurate at the high densities characteristic of freezing. For some theories such as the MWDA, SCELA, and GELA, this is not important for the solid phase as the effective densities that enter these theories tend to be about half the actual density. However, in all cases the liquid thermodynamics must also be evaluated, and this always requires densities at which the Percus–Yevick approximation is not very good. Since all one really needs for the liquid is the equation of state, it is common in these cases to use the Percus–Yevick approximation for the solid and to use the Carnahan–Starling approximation for the liquid because both can be understood as being accurate approximations in the relevant domains. For other DFTs that require the liquid-state DCF at all densities, such as RY, ELA, and WDA, this would be inconsistent and one must either suffice with Percus–Yevick or make use of the more accurate, but more complex, parameterization of Hendersen and Grundke [44] or the semi-phenomenological approximation of Baus and Colot [45].

The results of several calculations for liquid-FCC solid hard-sphere coexistence are shown in Table I. Rather than the value of the Gaussian parameter, the more physical Lindemann parameter L , defined as mean-squared displacement divided by the lattice constant, is reported. For the Gaussian model, one has $L = (3/\alpha a^2)^{1/2}$ for the FCC solid and $L = (2/\alpha a^2)^{1/2}$ for the BCC solid. All of the theories give reasonable results, with the GELA being the closest to the

TABLE I

Comparison of the Predictions of Various Effective-Liquid DFTs for the Freezing of Hard Spheres to Data from Simulation^a

Theory	EOS	$\bar{\eta}_{\text{liq}}$	$\bar{\eta}_{\text{sol}}$	P^*	L
RY ^b	PY	0.506	0.601	15.1	0.06
MWDA ^c	CS	0.476	0.542	10.1	0.097
ELA ^d	PY	0.520	0.567	16.1	0.074
SCELA ^e	CS	0.508	0.560	13.3	0.084
GELA ^e	CS	0.495	0.545	11.9	0.100
WDA ^{e,f}	CS	0.480	0.547	10.4	0.093
MC ^g	—	0.494	0.545	11.7	0.126

^aGiven are the liquid ($\bar{\eta}_{\text{liq}}$) and solid ($\bar{\eta}_{\text{sol}}$) packing fractions ($\eta = \pi\rho d^3/6$), the reduced pressure ($P^* = \beta P d^3$), and the Lindemann parameter (L) at bulk coexistence. For each theory, the equation of state used for the fluid, Percus–Yevick (PY), or Carnahan–Starling (CS) is indicated.

^bFrom Barrat et al. [49].

^cFrom Denton and Ashcroft [41].

^dFrom Baus and Colot [37].

^eFrom Lutsko and Baus [25].

^fFrom Curtin and Ashcroft [40].

^gFrom Hoover and Ree [57].

simulation values. One important defect shared by all theories is that they uniformly predict a value of the Lindemann parameter which is much too low. The significance of the apparent accuracy in describing some other properties at coexistence is therefore open to question. It is also possible to study freezing into other structures, such as the BCC and simple cubic (SC) lattices [25]. However, since these structures are metastable, little information is available with the exception of Curtin and Runge, who used a constrained simulation method to study hard spheres in a BCC configuration [46]. At $\bar{\rho}d^3 = 1.041$ they found an excess free energy relative to a uniform ideal gas of $\frac{1}{\bar{\rho}V} \beta F(\rho) - (\ln \bar{\rho} \Lambda^3 - 1) = 6.094$ and at $\bar{\rho}d^3 = 1.1$ they found the value 6.878. The WDA gives the values 5.975 and 6.771, respectively, while the GELA gives 6.118 and 6.991 using the PY DCF and 6.049 and 6.903 using the CS DCF [25]. This seems to confirm the trends seen in the FCC coexistence data. The accuracy of the various theories in predicting the pressure of the solid phase for all densities follows the same trends, with the GELA being very close to simulation. At high densities, problems develop with the MWDA where multiple solutions to the effective-density equation develop and where there are regions of no solution [47, 48]. At very high densities, the GELA seems to predict that the Lindemann parameter goes to zero at $\eta \simeq 0.736$, which is very near the FCC close packing density, $\eta = 0.74$, where the Lindemann parameter must be zero. However, for the BCC phase, the GELA predicts a Lindemann parameter that not only varies little with density, showing no sign of going to zero at BCC close packing, $\eta = 0.68$, but also

even increases somewhat with increasing density. All of this is highly unphysical and indicates a breakdown of the theory.

This generally satisfactory behavior does not translate to other systems. Barrat, Hansen, Pastore, and Waisman [49] used the RY and ELA theories to investigate the freezing of atoms interacting with an inverse-power potential, $v(r) = (\sigma/r)^n$. In the limit $n \rightarrow \infty$, these so-called “soft spheres” coincide with the usual hard spheres. For the DCF of the fluid, they used both the Rogers and Young integral equation [50] and the modified HNC scheme of Rosenfeld and Ashcroft [51]. Their conclusions were that neither theory stabilized the BCC phase even though from simulation, it is known that the BCC phase is the stable solid phase for $n \leq 6$ [52]. Laird and Kroll carried out a similar study using the MWDA, SCELA and GELA [53]. They found that the MWDA also predicted freezing into the FCC structure for all values of n with the numerical values of the freezing parameters worsening with decreasing n . Worse yet, the SCELA and GELA failed to predict freezing altogether for $n \leq 6$. De Kuijper, Vos, Barrat, Hansen, and Schouten investigated the ability of these theories to predict freezing for many other potentials including the Lennard-Jones and exponential-6 potentials often used to model simple liquids [54]. They found that the SCELA fails to predict freezing for the LJ potential while the MWDA fails at low temperatures but does predict freezing into an FCC structure at higher temperatures. The simple second-order perturbation theory predicts freezing but with poor values for the freezing parameters. The conclusion is that none of these theories appears to be reliably predictive as one moves away from the hard-sphere potential. Further details including a discussion of freezing in binary systems can be found in Ref. (55). There have been attempts to further modify these basic theories to give a better description of freezing. For example, Wang and Gast suggested modifying the MWDA prescription for the effective density so as to give the correct static-lattice free energy in the large α limit [56]. While this and other attempts have yielded significant improvements, the trend in recent years has been toward simpler theories that separate the hard core and attractive contributions to the free energy as discussed below.

2. *Liquid–Solid Interface*

These theories have also been used to study interfacial systems including fluids near walls and liquid–solid interfaces. We note in particular the work by Curtin [58], Ohensorge, Löwen, and Wagner [59, 60] and Marr and Gast [61] on the liquid–solid interface in Lennard-Jones systems, as well as the work of Kyrlidis and Brown [62] on the hard-sphere liquid–solid interface, all of which demonstrate the utility of DFT even in describing very inhomogeneous systems. A good summary of the work on wetting can be found in Evans [14]. Numerous applications of interest in chemical engineering can be found in Wu [17].

3. Properties of the Bulk Liquid State

One interesting application of DFT is to model correlations in the liquid state. The third- and higher-order DCFs can be calculated from any model DFT by functional differentiation. For example, with the MWDA theory,

$$F_{\text{ex}}[\rho] = N\psi_{\text{ex}}(\bar{\rho}_{\text{MWDA}}[\rho])$$

$$\bar{\rho}_{\text{MWDA}} = \frac{1}{N} \int w(r_{23}; \bar{\rho}_{\text{MWDA}}) \rho(\mathbf{r}_2) \rho(\mathbf{r}_3) d\mathbf{r}_2 d\mathbf{r}_3 \quad (102)$$

one has that

$$c_1(r; \bar{\rho}) = - \lim_{\rho(\mathbf{r}) \rightarrow \bar{\rho}} \frac{\delta \beta F_{\text{ex}}[\rho]}{\delta \rho(\mathbf{r})}$$

$$= - \lim_{\rho(\mathbf{r}) \rightarrow \bar{\rho}} \left(\beta \psi_{\text{ex}}(\bar{\rho}_{\text{MWDA}}[\rho]) + N \frac{\delta \bar{\rho}_{\text{MWDA}}[\rho]}{\delta \rho(\mathbf{r})} \psi'_{\text{ex}}(\bar{\rho}_{\text{MWDA}}[\rho]) \right) \quad (103)$$

Implicit differentiation of the equation for the effective density gives

$$N \frac{\delta}{\delta \rho(\mathbf{r}_1)} \bar{\rho}_{\text{MWDA}} = \frac{2 \int w(r_{12}; \bar{\rho}_{\text{MWDA}}) \rho(\mathbf{r}_2) d\mathbf{r}_2 - \bar{\rho}_{\text{MWDA}}}{1 - \frac{1}{N} \int \frac{\partial}{\partial \bar{\rho}_{\text{MWDA}}} w(r_{23}; \bar{\rho}_{\text{MWDA}}) \rho(\mathbf{r}_2) \rho(\mathbf{r}_3) d\mathbf{r}_2 d\mathbf{r}_3} \quad (104)$$

so that in the thermodynamic limit, in which the $1/N$ term in the denominator is negligible, the result is

$$c_1(r; \bar{\rho}) = - \lim_{\rho(\mathbf{r}) \rightarrow \bar{\rho}} \frac{\delta \beta F_{\text{ex}}[\rho]}{\delta \rho(\mathbf{r})}$$

$$= -(\beta \psi_{\text{ex}}(\bar{\rho}) + \psi'_{\text{ex}}(\bar{\rho}) \bar{\rho}) \quad (105)$$

because the MWDA weight function is normalized, $\int w(r; \bar{\rho}) d\mathbf{r} = 1$. This is the usual equilibrium result. In the uniform limit, the second functional derivative of the MWDA (and WDA) functionals give, by construction, the bulk DCF used to calculate the weighting function. The third-order DCF for hard spheres has been evaluated and compared to simulation, with some success using both the WDA [63] and the MWDA [64] models.

There is also a close connection between DFT and the hypernetted chain (HNC) approximation to classical liquid-state theory because, as noted by Kim and Jones [65] and separately by White and Evans [66], the MWDA implies the HNC for a bulk fluid. This is easily seen by considering the DFT calculation of the structure of the bulk fluid. As explained above, the PDF can be obtained by solving for the density profile generated by a particle fixed at the origin which acts as the

external field. In principle, the effective density is determined by the coupled equations

$$\begin{aligned}
 F_{\text{ex}}[\rho] &= N\psi_{\text{ex}}(\bar{\rho}_{\text{MWDA}}[\rho]) \\
 \bar{\rho}_{\text{MWDA}} &= \frac{1}{N} \int w(r_{23}; \bar{\rho}_{\text{MWDA}}) \rho(\mathbf{r}_2) \rho(\mathbf{r}_3) d\mathbf{r}_2 d\mathbf{r}_3 \\
 \rho(\mathbf{r}; [v]) &= \exp\left(\beta\mu - \beta v(r) - \frac{\delta \beta F_{\text{ex}}[\rho]}{\delta \rho(\mathbf{r}; [v])}\right)
 \end{aligned} \tag{106}$$

where $v(r)$ is the pair potential. However, rewriting the equation for the effective density as

$$\bar{\rho}_{\text{MWDA}} = \bar{\rho} + \frac{1}{N} \int w(r_{23}; \bar{\rho}_{\text{MWDA}}) (\rho(\mathbf{r}_2) - \bar{\rho}) (\rho(\mathbf{r}_3) - \bar{\rho}) d\mathbf{r}_2 d\mathbf{r}_3 \tag{107}$$

it is clear that the difference from the bulk density will be of order $1/N$, provided that the spatial density profile approaches the bulk density sufficiently quickly as one moves away from the center of the external field. Assuming this is the case, then in the thermodynamic limit $\bar{\rho}_{\text{MWDA}} = \bar{\rho}$, just as in the case of zero field. To solve for the density profile, the functional derivative of the MWDA excess free energy functional is also needed, and one finds using Eq. (104) that

$$\begin{aligned}
 \frac{\delta}{\delta \rho(\mathbf{r})} F_{\text{ex}}[\rho] &= \frac{\delta}{\delta \rho(\mathbf{r})} N\psi_{\text{ex}}(\bar{\rho}_{\text{MWDA}}[\rho]) \\
 &= \psi_{\text{ex}}(\bar{\rho}_{\text{MWDA}}[\rho]) + N \frac{\delta \bar{\rho}_{\text{MWDA}}[\rho]}{\delta \rho(\mathbf{r})} \psi'_{\text{ex}}(\bar{\rho}_{\text{MWDA}}[\rho]) \\
 &= \psi_{\text{ex}}(\bar{\rho}_{\text{MWDA}}[\rho]) + \frac{2\psi'_{\text{ex}}(\bar{\rho}_{\text{MWDA}}[\rho]) \int w(r_{12}; \bar{\rho}_{\text{MWDA}}) \rho(\mathbf{r}_2) d\mathbf{r}_2 - \bar{\rho}_{\text{MWDA}}}{1 - \frac{1}{N} \int \frac{\partial}{\partial \bar{\rho}_{\text{MWDA}}} w(\mathbf{r}_{23}; \bar{\rho}_{\text{MWDA}}) \rho(\mathbf{r}_2) \rho(\mathbf{r}_3) d\mathbf{r}_2 d\mathbf{r}_3}
 \end{aligned} \tag{108}$$

In the thermodynamic limit, the term proportional to $1/N$ in the denominator of the second term on the right does not contribute. Using the explicit form of the MWDA weight function, Eq. (82) and a little algebra gives

$$\begin{aligned}
 \frac{\delta}{\delta \rho(\mathbf{r})} F_{\text{ex}}[\rho] &= \psi_{\text{ex}}(\bar{\rho}) - \int \beta^{-1} c_2(r_{12}; \bar{\rho}) \rho(\mathbf{r}_2) d\mathbf{r}_2 - \bar{\rho}^2 \psi''(\bar{\rho}) - \bar{\rho} \psi'_{\text{ex}}(\bar{\rho}) \\
 &= \psi_{\text{ex}}(\bar{\rho}) + \bar{\rho} \psi'_{\text{ex}}(\bar{\rho}) - \int \beta^{-1} c_2(r_{12}; \bar{\rho}) (\rho(\mathbf{r}_2) - \bar{\rho}) d\mathbf{r}_2
 \end{aligned} \tag{109}$$

Noting that the bulk density is determined by the Euler–Lagrange equation which reduces to $\ln \bar{\rho} + \psi_{\text{ex}}(\bar{\rho}) + \bar{\rho} \psi'_{\text{ex}}(\bar{\rho}) = \mu$, the final result is

$$\rho(\mathbf{r}; [v]) = \bar{\rho} \exp\left(\beta\mu - \beta v(r) + \int c_2(r_{12}; \bar{\rho})(\rho(\mathbf{r}_2; [v]) - \bar{\rho}) d\mathbf{r}_2\right) \quad (110)$$

Thus, for the uniform system, one has

$$g(r_1; \mu) = \exp\left(-\beta v(r_1) + \bar{\rho} \int c_2(r_{12}; \bar{\rho})(g(r_2; \mu) - 1) d\mathbf{r}_2\right) \quad (111)$$

This is the HNC closure relation which, combined with the Ornstein–Zernike equation gives a complete theory of the bulk liquid state [21].

White and Evans also show that the theories are equivalent for a fluid near a wall, but not for other more confined geometries [66]. Denton and Ashcroft reversed the logic and used DFT to give new closures for the Ornstein–Zernike equation [67]. They also note [68] that Barrat, Hansen, and Pastore had previously shown that the RY theory also implies the HNC for a uniform fluid [69].

IV. FUNDAMENTAL MEASURE THEORY FOR HARD SPHERES

Fundamental Measure Theory (FMT) has proven to be one of the most successful methods of modeling the DFT of hard spheres in more than one dimension. It is strongly motivated by Percus’ results for the one-dimensional hard-sphere fluid as well as by the Scaled Particle Theory approach to liquid-state theory [10–12].

A. Motivation

1. Hard Rods

In many interesting circumstances, the statistical mechanics of hard spheres in one dimension—usually called hard rods—can be solved exactly [70]. Beginning in the 1970s, Percus cast the problem in the language of Density Functional Theory and gave the solution for arbitrary external field. This result has served as a touchstone in recent developments of DFT for hard spheres. Because it gives an intrinsically interesting example of exact DFT, Percus’ solution is outlined in Appendix A while the results are summarized here to provide motivation for the discussion of FMT below.

The great simplification of hard rods is that they only interact with nearest neighbors and they cannot move past one another. Thus, the grand partition function for rods of length d is

$$\Xi(\beta, \mu; [\phi]) = 1 + \int_{-\infty}^{\infty} \exp(-\beta \tilde{\phi}(q_1)) dq_1 + \sum_{n=2}^{\infty} \int_{-\infty}^{\infty} \exp\left(-\beta \sum_{i=1}^n \tilde{\phi}(q_i)\right) W(q_1, \dots, q_n) dq_1 \dots dq_n \quad (112)$$

where $\phi(x)$ is the external field, $\tilde{\phi}(x) = \phi(x) - \mu$, and $W(q_1, \dots, q_n)$ is one provided that $q_1 < q_2 - d < q_3 - 2d \dots$ and zero otherwise. Functional differentiation with respect to the field gives an expression for the local density, $\rho(x)$. As shown in Appendix A it is possible to eliminate the field in favor of the density thus arriving at

$$\ln \Xi(\beta, \mu; [\rho]) = \int_{-\infty}^{\infty} \frac{\frac{1}{2}(\rho(r+d/2) + \rho(r-d/2))}{1 - \int_{-d/2}^{d/2} \rho(r+y)dy} dr \quad (113)$$

This result is not directly useful for DFT because the density that appears in it is the equilibrium density: The field has been eliminated so that this is the equivalent of Eq. 23. However, as in the simple examples of exact DFT from the previous section, the relation between the field and the density can be used together with the the Euler–Lagrange equation to get

$$\begin{aligned} \frac{\delta \beta F[\rho]}{\delta \rho(\mathbf{r})} &= -\beta \tilde{\phi}(r) \\ &= \ln \rho(r) - \frac{1}{2} \ln \left(1 - \int_{r-d}^r \rho(y) dy \right) - \frac{1}{2} \ln \left(1 - \int_r^{r+d} \rho(y) dy \right) \\ &\quad + \frac{1}{2} \int_{-r-d/2}^{r+d/2} \left(\frac{\rho(x+d/2) + \rho(x-d/2)}{1 - \int_{-d/2}^{d/2} \rho(x+y) dy} \right) dx \end{aligned} \quad (114)$$

Functional integration as described in the last section gives the final result

$$\beta F[\rho] = \beta F_{\text{id}}[\rho] - \int \frac{1}{2} (\rho(x+d/2) + \rho(x-d/2)) \ln \left(1 - \int_{-d/2}^{d/2} \rho(x+y) dy \right) dx \quad (115)$$

As shown below, this beautiful, exact result plays a fundamental role in the construction of FMT.

2. Generalization to Higher Dimensions

In fact, Percus and co-workers speculated on how this might be generalized to more than one dimension [71–73]. It has the form of an integral over a local excess free energy that clearly depends on two quantities: the density evaluated at the “surface” of a hard rod centered at position x , $\rho(x \pm d/2)$, and the density averaged over the “volume” of a hard rod centered at position x ; these concepts are easily generalized to more than one dimension as will be seen below. This suggests

writing it in the form

$$\beta F_{\text{ex}}[\rho] = - \int_{-\infty}^{\infty} s(r) \ln(1 - \eta(r)) dr \quad (116)$$

where

$$\begin{aligned} \eta(r) &= \int_{-\infty}^{\infty} w_{\eta}(r-y) \rho(y) dy \\ s(r) &= \int_{-\infty}^{\infty} w_s(r-y) \rho(y) dy \end{aligned} \quad (117)$$

and the weight functions are $w_{\eta}(x) = \Theta(\frac{d}{2} - |x|)$ and $w_s(x) = \delta(\frac{d}{2} - |x|)$, where $\Theta(x)$ is the step function equal to 1 for $x > 0$ and zero otherwise. The first of these weights restricts integration to the volume of one of the hard rods, while the second restricts integration to its ‘‘surface.’’ In this form, the extrapolation to higher dimensions is obvious. In the context of his work on SPT, Rosenfeld realized that another important property of these ‘‘fundamental measures’’ is that their convolution gives the Mayer function for hard spheres $\Theta(d - |x|)$. To see why this is important, let us denote these, and possibly other, linear density functionals collectively as $n_{\alpha}(r) = \int_{-\infty}^{\infty} w_{\alpha}(r-y) \rho(y) dy$ and imagine that the excess free energy can be written, by analogy to Eq. (116), as

$$\beta F_{\text{ex}}[\rho] = \int \Phi(\{n_{\alpha}(\mathbf{r})\}) d\mathbf{r} \quad (118)$$

for some algebraic function of the measures, Φ . Then it follows that the DCF should be

$$c_2(\mathbf{r}_1, \mathbf{r}_2; [\rho]) = - \frac{\delta^2 \beta F_{\text{ex}}[\rho]}{\delta \rho(\mathbf{r}_1) \delta \rho(\mathbf{r}_2)} = - \sum_{\alpha\gamma} \int \frac{\partial^2 \Phi}{\partial n_{\alpha}(\mathbf{r}) \partial n_{\gamma}(\mathbf{r})} w_{\alpha}(\mathbf{r} - \mathbf{r}_1) w_{\gamma}(\mathbf{r} - \mathbf{r}_2) d\mathbf{r} \quad (119)$$

and, at zero density, this must become the negative of the Mayer function. Thus, if the free energy can be written in this form, the convolution of the weights must give a step function.

B. Rosenfeld’s FMT

Rosenfeld begins by noting that in three dimensions, the step function can be written as a convolution using three basic functions: $w_i^{(3)}(\mathbf{r}) = \Theta(\frac{d}{2} - r)$, $w_i^{(2)}(\mathbf{r}) = \delta(\frac{d}{2} - r)$, and $w_i^{(1)}(\mathbf{r}) = \hat{\mathbf{r}} \delta(\frac{d}{2} - r)$, where $\hat{\mathbf{r}} = \mathbf{r}/r$ is the unit vector and the index i is to distinguish different species (i.e., particles with different hard-sphere diameters). Note that the spatial integral of $w^{(3)}$ is the volume of a sphere with diameter d , that of $w^{(2)}$ is its area. This suggests also defining $w_i^{(1)}(\mathbf{r}) = w_i^{(2)}(\mathbf{r})/4\pi(d/2)$ and $w_i^{(0)}(\mathbf{r}) = w_i^{(2)}(\mathbf{r})/4\pi(d/2)^2$, which integrate to

give the radius of the sphere and unity, respectively. They therefore constitute the set of “fundamental measures” of the sphere and are the origin of the name of the theory. Denoting a convolution between two functions $f(\mathbf{r})$ and $g(\mathbf{r})$ as

$$f \otimes g \equiv \int f(\mathbf{r}_1 - \mathbf{r})g(\mathbf{r} - \mathbf{r}_2)d\mathbf{r} \quad (120)$$

it is easy to confirm that

$$\Theta\left(\frac{d_i + d_j}{2} - r_{12}\right) = w_3^i \otimes w_0^j + w_0^i \otimes w_3^j + w_2^i \otimes w_1^j + w_1^i \otimes w_2^j - \mathbf{w}_2^i \otimes \mathbf{w}_1^j - \mathbf{w}_1^i \otimes \mathbf{w}_2^j \quad (121)$$

where the scalar product is also taken in the final two terms on the right and where $\mathbf{w}_i^{(1)}(\mathbf{r}) = w_i^{(2)}(\mathbf{r})/4\pi(d/2)$. The reason for introducing the somewhat redundant $w_i^{(0)}$ and $w_i^{(0)}$ is that in the uniform limit, the resulting density variables correspond to variables occurring in SPT. If the density distribution of species i is $\rho_i(\mathbf{r})$ then the fundamental densities are defined as

$$n_\alpha(\mathbf{r}) = \sum_i \int w_i^{(\alpha)}(\mathbf{r} - \mathbf{r}_1)\rho(\mathbf{r}_1)d\mathbf{r}_1 \quad (122)$$

Rosenfeld next makes the ansatz that the functional $F[n]$ has the form given in Eq. (118) above. Then, if the density satisfies the Euler–Lagrange equation for some field, then from Eq. (123) we obtain

$$\begin{aligned} \Omega &= F_{\text{ex}}[\rho] - \int \left(k_B T \rho(\mathbf{r}) + \frac{\delta F_{\text{ex}}[\rho]}{\delta \rho(\mathbf{r})} \right) d\mathbf{r} \\ &= -k_B T \int \left(\rho(\mathbf{r}) - \Phi(\{n_\alpha(\mathbf{r})\}) + \sum_\alpha \frac{\partial \Phi}{\partial n_\alpha(\mathbf{r})} n_\alpha(\mathbf{r}) \right) d\mathbf{r} \end{aligned} \quad (123)$$

Since the grand potential is just $\Omega = -PV$, in a uniform system with $\rho(\mathbf{r}) = \bar{\rho}$, one has that

$$\beta P = \bar{\rho} - \Phi(\{n_\alpha\}) + \sum_{\alpha,i} \frac{\partial \Phi}{\partial n_\alpha} n_\alpha \quad (124)$$

Another relation is obtained using the ideas of SPT. As explained in Roth et al. [74], the chemical potential for inserting a single spherical particle is equal to the work of insertion. This consists of work done against the fluid pressure, PV , work done due to surface tension, proportional to the area of the sphere, and subdominant terms due to the dependence of surface tension on the radius of curvature. Thus, in the limit that the sphere becomes infinitely large, the work

done divided by the volume of the sphere is equal to the pressure, P . Thus, since in the bulk we have

$$\beta\mu_{\text{ex}}^i = \frac{\partial\Phi}{\partial\rho^i} = \frac{\partial\Phi}{\partial n_0} + \frac{\partial\Phi}{\partial n_1} R_i + \frac{\partial\Phi}{\partial n_2} S_i + \frac{\partial\Phi}{\partial n_3} V_i \quad (125)$$

this reasoning implies that

$$\frac{\partial\Phi}{\partial n_3} = \beta P \quad (126)$$

Combining this and Eq. (124) gives

$$\frac{\partial\Phi}{\partial n_3} = n_0 - \Phi(\{n_\alpha\}) + \sum_\alpha \frac{\partial\Phi}{\partial n_\alpha} n_\alpha \quad (127)$$

The final assumption made is that the dependence of Φ on the fundamental densities can be determined by dimensional analysis. Specifically, it is assumed that since Φ has units of inverse volume, it must be of the form

$$\Phi = f_0(n_3)n_0 + f_1(n_3)n_1n_2 + f_2(n_3)n_2^3 + f_3(n_3)\mathbf{n}_1 \cdot \mathbf{n}_2 + f_4(n_3)n_2(\mathbf{n}_2 \cdot \mathbf{n}_2) \quad (128)$$

In a single-component system, combinations such as n_1n_2/n_0 could occur; however, in a multicomponent system, such terms would not allow a virial expansion in all of the partial densities and so are ruled out. Substituting into Eq. (127) and treating the densities as independent variables gives

$$\begin{aligned} f'_0(n_3) &= 1 + n_3f'_0(n_3) \\ f'_1(n_3) &= f_1(n_3) + n_3f'_1(n_3) \\ f'_2(n_3) &= 2f_2(n_3) + n_3f'_2(n_3) \\ f'_3(n_3) &= f_3(n_3) + n_3f'_3(n_3) \\ f'_4(n_3) &= 2f_4(n_3) + n_3f'_4(n_3) \end{aligned} \quad (129)$$

Solution of these equations with the resulting integration constants chosen to give the correct low-density behavior results in the density functional model of Rosenfeld [75, 76]:

$$\Phi = -n_0 \ln(1-n_3) + \frac{n_1n_2 - \mathbf{n}_1 \cdot \mathbf{n}_2}{1-n_3} + \frac{1}{24\pi} \frac{n_2^3 - 3n_2(\mathbf{n}_2 \cdot \mathbf{n}_2)}{(1-n_3)^2} \quad (130)$$

(Note that in fact, the vector density measures are zero in a uniform system so that the last two terms in Eq. (128) should not be included [74]. Therefore the result depends on assuming that Eq. (127) continues to hold in a slightly *inhomogeneous* system.)

For pure (single-species) systems, an alternative notation that is commonly used in the literature emphasizes the basis functions rather than the fundamental measures. One defines $w^{(\eta)}(\mathbf{r}) = \Theta(\frac{d}{2}-r)$, $w^{(s)}(\mathbf{r}) = \delta(\frac{d}{2}-r)$ and $\mathbf{w}^{(v)}(\mathbf{r}) = \hat{\mathbf{r}}\delta(\frac{d}{2}-r)$ and denotes the corresponding density measures as $\eta(\mathbf{r})$, $s(\mathbf{r})$ and $v(\mathbf{r})$, and the free energy density functional is written as

$$\Phi = \Phi_1 + \Phi_2 + \Phi_3 \quad (131)$$

with

$$\begin{aligned} \Phi_1 &= -\frac{1}{\pi d^2} s \ln(1-\eta) \\ \Phi_2 &= \frac{1}{2\pi d} \frac{s^2 - v^2}{(1-\eta)} \\ \Phi_3 &= \frac{1}{24\pi} \frac{s^3 - 3sv^2}{(1-\eta)^2} \end{aligned} \quad (132)$$

Rosenfeld's model possesses several remarkable properties. The leading term of the free energy density is proportional to the exact functional for one-dimensional hard spheres, which is at least intuitively satisfying. In the bulk liquid, the local density is a constant, $\bar{\rho}$, $\eta = \pi\bar{\rho}d^3/6$ is the usual packing fraction, $s = \pi\bar{\rho}d^2 = 6\eta/d$, and the vector density measures vanish. The resulting expression for the free energy density, which is then just the bulk free energy per unit volume, becomes

$$f_{\text{ex}}(\rho) = \Phi = \bar{\rho} \left(-\ln(1-\eta) + \frac{3}{2}\eta \frac{2-\eta}{(1-\eta)^2} \right) \quad (133)$$

which is recognized as the Percus–Yevick compressibility equation of state [21]; it is of course the same as Eq. (130) without the vector terms, which is the usual result of the simplest form of SPT [10–12]. Finally, evaluating the DCF from Eq. (119) gives

$$c(r; \bar{\rho}) = -\Theta(d-r) \left(\frac{(1+2\eta)^2}{(\eta-1)^4} - 6\eta \frac{(1+\frac{\eta}{2})^2}{(\eta-1)^4} \left(\frac{r}{d}\right) + \frac{\eta(1+2\eta)^2}{2(\eta-1)^4} \left(\frac{r}{d}\right)^3 \right) \quad (134)$$

which again agrees with the Percus–Yevick result. Thus, the Rosenfeld FMT has the property that, at least in the case of hard spheres, it is completely consistent with the Percus–Yevick hard-sphere theory. In many ways, this was, and remains, one of its most attractive features. In fact, an alternative derivation of this functional was given by Kierlik and Rosinberg [77] who, rather than introduce

the fundamental measure weights a priori, instead demanded that the SPT equation of state hold (that is, Eq. (130) without the vector terms) and asked what weights one would need in Eq. (122) to get the Percus–Yevick DCF. The resulting theory was subsequently shown to be mathematically identical to Rosenfeld’s [78].

C. Refinement of FMT

Despite the early successes, it was also recognized that the Rosenfeld FMT did not give an adequate description of hard-sphere statistical mechanics. The two most important issues had to do with the seemingly independent problems of the solid phase [75] and of the description of reduced dimension systems such as quasi-one-dimensional pores [79].

The calculation of the free energy of the solid phase within the Gaussian approximation requires knowledge of the local densities. From the explicit forms of the weights, it is easy to see that the local densities are related by

$$\begin{aligned} s(\mathbf{r}; d) &= 2 \frac{\partial}{\partial d} \eta(\mathbf{r}; d) \\ \mathbf{v}(\mathbf{r}; d) &= \nabla \eta(\mathbf{r}; d) \end{aligned} \quad (135)$$

so that once the local packing fraction is calculated, the other densities follow easily. Using the Gaussian model for the densities, straightforward calculation gives

$$\eta(\mathbf{r}) = (\bar{\rho}/\bar{\rho}_{\text{latt}}) \sum_{j=0}^{\infty} \tilde{\eta}(|\mathbf{r}-\mathbf{R}_j|) = \bar{\rho} \sum_{j=0}^{\infty} \exp(-i\mathbf{K}_j \cdot \mathbf{r}) \exp(-K_j^2/2\alpha) \tilde{\eta}(K_j) \quad (136)$$

where $\bar{\rho}$ is the average density, $\bar{\rho}_{\text{latt}}$ is the density of the lattice sites, the first sum is over lattice vectors, \mathbf{R}_j , and the second is over reciprocal lattice vectors, \mathbf{K}_j and

$$\begin{aligned} \tilde{\eta}(r) &= \frac{1}{2} \left(\operatorname{erf} \left(\sqrt{\alpha} \left(r + \frac{d}{2} \right) \right) - \operatorname{erf} \left(\sqrt{\alpha} \left(r - \frac{d}{2} \right) \right) \right) \\ &\quad - \frac{1}{2r} \sqrt{\frac{1}{\alpha d^2 \pi}} \left(\exp \left(-\alpha \left(r - \frac{d}{2} \right)^2 \right) - \exp \left(-\alpha \left(r + \frac{d}{2} \right)^2 \right) \right) \\ \tilde{\eta}(K) &= \frac{1}{6} \pi \bar{\rho} d^3 \left(j_0 \left(\frac{Kd}{2} \right) + j_2 \left(\frac{Kd}{2} \right) \right) \end{aligned} \quad (137)$$

The problem is that solids typically have rather large values of αd^2 (e.g., on the order of 100), and this causes the local packing fraction to be very close to one since (with $\bar{\rho}_{\text{latt}} = \bar{\rho}$)

$$\tilde{\eta}(0) = 1 - \frac{(\alpha d^2)^{1/2}}{\sqrt{\pi}} \exp\left(-\frac{1}{4}\alpha d^2\right) + \dots \quad (138)$$

leading to possibly large contributions to the free energy since Φ diverges for $\eta = 1$. However, at these points it is also the case that

$$\tilde{s}(0) = \frac{1}{d\sqrt{\pi}} (\alpha d^2)^{3/2} e^{-\frac{1}{4}\alpha d^2} \quad (139)$$

so that the interplay between the various terms must be examined carefully. This was done by Rosenfeld et al. [80], who noted that the Φ_2 contribution to the free energy density did not destabilize the solid because of a cancelation in the numerator between the s^2 and v^2 terms. However, no such cancelation occurs in the Φ_3 term, so the model diverges for highly localized densities. This suggested modifying Φ_3 in such a way that a similar cancelation occurred while at the same time retaining the exact connection to the Percus–Yevick distribution function. They proposed using an expression of the form

$$\Phi_3 = \frac{1}{24\pi} \frac{s^3}{(1-\eta)^2} f(\xi) \quad (140)$$

where $\xi^2 = v^2/s^2$. Setting $f(\xi) = 1 - 3\xi^2$ corresponds to the original Rosenfeld functional while $f(\xi) = (1 - \xi^2)^3$ has all of the desired properties. Another possible choice is $f(\xi) = 1 - 3\xi^2 + 2\xi^3$. The first modification will be referred to as the RSLT theory, while the second will be called the RSLT2 theory. Both of these modifications stabilize the solid without affecting the properties of the bulk fluid.

D. Dimensional Reduction and the Tarazona Functional

The divergences that occur in the solid are due to the contributions of density distributions that are highly localized at the lattice sites. This eventually led Rosenfeld, Tarazona, and others to study in detail the description of quasi-zero-dimensional systems. The end result was a new approach to the derivation of FMT which points the way to eliminating the divergences that prevent application to the solid phase.

Suppose a field is used which is infinite everywhere except for a cavity, centered at the origin, that is infinitesimally larger than a hard sphere. The average density distribution must therefore be $\rho(\mathbf{r}) = N\delta(\mathbf{r})$, where $0 < N < 1$ is the average occupancy. Consider the first contribution to the Rosenfeld

functional written as

$$F_1 = - \int d\mathbf{r} \psi_1(\eta(\mathbf{r})) \int ds \rho(\mathbf{r} + \mathbf{s}) w_D(s) \quad (141)$$

where $\psi_1(\eta) = \ln(1-\eta)$, $w_D(s) = S_D^{-1}(d) \delta(\frac{d}{2}-s)$, and $S_D(d)$ is the area of the D -sphere with diameter d . Noting that

$$\eta(\mathbf{r}) = \int_{-\infty}^{\infty} \Theta\left(\frac{d}{2} - |\mathbf{r}-\mathbf{r}'|\right) \rho(\mathbf{r}') d\mathbf{r}' = N\Theta\left(\frac{d}{2} - r\right) \quad (142)$$

and using $\delta(d/2 - x) = 2 \frac{\partial}{\partial d} \Theta(d/2 - x)$, one finds

$$F_1 = -S_D^{-1} \int d\mathbf{r} \psi_1(\eta(\mathbf{r})) N \delta\left(s - \frac{d}{2}\right) = S_D^{-1} \frac{\partial}{\partial(d/2)} \int \Phi_0(\eta(\mathbf{r})) d\mathbf{r} \quad (143)$$

where $\Phi_0(\eta)$ is the exact zero- d functional,

$$\Phi_0(\eta) = (1 - \eta) \ln(1 - \eta) - (1 - \eta) \quad (144)$$

Notice that for $r < d/2$, we have $\eta = N$, while for $r > d/2$ we have $\eta = 0$, and so $\Phi_0(\eta) = 0$. Thus, the integral gives

$$F_1 = S_D^{-1} \frac{\partial}{\partial(d/2)} V_D(d) \Phi_0(N) = \Phi_0(N)$$

which agrees with the exact result, Eq. (37).

Consider next the distribution for a cavity that is the union of two such quasi-zero-dimensional cavities. If the centers are closer than the hard-sphere diameter (so that the two cavities overlap), the combined cavity can still only hold one hard sphere at a time and the exact result is again given by Eq. (37). If one of the cavities is centered at the origin and the other is centered on \mathbf{R} , then the density will be $\rho(\mathbf{r}) = N_1 \delta(\mathbf{r}) + N_2 \delta(\mathbf{r}-\mathbf{R})$ and we again find

$$F_1 = -S_D^{-1} \frac{\partial}{\partial(d/2)} \int \Phi_0(\eta(\mathbf{r})) d\mathbf{r} \quad (145)$$

Define the region V_1 to be all points such that $r < d/2$ and V_2 to be all points such that $|\mathbf{r}-\mathbf{R}| < d/2$. Let their intersection be $V_{12} = V_1 \cap V_2$ and let $|V_i|$ be the volume of V_i . Then, $\eta(\mathbf{r})$ is N_1 in $V_1 - V_{12}$ (i.e., in V_1 but excluding V_{12}) and N_2 in $V_2 - V_{12}$ and $N = N_1 + N_2$ in V_{12} so

$$\int \Phi_0(\eta(\mathbf{r})) d\mathbf{r} = |V_1 - V_{12}| \Phi_0(N_1) + |V_2 - V_{12}| \Phi_0(N_2) + |V_{12}| \Phi_0(N) \quad (146)$$

Now, specializing to three dimensions, $|V_1| = |V_2| = \frac{4\pi}{3} \left(\frac{d}{2}\right)^3$ while we note for later use that the volume of intersection of two spheres with diameters d_1 and d_2 is

$$|V_{12}| = \frac{\pi}{12} \left(R(d_1 + d_2 + R) - \frac{3}{4}(d_1 - d_2)^2 \right) \frac{(d_1 + d_2 - 2R)^2}{4R} \quad (147)$$

so $|V_{12}| = \frac{1}{12} \pi (2d + R)(R - d)^2$. Hence

$$F_1 = \Phi_0(N) - \frac{R}{d} (\Phi_0(N) - \Phi_0(N_1) - \Phi_0(N_2)) \quad (148)$$

This differs from the exact result due to the term proportional to R . Tarazona and Rosenfeld suggest that the natural way to correct the functional is to introduce a correction to Φ_1 involving two-body contributions. Generalizing the expression for Φ_1 , they propose that the correction be written as

$$F_2 = - \int d\mathbf{r} \psi(\boldsymbol{\eta}(\mathbf{r})) \int d\mathbf{s}_1 d\mathbf{s}_2 \rho(\mathbf{r} + \mathbf{s}_1) w(s_1) \rho(\mathbf{r} + \mathbf{s}_2) w(s_2) P(\mathbf{s}_1, \mathbf{s}_2) \quad (149)$$

A simple calculation, given in Appendix B, gives

$$\begin{aligned} F_2 &= 4\pi \frac{d}{2} \left(\frac{1}{4\pi(d/2)^2} \right)^2 \int d\mathbf{r} \psi''_0(\boldsymbol{\eta}(\mathbf{r})) \\ &\quad \times \int d\mathbf{s}_1 d\mathbf{s}_2 \rho(\mathbf{r} + \mathbf{s}_1) w(s_1) \rho(\mathbf{r} + \mathbf{s}_2) w(s_2) \left(\frac{d^2}{4} - \mathbf{s}_1 \cdot \mathbf{s}_2 \right) \\ &= \frac{1}{2\pi d} \int d\mathbf{r} \psi''_0(\boldsymbol{\eta}(\mathbf{r})) (s^2(\mathbf{r}) - v^2(\mathbf{r})) \end{aligned} \quad (150)$$

which is the same as the second contribution to the Rosenfeld functional.

So far, this exercise has just resulted in a somewhat different derivation of the Rosenfeld functional. Tarazona and Rosenfeld went on to consider the contributions of cavities formed by the intersection of three spherical cavities. They showed that the combination $\Phi_1 + \Phi_2$ does not give the correct result and thus motivates the inclusion of a three-body term, Φ_3 . They discussed its properties, but an explicit form was only given later by Tarazona [83]. The result is expressed in terms of a tensor density measure,

$$T_{ij}(\mathbf{r}_1) = \int \rho(\mathbf{r}_2) \frac{r_{12,i} r_{12,j}}{r_{12}^2} \delta\left(\frac{d}{2} - r_{12}\right) dr_2 \quad (151)$$

as

$$\Phi_3 = \frac{3}{16\pi(1-\eta)^2} (\mathbf{v} \cdot \mathbf{T} \cdot \mathbf{v} - s v^2 - \text{Tr}(\mathbf{T}^3) + s \text{Tr}(\mathbf{T}^2)) \quad (152)$$

where $\text{Tr}(\mathbf{A})$ indicates the trace of the tensor \mathbf{A} . Following Roth et al. [74], this can also be written in a more revealing form by separating the tensor into its trace and trace-less parts as

$$\begin{aligned} T_{ij}(\mathbf{r}_1) &= \frac{1}{3} s(\mathbf{r}_1) \delta_{ij} + U_{ij}(\mathbf{r}_1) \\ U_{ij}(\mathbf{r}_1) &= \int \rho(\mathbf{r}_2) \left(\frac{r_{12,i} r_{12,j}}{r_{12}^2} - \delta_{ij} \right) \delta \left(\frac{d}{2} - r_{12} \right) dr_2 \end{aligned} \quad (153)$$

in terms of which the functional becomes

$$\Phi_3 = \frac{1}{24\pi(1-\eta)^2} \left(s^3 - 3s v^2 + \frac{9}{2} (\mathbf{v} \cdot \mathbf{U} \cdot \mathbf{v} - \text{Tr}(U^3)) \right) \quad (154)$$

This is a more natural representation in the sense that in a uniform liquid, both \mathbf{v} and \mathbf{U} vanish. It is also interesting because connections can be made to some of the earlier models mentioned above. Obviously, taking $U = 0$ gives the original Rosenfeld functional. One might imagine trying to approximate the tensor using the simpler densities as, for example,

$$U_{ij} \sim A \frac{v_i v_j - \frac{1}{3} v^2 \delta_{ij}}{s} \quad (155)$$

where the prefactor is undetermined and the constraint on forming the right-hand side is that it must be a traceless tensor that scales linearly with the density. Putting this into Φ_3 gives

$$\Phi_3 \sim \frac{s^3}{24\pi(1-\eta)^2} (1 - 3\xi^2 + 3A\xi^4 - A^3\xi^6) \quad (156)$$

Taking $A = 1$, the term in brackets becomes $(1 - \xi^2)^3$, which is the same as the empirical model proposed by Rosenfeld et al. [80]. Tarazona has observed that Eq. 152 could also be guessed by postulating the need for a tensor density, constructing the lowest-order expression that vanishes in one dimension and that agrees with the first two orders of the virial expansion of the DCF in three dimensions, and guessing the prefactor $(1 - \eta)^{-2}$ based on an analogy with the first two parts of the free energy [82].

The Tarazona functional has several significant properties in regard to the solid phase [83]. First, and perhaps most importantly, it stabilizes the solid phase and makes a reasonable prediction for liquid–solid coexistence (see Table II).

TABLE II
Comparison of the Predictions of Various FMT DFTs for the Freezing of Hard Spheres to Data from Simulation^a

Theory	EOS	$\bar{\eta}_{\text{liq}}$	$\bar{\eta}_{\text{sol}}$	P^*	L
RSLT ^b	PY	0.491	0.540	12.3	1.06
Tarazona ^c	PY	0.467	0.516	9.93	0.145
White Bear ^{c,d}	CS	0.489	0.536	11.3	0.132
MC ^e	—	0.494	0.545	11.7	0.126

^aGiven are the liquid, $\bar{\eta}_{\text{liq}}$, and solid, $\bar{\eta}_{\text{sol}}$, packing fractions, the reduced pressure $P^* = \beta P d^3$ and the Lindemann parameter, L , at bulk coexistence. For each theory, the equation of state used for the fluid, Percus–Yevick(PY) or Carnahan–Starling (CS), is indicated. The Lindemann ratio for all three theories, calculated in the Gaussian approximation, is taken from Ref. 81.

^bFrom Rosenfeld et al. [80].

^cFrom Tarazona [82].

^dFrom Roth et al. [74].

^eFrom Hoover and Ree [57].

In fact, the description of the solid is rather good and it is the fact that the uniform liquid is described by the Percus–Yevick equation of state that is responsible for the difference from simulation. Tarazona also showed that the Lindemann parameter (i.e., the width of the Gaussians) is in good agreement with simulation at all densities and, in particular, that it vanishes as the density of the solid approaches close packing. Of the older, liquid-based DFTs, only the GELA had shown similar behavior and then only for the FCC phase. One of the virtues of FMT is that it contains enough geometrical information about hard spheres to show the expected divergences at close-packing. Groh and Mulder investigated the description of the solid phase without making the Gaussian approximation [28]. Their results confirm the improvement of the Tarazona model over earlier versions of FMT and also support the accuracy of the Gaussian approximation.

In a subsequent investigation of hard-sphere mixtures, Cuesta et al. related the ability of the FMT model to accurately describe these quasi-zero-dimensional systems to the low-density expansion of the three-body direct correlation function [84]. They showed that to describe mixtures, a third-order tensor density measure must also be introduced. However, the theory is subject to instabilities leading to the possibility of infinitely negative free energies thus leaving its status in doubt. Their conclusion is that the natural extension of the Tarazona functional, Eq. (152), is preferable even though it is not formally as accurate as the more complex form.

E. The White-Bear Functional

One of the nice features of the various forms of FMT so far described is that the second functional derivative of the free energy functional with respect to density gives the Percus–Yevick DCF. However, this necessarily implies that the equation

of state for the uniform fluid is the Percus–Yevick equation of state which is known to be inaccurate at moderate to high densities. There have therefore been several attempts to build in a more accurate equation of state. Roth, Evans, Lang, and Kahl proposed what is known as the “white-bear” functional based on a modified version of Rosenfeld’s original derivation of FMT for mixtures [74] and a similar proposal for the monotonic system was made by Tarazona [82]. Recall that Eq. (124) above relates the pressure to the FMT ansatz and that Rosenfeld then goes on to eliminate the pressure using relations from SPT. Roth et al instead simply insert an empirical expression for the pressure written in terms of the density measures. The particular expression they use is the Mansoori–Carnahan–Starling–Leland (MCSL) expression which is a generalization of the Carnahan–Starling equation of state to mixtures [85]. The result is

$$\Phi_3 = \frac{s^3 - 3sv^2}{36\pi\eta^2(1-\eta)^2} \left(\eta + (1-\eta)^2 \ln(1-\eta) \right) \quad (157)$$

They go on to propose that the factor $s^3 - 3sv^2$ be replaced by the expression occurring in Tarazona’s functional to give the final white-bear functional,

$$\Phi_3 = \frac{s^3 - 3sv^2 + \frac{9}{2}(\mathbf{v} \cdot \mathbf{U} \cdot \mathbf{v} - \text{Tr}(U^3))}{36\pi\eta^2(1-\eta)^2} \left(\eta + (1-\eta)^2 \ln(1-\eta) \right) \quad (158)$$

Just as the uniform fluid is now described by the MCSL equation of state, this functional does not reproduce the Percus–Yevick DCF. A simple calculation gives the Percus–Yevick form,

$$c(r; d) = \left(a_0 + a_1 \frac{r}{d} + a_3 \left(\frac{r}{d} \right)^3 \right) \Theta(d-r) \quad (159)$$

but with coefficients,

$$\begin{aligned} a_0 &= -\frac{1 + 4\eta + 3\eta^2 - 2\eta^3}{(1-\eta)^4} \\ a_1 &= \frac{2 - \eta + 14\eta^2 - 6\eta^3}{(1-\eta)^4} + \frac{2 \ln(1-\eta)}{\eta} \\ a_3 &= \frac{-3 + 10\eta - 15\eta^2 + 5\eta^3}{(1-\eta)^4} - \frac{3 \ln(1-\eta)}{\eta} \end{aligned} \quad (160)$$

When compared to computer simulation, this expression is shown to be more accurate, compared to simulations, than the Percus–Yevick approximation [74]. Roth et al also show some small improvement over the Rosenfeld functional in the description of a fluid near a wall. A notable success is in giving much better values

for liquid–solid coexistence than in the original theory of Tarazona (see Table II) due to the improved equation of state for the uniform liquid.

F. Calculating the Densities

In applications, one often needs to evaluate the density measures for particular parameterizations of the density (e.g., the Gaussian model of the solid) and/or for densities with particular symmetries (planar, spherical, . . .). The tensor density measures in particular appear complex, but their evaluation is not difficult when performed using a generating function. Consider in particular the functional

$$\tau(\mathbf{r}_1) = \frac{1}{2} \int d\mathbf{r}_2 \rho(\mathbf{r}_2) \left(\left(\frac{d}{2} \right)^2 - r_{12}^2 \right) \Theta \left(\frac{d}{2} - r_{12} \right) \quad (161)$$

It is easy to see that from this single scalar, all of the density measures up to the second-rank tensor follow:

$$\begin{aligned} \eta(\mathbf{r}) &= \frac{4}{d} \frac{\partial}{\partial d} \tau(\mathbf{r}) \\ s(\mathbf{r}) &= 2 \frac{\partial}{\partial d} \eta(\mathbf{r}) \\ v_i(\mathbf{r}) &= -\partial_i \eta(\mathbf{r}) \\ T_{ij}(\mathbf{r}) &= \frac{2}{d} \eta(\mathbf{r}) \delta_{ij} + \frac{2}{d} \partial_i \partial_j \tau(\mathbf{r}) \end{aligned} \quad (162)$$

Generating functionals that give all of these as well as even higher-order densities can be constructed by including additional factors of $\left(\frac{d}{2}\right) - r_{12}$ in the integral. In a planar geometry for which $\rho(\mathbf{r}) = \rho(z)$, one has

$$\tau(z) = \frac{\pi}{64} \int_{-d/2}^{d/2} \rho(z_1 + z) (d - 2z_1)^2 (d + 2z_1)^2 dz_1 \quad (163)$$

while in a spherical geometry, $\rho(\mathbf{r}) = \rho(r)$ and

$$\begin{aligned} \tau(r) &= \frac{\pi}{4} \Theta \left(r - \frac{d}{2} \right) \frac{1}{r} \int_{-d/2}^{d/2} \rho(r_1 + r) \left(\left(\frac{d}{2} \right)^2 - r_1^2 \right)^2 (r_1 + r) dr_1 \\ &+ \frac{\pi}{4} \Theta \left(\frac{d}{2} - r \right) \frac{1}{r} \int_{d/2-2r}^{d/2} \rho(r_1 + r) \left(\left(\frac{d}{2} \right)^2 - r_1^2 \right)^2 (r_1 + r) dr_1 \\ &+ 2\pi \Theta \left(\frac{d}{2} - r \right) \int_0^{d/2-r} \rho(r_1) \left(\left(\frac{d}{2} \right)^2 - r_1^2 - r^2 \right) r_1^2 dr_1 \end{aligned} \quad (164)$$

Finally, the Gaussian parameterization of the solid phase gives

$$\tau(\mathbf{r}_1) = x \sum_n \hat{\tau}(\mathbf{r}_1 - \mathbf{R}_n) \quad (165)$$

with

$$\begin{aligned} \hat{\tau}(\mathbf{r}_1) &= \frac{1}{2} \left(\frac{\alpha}{\pi} \right)^{3/2} \int dr_2 \exp(-\alpha r_2^2) \left(\left(\frac{d}{2} \right)^2 - r_{12}^2 \right) \Theta \left(\frac{d}{2} - r_{12} \right) \\ &= - \frac{x}{16\sqrt{\pi}\alpha^{3/2}r_1} \left(\begin{array}{c} 2(2-\alpha r_1 d + 2\alpha r_1^2) \exp\left(-\alpha \left(r_1 + \frac{d}{2}\right)^2\right) \\ -2(2+\alpha r_1 d + 2\alpha r_1^2) \exp\left(-\alpha \left(r_1 - \frac{d}{2}\right)^2\right) \\ + \sqrt{\alpha} r_1 (6-\alpha d^2 + 4\alpha r_1^2) \sqrt{\pi} \left(\operatorname{erf}\left(\sqrt{\alpha} \left(r_1 + \frac{d}{2}\right)\right) \right) \\ - \operatorname{erf}\left(\sqrt{\alpha} \left(r_1 - \frac{d}{2}\right)\right) \end{array} \right) \end{aligned} \quad (166)$$

The representation in reciprocal space is much simpler:

$$\tau(\mathbf{r}) = x\bar{\rho} \sum_n \exp(i\mathbf{K}_n \cdot \mathbf{r}) \exp(-K_n^2/4\alpha) \tilde{\tau}(\mathbf{K}_n) \quad (167)$$

with

$$\begin{aligned} \tilde{\tau}(\mathbf{K}) &= -\pi \frac{d^2 K^2 \sin \frac{1}{2} Kd - 12 \sin \frac{1}{2} Kd + 6Kd \cos \frac{1}{2} Kd}{K^5} \\ &= \left(\frac{d}{2} \right)^5 \frac{4\pi}{105} \left(7j_0 \left(\frac{Kd}{2} \right) + 10j_2 \left(\frac{Kd}{2} \right) + 3j_4 \left(\frac{Kd}{2} \right) \right) \end{aligned} \quad (168)$$

where $j_n(x)$ is the n th-order spherical Bessel function.

G. Further Developments and Open Questions

The main virtues of FMT are (a) its internal consistency in that it does not require one DCF as input and imply another via the functional derivative of the model free energy functional and (b) its agreement with exact results in one and quasi-zero

dimensions. The first property is shared by the MWDA and WDA effective liquid theories, but the second is particular to FMT.

Fundamental Measure Theory has been successfully used in a number of problems. In his original paper, Rosenfeld showed that it makes reasonable predictions for the three-body DCF [75]. Kierlik and Rosinberg found good results using the theory, together with a mean-field treatment of the long-ranged part of the potential, to describe adsorption of Lennard-Jones atoms at a wall [77, 79]. As discussed by Roth et al. [74], Rosenfeld's original FMT also gives a good description of hard spheres near a hard wall, and the white-bear functional is even better. Warshavsky and Song performed a remarkably difficult calculation of the free energy of the hard-sphere liquid–solid interface using FMT and found good results for the surface tension [86]. Similar results were found by Lutsko using a gradient theory constructed from FMT [87]. As discussed in the following section, FMT is widely used to model the short-ranged repulsion typical of simple fluids.

Despite its successes, there are still obstacles in the description of the solid phase in FMT. One problem is the development of multiple metastable solid states. Recall that in the Gaussian approximation, the value of the width of the Gaussians is determined by minimizing the free energy. Normally, one expects to find two minima: one at infinite width corresponding to the uniform liquid and one at some finite width corresponding to the solid. As shown by Lutsko [81], at high densities, the RSLT theory gives two nonzero minima for the FCC solid which, if taken seriously, would mean that there was a metastable solid phase. More seriously, the RSLT, Tarazona, and white-bear functionals all show two BCC solids for some density ranges, with the anomaly affecting the smallest range of densities in the case of the white-bear functional. Furthermore, while in all three theories one of the branches does show the correct vanishing of the Lindemann parameter at high densities, its behavior at intermediate densities is not monotonic, which is unphysical and not so different from what is found with the liquid-based theories. In fact, the only one of the three theories for which the *stable* branch of the free energy curve shows a vanishing Lindemann parameter is the Tarazona theory. The result is that the theory giving the best description of FCC melting (the white-bear) gives an unphysical picture of the BCC solid while the one giving the best description of the BCC phase (the Tarazona theory) gives a poor description of FCC melting and unphysical behavior for the BCC phase at intermediate densities.

Finally, it should be noted that various attempts have been made to extend FMT to other hard-core objects. Rosenfeld [88] has attempted to generalize the theory to hard, convex but nonspherical bodies while Cuesta and co-workers have constructed FMTs for parallel hard cubes [89, 90], hard-core lattice gases [91] and parallel hard cylinders [92]. Because these cases are all either very technical or somewhat artificial, the reader is referred to the literature for further details.

V. BEYOND HARD SPHERES

Fundamental Measure Theory gives a reasonable approximation to the DFT for hard spheres. Especially satisfying is the fact that it is constructed to agree with the exact DFT in several limiting cases and that it is closely related to the well-known Percus–Yevick theory (and SPT) in three dimensions. It is therefore natural to wonder whether the approach can be extended beyond hard objects. Rosenfeld’s original development of FMT was closely tied to the geometry of hard spheres, and the later developments were intimately related to low-dimensional exact solutions that do not exist for long-ranged potentials. Thus the attempts that have been made are necessarily somewhat heuristic and, in fact, have met with mixed success [93, 94]. It is therefore the case that most applications to realistic potentials have relied on a separation of the contributions to the free energy into a hard-core contribution, modeled by FMT or one of the earlier DFTs for hard spheres, and a contribution due to the long-ranged interaction which is usually handled in a mean-field approximation. In this section, I discuss the basic construction of these models and give several illustrative examples of their application in practice.

It is important to specify what type of material is to be modeled. The primary distinction is between entities that interact via a potential with a strong short-ranged repulsion (such as simple liquids, colloids, proteins, . . .) and soft matter, for which the interaction involves a weak short-ranged repulsion (such as some polymers). Indeed, in the extreme case that interparticle interaction is very *softly* repulsive (i.e., not divergent as $r \rightarrow 0$) and decays to zero at large distances, Likos et al. have shown that the Random Phase Approximation, $c(r) \sim -\beta v(r)$, is nearly exact at high densities [95]. A good quality, density-independent DCF allows for the construction of the free energy functional without further approximation. Thus, attention here will be focused on the first case of a strong repulsion for which such useful results are not available.

The underlying idea is that the DFT free energy functional is written as

$$F[\rho] = F_{id}[\rho] + F_{HS}([\rho]; d) + F_l[\rho] \quad (169)$$

where the first term on the right is the (exact) ideal-gas contribution, the second is the hard-sphere contribution (which depends on some hard-sphere diameter, d , which must be specified) and the last contribution accounts for the long-ranged interactions. This is motivated by the fact that the Mayer function for potentials with a strong short-ranged potential is quite similar to that for hard spheres, thus suggesting that the statistical mechanics of the latter might be viewed as “hard-spheres plus a correction.” Furthermore, the analogy to thermodynamic perturbation theory is obvious. Since the basic physical intuition of separating the contributions into one modeled as a hard-core and a mean-field treatment of the attractive part is the same as that underlying the van der Waals equation of state, I will refer to these as van der Waals models (VdW) models. They are also often

referred to in the literature as “mean-field models,” although this is somewhat misleading because the different terms are actually treated at different levels of approximation. The two elements that remain to be specified are the hard-sphere diameter and the form of the long-ranged (or “tail”) contribution.

An important concept is the division of the pair interaction potential, $v(r)$, into a short-ranged repulsive part, $v_0(r)$, and a long-ranged, attractive tail, $w(r)$. Taking the Lennard-Jones potential as an illustrative example,

$$v_{\text{LJ}}(r) = 4\epsilon \left(\left(\frac{\sigma}{r} \right)^{12} - \left(\frac{\sigma}{r} \right)^6 \right) \quad (170)$$

there are two widely used choices which are taken from thermodynamic perturbation theory. The first is the Barker–Henderson (BH) division [21, 96],

$$\begin{aligned} v_0^{(\text{BH})}(r) &= v_{\text{LJ}}(r)\Theta(r_0-r) \\ w^{(\text{BH})}(r) &= v_{\text{LJ}}(r)\Theta(r-r_0) \end{aligned} \quad (171)$$

where the division is made at the point at which the potential is equal to zero, $v_{\text{LJ}}(r_0) = 0$, giving $r_0 = \sigma$. The second is that used in the Weeks–Chandler–Anderson (WCA) theory [27, 97–99]

$$\begin{aligned} v_0^{(\text{WCA})}(r) &= (v_{\text{LJ}}(r) - v_{\text{LJ}}(r_m))\Theta(r_m - r) \\ w^{(\text{WCA})}(r) &= v_{\text{LJ}}(r_m)\Theta(r_m - r) + v_{\text{LJ}}(r)\Theta(r - r_m) \end{aligned} \quad (172)$$

where the division is made at the minimum of the potential, $v'_{\text{LJ}}(r_m) = 0$, giving $r_m = 2^{1/6}\sigma$. The effective hard-sphere diameter is calculated using the $v_0(r)$ contribution. In the BH theory, it is given as

$$d_{\text{BH}}(T) = \int_0^{r_0} (1 - \exp(-\beta v_0(r))) dr \quad (173)$$

which is chosen so as to optimize the representation of the short-ranged part of the potential by a hard-sphere interaction (see, e.g., the discussion in Ref. 21). Many other definitions occur in the literature on thermodynamic perturbation theory including that of the WCA theory [21, 97–99], the Lado theory [100] and the Mansoori–Canfield–Rasaiah–Stell theory [85]. While superior for use in thermodynamic perturbation theory in some situations (particularly at high density), these give density-dependent diameters and involve the PDF for hard spheres, both of which are problematic for DFT. A density-dependent diameter complicates the DFT because it adds an additional density dependence to the (already complicated) functionals. The need for the PDF is not too burdensome for liquids, but is more problematic for the solid phase (although there are available empirical [35, 101] and DFT-based [102–104] models) and is very difficult for interfacial problems

involving, for example, transitions from liquid to solid. For these reasons, it is simpler to use the density-independent BH hard-sphere diameter or to use a diameter calculated for the bulk liquid. Other viable options would be the density-independent diameter obtained by matching the second virial coefficient of the hard-sphere and short-ranged interactions as used by Paricaud [105].

A. Treatment of the Tail Contribution: Perturbative Theories

Returning to the exact formalism described in Section II.C, it is clear that the excess free energy functional is linear in the DCF. An exact separation into “short-ranged” and “long-ranged” contributions can therefore be made starting with the exact DCF by writing

$$c_2(\mathbf{r}_1, \mathbf{r}_2; [\rho]) = c_2^{\text{HS}}(\mathbf{r}_1, \mathbf{r}_2; d, [\rho]) + \Delta c_2(\mathbf{r}_1, \mathbf{r}_2; d, [\rho]) \quad (174)$$

where the first term on the right is the exact DCF for hard spheres and the second term is defined by this expression. The excess free energy functional given in Eq. (44) will then also be a sum of a hard-sphere contribution and a part primarily related to long-ranged interactions,

$$\begin{aligned} \frac{1}{V}\beta F[\rho] &= \beta F^{\text{HS}}(d, [\rho]) + \Delta\beta f_{\text{ex}}(\bar{\rho}_0; d) + \frac{\partial\Delta\beta f_{\text{ex}}(\bar{\rho}_0; d)}{\partial\bar{\rho}_0}(\bar{\rho} - \bar{\rho}_0) \\ &\quad - \frac{1}{V}\int_0^1 d\lambda \int_0^\lambda d\lambda' \int d\mathbf{r}_1 d\mathbf{r}_2 \Delta c_2(\mathbf{r}_1, \mathbf{r}_2; d, [(1-\lambda')\rho_0 + \lambda'\rho]) \\ &\quad \times (\rho(\mathbf{r}_1) - \bar{\rho})(\rho(\mathbf{r}_2) - \bar{\rho}) \end{aligned} \quad (175)$$

where “ Δ ” always refers to the difference between the exact quantity and the corresponding hard-sphere quantity. The hard-sphere and long-ranged contributions can be handled differently. For the hard-sphere part, it is natural to use the FMT functional. For the remainder, all of the liquid-based theories discussed above remain viable options. However, since models like the MWDA, SCELA, and GELA work best for hard spheres and become less reliable as one moves to softer potentials, there is little incentive to use them for the long-ranged contribution. That leaves something like the simple perturbative theory of Ramakrishnan and Yussouff, Eq. (72), as the only viable option. Taking the reference state to be the uniform liquid and truncating at lowest order gives

$$\begin{aligned} \frac{1}{V}\beta F[\rho] &= \beta F^{\text{HS}}(d, [\rho]) + \Delta\beta f_{\text{ex}}(\bar{\rho}_0; d) + \frac{\partial\Delta\beta f_{\text{ex}}(\bar{\rho}_0; d)}{\partial\bar{\rho}_0}(\bar{\rho} - \bar{\rho}_0) \\ &\quad - \frac{1}{2V}\int d\mathbf{r}_1 d\mathbf{r}_2 \Delta c_2(r_{12}; \bar{\rho}_0, d)(\rho(\mathbf{r}_1) - \bar{\rho}_0)(\rho(\mathbf{r}_2) - \bar{\rho}_0) \end{aligned} \quad (176)$$

which is an expression employed by Rosenfeld [106] using a DCF calculated from the MHNC and by Tang [107] using his first order mean spherical approximation.

For the case of a uniform solid or for a fluid near a wall, an obvious choice for the reference state exists (the average density of the solid and the bulk density of the fluid, respectively). However, this cannot be a “universal” functional because it obviously fails if the target state, $\rho(\mathbf{r}_1)$, is a uniform liquid with a different density than the reference state. This problem could be fixed if one kept the integration over density space and used, for example,

$$\begin{aligned} \frac{1}{V}\beta F[\rho] &= \beta F^{\text{HS}}(d, [\rho]) + \Delta\beta f_{\text{ex}}(\bar{\rho}_0; d) + \frac{\partial\Delta\beta f_{\text{ex}}(\bar{\rho}_0; d)}{\partial\rho_0}(\bar{\rho} - \bar{\rho}_0) \\ &\quad - \frac{1}{V} \int_0^1 d\lambda \int_0^\lambda d\lambda' \int d\mathbf{r}_1 d\mathbf{r}_2 \Delta c_2(r_{12}; d, (1-\lambda')\rho_0 + \lambda'\bar{\rho}) \\ &\quad \times (\rho(\mathbf{r}_1) - \bar{\rho}_0)(\rho(\mathbf{r}_2) - \bar{\rho}_0) \end{aligned} \quad (177)$$

which now gives the correct result when $\rho(\mathbf{r}) = \bar{\rho}$ for all values of the reference state. I am not aware of this having been used in practice. In fact, despite solving the problem of the uniform-liquid limit, this expression is still not satisfactory. Using the average bulk density for the reference density is reasonable in the examples given above, but for a problem such as the planar liquid–vapor interface, it makes little sense.

All of this suggest the use of a position-dependent reference density. The various models discussed in Section III.B.2 a can be used to construct local density approximations to the tail contribution. Some of these have been discussed in Ref. [42], where they were shown to give reasonable results for the description of liquid–vapor interfaces. However, the complexity of these models together with the fact that they are inconsistent in the sense discussed in Section III.B.1. e has led to other approaches being adopted.

B. Approaches Based on PDF

Once the free energy is broken into a hard-sphere contribution and the contribution due to the attractive part of the potential, it is natural to note the similarity to liquid-state perturbation theory where one has, at first order,

$$F(\rho; T) = F_{\text{hs}}(\rho d^3; T) + \frac{1}{2} \int w(r_{12}) g_{\text{hs}}(r_{12}; d, T, \rho) d\mathbf{r}_1 d\mathbf{r}_2 \quad (178)$$

The idea is to use the last term on the right as a model for the treatment of the tail. Just as in the case of the DCF-based models, the problem is how to generalize this for an inhomogeneous system. Various proposals have been made such as that of Sokolowski and Fischer [108],

$$\Delta F[\rho] = \frac{1}{2} \int w(r_{12}) \rho(\mathbf{r})_1 \rho(\mathbf{r})_2 g_{\text{hs}}(r_{12}; d, T, \tilde{\rho}(\mathbf{r}_1, \mathbf{r}_2)) d\mathbf{r}_1 d\mathbf{r}_2. \quad (179)$$

with

$$\begin{aligned}\tilde{\rho}(r_1, r_2) &= \frac{1}{2}(\tilde{\rho}(r_1) + \tilde{\rho}(r_2)) \\ \tilde{\rho}(r_1) &= \frac{3}{4\pi R^3} \int \Theta(R-r)\rho(r)dr\end{aligned}\tag{180}$$

where R is chosen to be some physically reasonable value on the order of the length scale of the potential. Sokolowski and Fischer found this to give good results for liquid–vapor coexistence and for the qualitative behavior of the liquid–wall interface. Wadewitz and Winkelmann applied a variant of the model to the calculation of Lennard-Jones surface tension and found reasonable results with the quality deteriorating with decreasing range of the potential [109]. A similar theory was also studied by Tang, Scriven, and Davis [110].

The advantage of these approximations is that one makes use of the well-developed machinery of thermodynamic perturbation theory and thereby assures a reasonable equation of state, at least for the bulk liquid. The drawback is that there is little relation to the DCF-based formalism of exact DFT. Furthermore, the dominant contribution to the DCF implied by Eq. (179) is likely to be $w(r_{12})g_{hs}(r_{12}; d, T, \tilde{\rho}(\mathbf{r}_1, \mathbf{r}_2))$, which, in a dense fluid, will exhibit strong oscillations coming from the hard-sphere PDF whereas such oscillations are not seen in simulation (see, e.g., Fig. 2 below).

C. Mean-Field Theories

Some of the inconsistencies of the effective-liquid approach to the tail contribution are avoided if Δc_2 is independent of density. The low-density limit of the DCF for any system (no matter what the density distribution) is

$$\lim_{\bar{\rho} \rightarrow 0} \Delta c_2(\mathbf{r}_1, \mathbf{r}_2; d, [\rho]) = -(1 - \exp(-\beta v(r))) + \Theta(d-r)\tag{181}$$

which can be used as the desired approximation. It is more common, though, to break up the potential into a short-ranged repulsion and a long ranged attraction. Then, noting that the hard-sphere part of the DCF is supposed to model the short-ranged attraction, one has that $\exp(-\beta v_0(r)) \sim \Theta(r-d)$ so that

$$\begin{aligned}\lim_{\bar{\rho} \rightarrow 0} \Delta c_2(\mathbf{r}_1, \mathbf{r}_2; d, [\rho]) &= -(1 - \exp(-\beta v_0(r))\exp(-\beta w(r))) + \Theta(d-r) \\ &\simeq \Theta(r-d)(\exp(-\beta w(r)) - 1)\end{aligned}\tag{182}$$

At high temperatures, this gives the so-called Mean Spherical Approximation

$$\lim_{\beta \rightarrow 0} \lim_{\bar{\rho} \rightarrow 0} \Delta c_2(\mathbf{r}_1, \mathbf{r}_2; d, [\rho]) \simeq -\Theta(r-d)\beta w(r_{12})\tag{183}$$

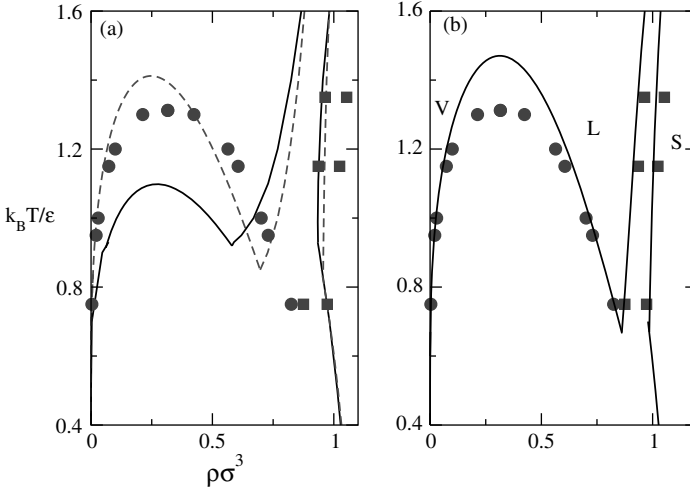


Figure 1. The phase diagram for the Lennard-Jones vapor (V), liquid (L), and FCC solid (S) calculated using different approximations. In all cases, the hard-sphere contribution is calculated using the white-bear FMT functional. (a) The tail contribution is calculated using Eq. 184 with both the BH (full line) and WCA (broken line) expressions for the long-ranged part of the potential. [Equation (173) was used to calculate the hard-sphere diameter in both cases.] The simulation data of Verlet and Levesque [113] and of Hansen and Verlet [114] are shown as symbols. (b) The result of using Eq. (186) with $w = 0$ and the effective hard-sphere diameter and perturbation theory of Ree et al. [115, 116].

For reasons discussed below, the preceding step function is often dropped and the approximation $\Delta c_2 \simeq -\beta w(r_{12})$ is used instead. It is interesting that besides being the expected result in the low-density, high-temperature limit, there is also evidence that this approximation becomes exact at high densities, at least in two dimensions [111]. This gives the mean-field result

$$F_l[\rho] = \frac{1}{2} \int \rho(\mathbf{r}_1) \rho(\mathbf{r}_2) w(r_{12}) d\mathbf{r}_1 d\mathbf{r}_2 \quad (184)$$

which has been used since the 1970's. Figure 1 shows the coexistence curves calculated using this model for the two choices of the tail function and the data from simulations. The liquid–vapor coexistence curve calculated using $w^{BH}(r)$ is significantly below the data while that calculated using $w^{WCA}(r)$ is above it. The difference is primarily due to the extension of the tail function into the core in the WCA model [compare Eq. (171) to Eq. (172)]. For the uniform fluid, one has that

$$\frac{1}{V} F_l^{(WCA)}(\bar{\rho}) = 2\pi\bar{\rho}^2 \int_0^\infty w^{(WCA)}(r) dr = \frac{2\pi}{3} \bar{\rho}^2 v_{LJ}(r_m) d^3 + 2\pi\bar{\rho}^2 \int_d^\infty w^{WCA}(r) dr \quad (185)$$

The first term on the right is due to the extension of the “tail” into the core, while the second term is not very different from the full contribution of the BH tail. This is the reason for extending the tail contribution into the core: At least for a Lennard-Jones fluid, it appears to move the bulk liquid–vapor part of the phase diagram in the direction of the simulation results. Because the contribution of the tail function inside the core is of little importance in thermodynamic perturbation theory, the importance of this contribution to the VdW model is somewhat disturbing. In fact, this effect has been exploited by Curtin and Ashcroft [112] to give a better model for the LJ phase diagram by replacing $w^{(\text{WCA})}(r)$ by $w^{(\text{CA})}(r) = w^{(\text{WCA})}(r)\Theta(r-r_*)$ with r_* chosen to be half the FCC nearest-neighbor distance. The rationale behind this choice is unclear except that it improves agreement of the phase diagram with the data. This model was subsequently used by Ohensorge, Löwen, and Wagner [59, 60] in an investigation of the liquid–solid interface near the triple point.

It is clear from Fig. 1 that the simple mean-field treatment of the tail is not very accurate, even for the liquid–vapor coexistence curve. Because the equation of state for the fluid can be relatively accurately calculated by other means (e.g., thermodynamic perturbation theory), this suggests introducing a correction based on this knowledge. For example, Lu, Evans, and Telo da Gamma [117] used a mean-field model but adjusted the hard-sphere diameter so as to reproduce the empirical liquid–vapor coexistence curve. For solids, a particularly simple model can be formulated in the context of the Gaussian density parameterization [Eq. (1.54)] where, for an inhomogeneous system, one allows the parameters, the average density $\bar{\rho} = x\bar{\rho}_{\text{latt}}$, and the width of the Gaussians, α , to depend on position. Then, a very simple model giving the desired equation of state for the liquid is

$$F_l[\rho] = \frac{1}{2} \int \rho(\mathbf{r}_1)\rho(\mathbf{r}_2)w(r_{12})d\mathbf{r}_1d\mathbf{r}_2 + \int \Delta f(\bar{\rho}(\mathbf{r}))d\mathbf{r} \quad (186)$$

where $\Delta f(\rho)$ is the correction to the VdW model needed to give the known equation of state for the bulk liquid. An even simpler approximation drops the first term on the right altogether and models the tail solely through the effective liquid term. Both Curtin [58] and Lutsko and Nicolis [118] used this approximation to calculate the bulk equation of state for both the liquid and the solid. The phase diagram for the Lennard-Jones system is shown in Fig. 1. As is typical of all mean-field approaches, the equation of state (calculated using thermodynamic perturbation theory) is not accurate near the critical point. Otherwise, the predicted phase diagram is quantitatively very good. Similar results were obtained for the ten Wolde–Frenkel potential model for globular proteins [118]. The reason this works so well for the FCC solid is that the coordination in the solid and in the dense liquid is very similar so that the local environment of the atoms is not too different in the two systems. This approximation would not be expected to work for a BCC solid where something like the first term on the right in Eq. (186) would be necessary to account for the different structure.

A more elaborate modification of the VdW model which is closer to the spirit of FMT has recently been proposed [42] based on the observation that the simple VdW model implies a DCF in the uniform fluid of the form

$$c_2^{\text{VdW}}(r_{12}; \bar{\rho}) = c_2^{\text{FMT}}(r_{12}; \bar{\rho}, d) - \beta w(r_{12}) \quad (187)$$

provided that the hard-sphere diameter does not depend on the density. Comparison of this model to the DCF as determined by computer simulation shows that, at least in the dense fluid, most of the difference lies in the core region and, in fact, that the difference between the observed correlation function and the hard-sphere contribution is roughly linear in r . Motivated by the work of Tang [119], which primarily involves a complicated estimate of the DCF in the core region, this suggested that one might correct the correlations in the core by adding a linear contribution,

$$c_2^{\text{VdW}}(r_{12}; \bar{\rho}) = c_2^{\text{FMT}}(r_{12}; \bar{\rho}, d) + \Theta(d-r) \left(a_0(\bar{\rho}) + a_1(\bar{\rho}) \frac{r}{d} \right) - \beta w(r_{12}) \quad (188)$$

with intercept and slope chosen so that the resulting DCF is continuous and gives some known equation of state via the compressibility equation [120],

$$\begin{aligned} -\beta w(d_+) &= c_2^{\text{FMT}}(d_+; \bar{\rho}, d) + (a_0(\bar{\rho}) + a_1(\bar{\rho})) - \beta w(d_-) \\ f_{\text{ex}}(\bar{\rho}) &= f_{\text{ex}}^{\text{HS}}(\bar{\rho}) - 4\pi d^3 \int_0^1 (1-\lambda) \left(\frac{1}{3} a_0(\lambda \bar{\rho}) + \frac{1}{4} a_1(\lambda \bar{\rho}) \right) + 2\pi \bar{\rho}^2 \int_0^\infty w(r) dr \end{aligned} \quad (189)$$

where $f_{\text{ex}}(\bar{\rho})$ is the (excess part of the) desired equation of state for the uniform liquid and where the notation d_\pm indicates the quantity evaluated at the hard-sphere diameter as it is approached from r greater than (+) or less than (-) d . In the spirit of the older liquid-based theories that often required the DCF of the uniform liquid as input, the equation of state is an input of the present theory and so must be determined, for example, from thermodynamic perturbation theory, the First-Order Mean Spherical Approximation of Tang [119], simulation, liquid-state integral equations, or some other source. As shown in Fig. 2, the improvement in the description of the DCF can be significant.

The second ingredient of the improved VdW model is to modify the free energy functional so as to be consistent with the modified DCF using the ideas of FMT. Following the approach of Kierlik and Rosinberg [77], who started with Rosenfeld's ansatz and demanded that it reproduce the Percus-Yevick DCF, one can do the same but demand that the desired core correction be obtained. The details are given in Ref. 42 and are straightforward, leading to

$$F[\rho] = F_{\text{id}}[\rho] + F_{\text{HS}}([\rho]; d) + F_{\text{core}}([\rho]; d) + F_I[\rho] \quad (190)$$

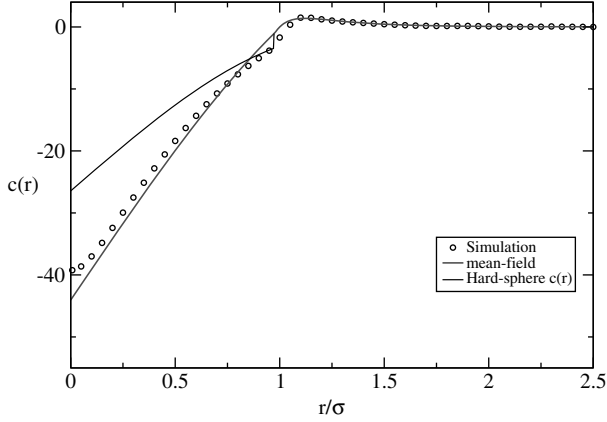


Figure 2. The DCF for a Lennard-Jones fluid at $T^* = 0.72$ and $\rho\sigma^3 = 0.85$ as determined from the model with the linear core correction, lower line, and the simulation data of Llano-Restrepo and Chapman [121]. The hard-sphere contribution to the DCF is shown as the upper line. From Ref. [120], where further details can be found.

with

$$\begin{aligned}
 F_{\text{core}}([\rho]; d) &= \int \Phi_{\text{core}}(\mathbf{r}; [\rho]; d) d\mathbf{r} \\
 \Phi_{\text{core}}(\mathbf{r}; [\rho]; d) &= \frac{1}{\pi d^2} j_1(\eta(\mathbf{r})) s(\mathbf{r}) + \frac{1}{\pi d} j_2(\eta(\mathbf{r})) (s^2(\mathbf{r}) - v^2(\mathbf{r})) \\
 &\quad + \frac{1}{\pi} j_3(\eta(\mathbf{r})) s(\mathbf{r}) (s^2(\mathbf{r}) - 3v^2(\mathbf{r}))
 \end{aligned} \tag{191}$$

The quantities $\eta(\mathbf{r})$, and so on, are the density measures from FMT. Defining

$$\beta\phi_{\text{core}}(\bar{\rho}) = \frac{1}{\rho} \left(f_{\text{ex}}(\bar{\rho}) - f_{\text{HS}}(\bar{\rho}) - \frac{1}{V} F_l(\bar{\rho}) \right) \tag{192}$$

the functions $j_n(\eta)$ are given by

$$\begin{aligned}
 j_1(\eta) &= \beta\phi_{\text{core}}(\bar{\rho}) + 3\eta(a_0(\bar{\rho}) + a_1(\bar{\rho})) + 72\eta^2 j_3(\eta) \\
 j_2(\eta) &= -\frac{1}{2}(a_0(\bar{\rho}) + a_1(\bar{\rho})) - 18\eta j_3(\eta) \\
 j_3(\eta) &= \frac{1}{36\eta^2} \left[\frac{1}{2} \left(\beta\phi_{\text{core}}(\bar{\rho}) - \bar{\rho} \frac{\partial}{\partial \bar{\rho}} \beta\phi(\bar{\rho}) - \beta\phi_{\text{core}}(0) \right) \right. \\
 &\quad \left. + 3 \int_0^\eta \eta \frac{d}{d\eta} c_{\text{HS}}(d_-; \bar{\rho}; d) d\eta \right]
 \end{aligned} \tag{193}$$

where $\bar{\rho} = \bar{\rho}(\eta) = 6\eta/(\pi d^3)$.

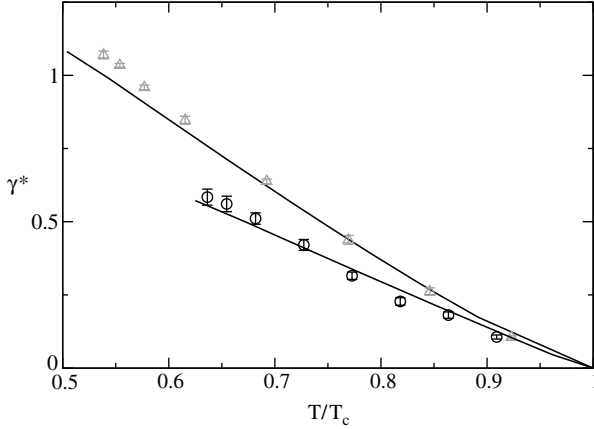


Figure 3. The surface tension for a Lennard-Jones fluid with a cutoff of 6σ (upper curve), and 2.5σ (lower curve). The solid lines are the result of the DFT calculations [42] and the data are from Grosfils and Lutsko [122]. The temperatures are scaled to the critical temperature while the dimensionless surface tension is $\gamma^* = \gamma\sigma^2/\varepsilon$.

Figure 3 shows the excess free energy per unit area (the surface tension) for the planar Lennard-Jones vapor–fluid interface calculated using this model for different values of the cutoff of the potential and as determined by simulation [42]. The surface tension is very sensitive to the range of the potential, and this property can be used to test the robustness of a theory. The results are in good agreement with simulation, with most of the difference being due to inaccuracies in the equation of state at the small cutoff. For DFT to be useful, it must be transferable which is to say a given model must give reasonable results for a variety of potentials. The variation of surface tension with cutoff is one such test. As another illustration, the surface tension for the potential

$$v(r) = v_{\text{HS}}(r, d) + \frac{4\varepsilon}{\alpha^2} \left(\left(\left(\frac{r}{\sigma} \right)^2 - d^2 \right)^{-6} - \alpha \left(\left(\frac{r}{\sigma} \right)^2 - d^2 \right)^{-3} \right) \quad (194)$$

has also been calculated and compared to simulation. For $d = 0$ and $\alpha = 1$, this reduces to the Lennard-Jones potential; while for $d = \sigma$ and $\alpha = 50$, it is the interaction used by ten Wolde and Frenkel to model globular proteins [123]. Figure 4 shows the surface tension for various parameters, all with a cutoff of 2.8σ . In this case, the required equation of state is calculated using first-order thermodynamic perturbation theory, and the results are again seen to be in good agreement with the theory.

Figures 5 and 6 show the predicted density distribution for a Lennard-Jones fluid near a hard wall, along with the results of Grand Canonical Monte Carlo

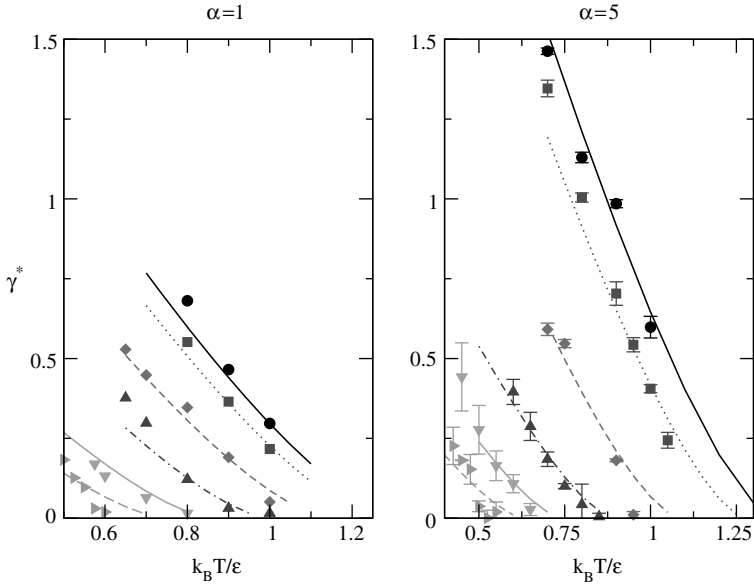


Figure 4. The surface tension for the potential given in Eq. (94) with a cutoff of 2.8σ , for different values of the hard-core diameter and for two different values of α . The points are from simulation with $d = 0.0$ (circles), 0.2 (squares), 0.4 (diamonds), 0.6 (triangles), 0.8 (triangles down), and 1.0 (triangles right). The lines are from the DFT calculations [124].

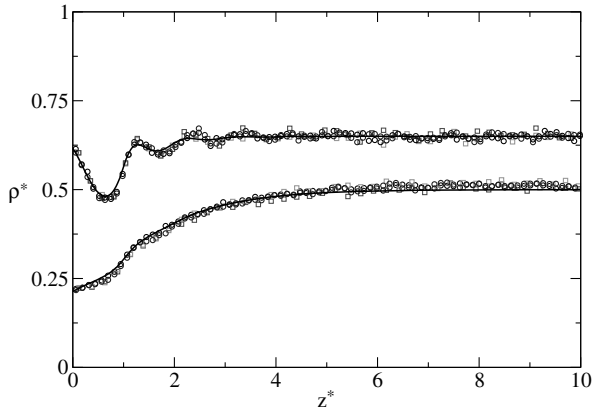


Figure 5. Structure of the Lennard-Jones fluid near a hard wall as determined from simulation (symbols) and the theory (lines). The simulations come from two runs each using cells with aspect ratio $1 \times 1 \times 2$ (circles), and $1 \times 1 \times 4$ (squares). The upper curve and data are for a chemical potential corresponding to bulk density $\rho^* = \rho\sigma^3 = 0.65$ and the lower curve for density $\rho^* = 0.50$. From Lutsko [42].

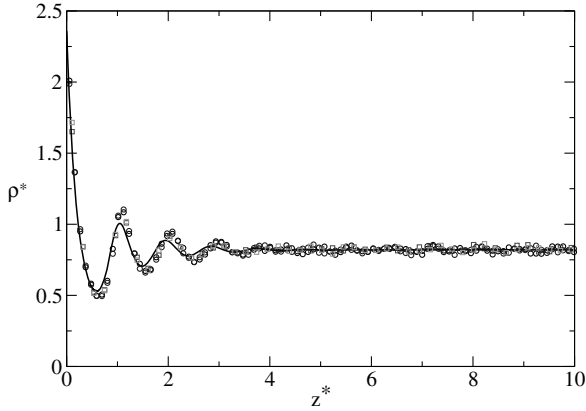


Figure 6. Same as Fig. 5 except that the bulk density is $\rho^* = 0.85$. From Lutsko [42].

simulations as reported in Ref. 42. Again, the quantitative agreement is very good. Furthermore, it is significant that, because of its self-consistent structure, this relatively simple theory satisfies the exact sum rule that the density at the wall, $\rho(0)$, is the pressure in the bulk liquid, far from the wall, divided by the temperature (see Refs. 125, 126 and Appendix C). Physically, this is just a manifestation of the fact that the pressure in an equilibrium system must be uniform together with the fact that, when interacting with the wall, the particles behave like an

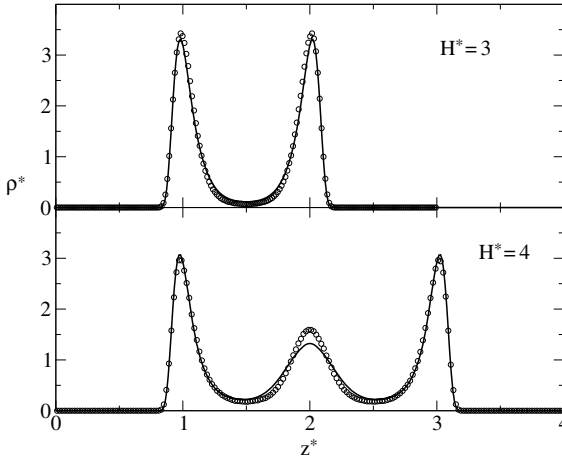


Figure 7. Comparison of the density distribution of a Lennard-Jones fluid within slit pores of size $H^* = 3$ and $H^* = 4$ as calculated from the theory (lines) and as determined from simulation (symbols). From Lutsko [42].

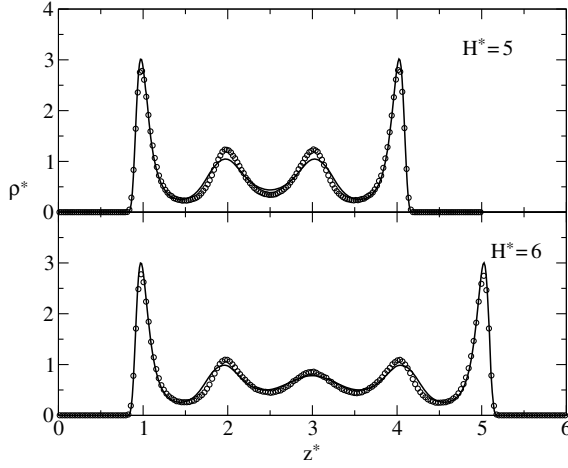


Figure 8. Comparison of the density distribution of a Lennard-Jones fluid within slit pores of size $H^* = 5$ and $H^* = 6$ as calculated from the theory (lines) and as determined from simulation (symbols). From Lutsko [42].

ideal gas. A final illustration is given in Figs. 7 and 8, which illustrate the predicted and observed density distribution of a Lennard-Jones fluid in a slit pore. A slit pore consists of two walls separated by some distance, H . The interaction between the fluid atoms and the walls was based on Steele's model [127, 128] of the average interaction of an atom with a 100 plane of an FCC solid, in which the potential felt by an atom a perpendicular distance z from the wall is

$$V_{\text{wall}}(z) = 2\pi\epsilon \left(\frac{2}{5} \left(\frac{\sigma}{z} \right)^{10} - \left(\frac{\sigma}{z} \right)^4 - \frac{\sqrt{2}}{3 \left(\frac{z}{\sigma} + 0.61/\sqrt{2} \right)^3} \right) \quad (195)$$

The chemical potential was set to a value that corresponds to the bulk density $0.5925/\sigma^3$, the temperature was $k_B T = 1.2\epsilon$, and the intermolecular potential was cut off at a distance of 6σ . Again, the predicted density distribution is in good agreement with the simulations.

There have been many other applications of the general idea of writing the free energy as a sum of a hard-sphere contribution and of a mean-field treatment of the long-ranged part of the interaction. As just one example, Archer, Pini, Evans, and Reatto [129] have recently made an interesting study of colloidal fluids with competing interactions. In their work, DFT is compared to a sophisticated form of liquid-state theory and is found to predict interesting behavior (banding) in regions where the liquid-state theory has no solution.

VI. EXTENSIONS AWAY FROM EQUILIBRIUM

It seems intuitively obvious that if the local density of a system is perturbed, by applying some field, and then released, by removing the field, its relaxation will somehow be governed by the free energy surface $F[\rho]$. This idea, in less general forms, is quite old and obviously related to early work by Cahn as well as to the time-dependent Ginzburg–Landau model. In recent years, the idea has been developed into a set of techniques that combine the detailed free energy models developed in equilibrium DFT with methods of non-equilibrium statistical mechanics so as to allow for the description of dynamical transitions in complex systems. In the following, attention will mostly be given to the developments called Dynamical Density Functional Theory, with some discussion given also to the recent introduction of energy-surface methods for mapping out transition pathways.

A. Dynamical DFT

Density Functional Theory as described so far is a theory concerning equilibrium systems; and, as such, dynamics plays no role. Dynamical Density Functional Theory (DDFT), is an attempt to extend the ideas of DFT to dynamical properties. Intuitively, one expects that the free energy functionals used in DFT would play some role in determining the dynamics for systems out of equilibrium. For example, consider diffusion where number is conserved and so the density must obey a conservation law of the form

$$\frac{\partial \rho(\mathbf{r}, t)}{\partial t} = \nabla \cdot \mathbf{J}(\mathbf{r}, t) \quad (196)$$

where \mathbf{J} is the number current. Assuming linear response and local equilibrium, the theory of non-equilibrium thermodynamics tells us that the thermodynamic force driving diffusion is the gradient in the local chemical potential [130] so, near equilibrium, one expects the current to have the form $\mathbf{J} = \mathbf{L} \cdot \nabla \mu(\mathbf{r}, t)$ where the tensor \mathbf{L} is a transport coefficient related to the diffusion constant. If the system is in local equilibrium, the local chemical potential should be given by the Euler–Lagrange equation at each point so that the diffusion law becomes, in the simplest case of an isotropic system,

$$\frac{\partial \rho(\mathbf{r}, t)}{\partial t} = \nabla \cdot (L \nabla \mu(\mathbf{r}, t)) = \nabla \cdot \left(L \nabla \frac{\delta F[\rho]}{\delta \rho(\mathbf{r}, t)} \right) \quad (197)$$

Practical calculations based on nontrivial free energy models go back at least to Cahn [131]. A similar development for nonconserved variables, and including a fluctuating force, is called the Time-Dependent Ginzburg–Landau Theory and is a standard tool in the investigation of dynamical critical phenomena [132].

Notice that for a low-density system, $F[\rho] \sim F_{id}[\rho]$ giving

$$\frac{\partial \rho(\mathbf{r}, t)}{\partial t} \sim \nabla \cdot (L\rho(\mathbf{r}, t)^{-1} \nabla \rho(\mathbf{r}, t)) \quad (198)$$

which is the diffusion equation with a diffusion coefficient $D = L/\rho$. The diffusion coefficient diverges as the density goes to zero because the motion of each atom becomes ballistic—not diffusive—in the zero density limit. For mixtures, the limit of the density of *one* component going to zero does not produce ballistic motion since the finite component—the bath—still produces diffusive behavior. For the case of two components, with the tracer component, ρ_t , at vanishing low density and the bath component at low, spatially uniform, finite density ρ_b , where one has $\rho(\mathbf{r}, t)^{-1} = (\rho_t(\mathbf{r}, t) + \rho_b)^{-1} \sim \rho_b^{-1}$, the transport law becomes

$$\frac{\partial \rho_t(\mathbf{r}, t)}{\partial t} \sim \nabla \cdot (L\rho_b^{-1} \nabla \rho_t(\mathbf{r}, t)) \quad (199)$$

Now, if one supposes that the bath can be treated as a passive background, serving only to damp the dynamics of the tracers, and that the tracers can be treated as being in local equilibrium, then one might expect that for finite tracer density, Eq. (197) could be applicable with $F[\rho]$ being an effective free energy for the tracers. However, to be consistent with Eq. (199) in the low-density limit, one must assume that the transport coefficient is replaced by $L \rightarrow \Gamma\rho(\mathbf{r}, t)$, for some constant Γ , giving

$$\frac{\partial \rho}{\partial t} = \nabla \cdot \left(\Gamma\rho(\mathbf{r}, t) \nabla \frac{\delta F[\rho]}{\delta \rho(\mathbf{r}, t)} \right) \quad (200)$$

which is generally referred to as DDFT in the literature. This equation is assumed to describe the evolution of the density of a system subject to damping such as a colloidal fluid. Other systems for which the assumption of the passivity of the background is perhaps less plausible would include mixtures of similar species and the extreme case of self-diffusion.

The general form has a long history in the theory of non-equilibrium statistical mechanics. It is related to “Model B” in Hohenberg and Halperin’s review of the theory of dynamical critical phenomena [132]. Some of the earliest uses of this and similar models, aside from that of Cahn, are Munakata [133, 134], Bagchi [135] and Dieterich [136]. The standard statistical mechanical approach to the derivation of equations such as Eq. (200) is by means of projection operators. For DDFT, the most complete analysis is probably that of Kawasaki [137]. An interesting derivation for granular systems was recently given by Tarazona and Marconi based on a multiscale expansion of the Enksog equation [138]. A very clear discussion of the relation between DDFT, the “extended” DDFT (i.e., DDFT including the local velocity), and conventional kinetic theory in the context of the

glass transition can be found in Das [139]. Kirkpatrick and Wolynes [140] discuss the relation between equilibrium DFT and “extended” DDFT in the context of the glass transition. Chan and Finken discuss the formulation of an axiomatic DDFT in analogy to equilibrium DDFT [141]. Here, by way of illustration of the physical ideas involved, an intermediate route, based on recent work of Evans and Archer and of Marconi and Tarazona, will be followed wherein the introduction of the assumption of local equilibrium in otherwise exact balance laws leads to DDFT.

1. Some ideas from Kinetic Theory

In order to discuss DDFT, it is first useful to review some basic ideas of kinetic theory. Consider a system of N particles (atoms, molecules, colloidal particles, . . .) evolving under Newtonian dynamics. For simplicity, attention will be restricted here to entities having no internal structure so that they are fully described by their positions \mathbf{q}_i and momenta \mathbf{p}_i , which together constitute the particle’s phase $x_i = \mathbf{q}_i, \mathbf{p}_i$. The collection of all phases will be denoted $\Gamma_N = \{x_i\}_{i=1}^N$. The time-dependent N -body distribution $f(\Gamma_N; t)$ gives the probability to find the first particle with phase x_1 , the second with phase x_2 , and so on. It satisfies the Liouville equation,

$$\frac{\partial}{\partial t} f(\Gamma_N; t) + \sum_{i=1}^N \frac{\mathbf{p}_i}{m} \cdot \frac{\partial}{\partial \mathbf{q}_i} f(\Gamma_N; t) + \sum_{i=1}^N \frac{\partial}{\partial \mathbf{p}_i} \cdot \mathbf{F}_i f(\Gamma_N; t) = 0 \quad (201)$$

where \mathbf{F}_i is the total force acting on particle i . It will be the sum of any external forces, such as that due to an external field, and the internal forces due to the interparticle interaction potential so that for pair potentials it is

$$\mathbf{F}_i = \mathbf{F}_i^{\text{ext}} - \sum_{j \neq i} \frac{\partial}{\partial \mathbf{q}_i} v(q_{ij}) \quad (202)$$

Notice that the evolution of the phase function is deterministic and that stochasticity enters through the distribution of initial conditions. Defining the reduced distributions as

$$\rho_m(x_1, \dots, x_m) = \frac{N!}{(N-m)!} \int f(\Gamma_N; t) dx_{m+1}, \dots, dx_N \quad (203)$$

and integrating the Liouville equation over particles $m+1, \dots, N$ gives an equation for the m -body distribution containing a contribution due to the $(m+1)$ -body distribution. This set of equations is known as the BBGKY hierarchy [142]. The first equation of the hierarchy is

$$\frac{\partial}{\partial t} \rho_1(x_1; t) + \frac{\mathbf{p}_1}{m} \cdot \frac{\partial}{\partial \mathbf{q}_1} \rho_1(x_1; t) + \frac{\partial}{\partial \mathbf{p}_1} \cdot \mathbf{F}_1^{\text{ext}} \rho_1(x_1; t) = \frac{\partial}{\partial \mathbf{p}_1} \cdot \int \frac{\partial v(q_{12})}{\partial \mathbf{q}_1} \rho_2(x_1, x_2; t) dx_2 \quad (204)$$

In equilibrium, the distributions are time-independent and the velocities are always distributed as Maxwellians so that

$$\begin{aligned}\rho_1(x_1; t) &\rightarrow \rho(\mathbf{q}_1)\varphi(\mathbf{p}_1; \mathbf{u}, T) \\ \rho_2(x_1, x_2; t) &\rightarrow \rho(\mathbf{q}_1, \mathbf{q}_2)\varphi(\mathbf{p}_1; \mathbf{u}, T)\varphi(\mathbf{p}_2; \mathbf{u}, T)\end{aligned}\quad (205)$$

where $\rho(\mathbf{q}_1)$ is the usual one-body density, $\rho(\mathbf{q}_1, \mathbf{q}_2)$ is the two-particle reduced distribution, which is related to the PDF as discussed in Section II, and the Maxwellian velocity distribution is

$$\varphi(\mathbf{p}; \mathbf{u}, T) = \left(\frac{1}{2\pi mk_B T}\right)^{D/2} \exp\left(-\frac{(\mathbf{p}-\mathbf{u})^2}{2mk_B T}\right)\quad (206)$$

(The center of mass velocity \mathbf{u} plays no role here, but we include it for the sake of a later discussion.) Substituting this into the equation for the one-body equation, multiplying through by \mathbf{p}_1 and integrating over \mathbf{p}_1 gives

$$-k_B T \frac{\partial}{\partial \mathbf{q}_1} \rho(\mathbf{q}_1) + F_1^{\text{ext}} \rho(\mathbf{q}_1) = \int \frac{\partial v(q_{12})}{\partial \mathbf{q}_1} \rho(\mathbf{q}_1, \mathbf{q}_2) dx_2\quad (207)$$

In equilibrium, the density satisfies the Euler–Lagrange equation, Eq. (31), and using it in the left-hand side gives

$$-\rho(\mathbf{q}_1) \frac{\partial}{\partial \mathbf{q}_1} \frac{\delta F_{\text{ex}}[\rho]}{\delta \rho(\mathbf{q}_1)} = \int \frac{\partial \beta v(q_{12})}{\partial \mathbf{q}_1} \rho(\mathbf{q}_1, \mathbf{q}_2) dx_2\quad (208)$$

which is the well-known first member of the Yvon–Born–Green hierarchy equation [21]. This exact, equilibrium relation plays a central role in several recent derivations of DDFT as described below.

2. A Simple Kinetic-Theory Approach

In general, the one-body density $\rho_1(x_1; t)$ depends on both position and velocity in nontrivial ways which are hard to calculate due to the coupled nature of the BBGKY hierarchy. However, integrating it over momenta gives the local density,

$$\rho(\mathbf{r}; t) = \int \delta(\mathbf{r}-\mathbf{q}_1) \rho_1(x_1; t) dx_1\quad (209)$$

and this satisfies a simple continuity equation. Multiplying the first BBGKY equation by $\delta(\mathbf{r}-\mathbf{q}_1)$ and integrating over momentum gives

$$\frac{\partial}{\partial t} \rho(\mathbf{r}; t) + \nabla \rho(\mathbf{r}; t) \mathbf{v}(\mathbf{r}; t) = 0$$

where the local velocity is defined as

$$\rho(\mathbf{r}; t) \mathbf{v}(\mathbf{r}; t) = \int \frac{1}{m} p_1 \delta(\mathbf{r}-\mathbf{q}_1) \rho_1(x_1; t) dx_1\quad (210)$$

The equation for the density has the expected form with the number current $\mathbf{J}(\mathbf{r}; t) = \rho(\mathbf{r}; t)\mathbf{v}(\mathbf{r}; t)$. A balance equation for the local velocity can be obtained in a similar way, by multiplying the first BBGKY equation by $\frac{\mathbf{p}_i}{m}\delta(\mathbf{r}-\mathbf{q}_i)$ and integrating to get

$$\begin{aligned} & m \frac{\partial}{\partial t} \rho(\mathbf{r}; t) \mathbf{v}(\mathbf{r}; t) + \nabla \cdot \int \frac{\mathbf{p}_1 \mathbf{p}_1}{m} \delta(\mathbf{r}-\mathbf{q}_1) \rho_1(x_1; t) dx_1 - \mathbf{F}^{\text{ext}}(\mathbf{r}; t) \rho(\mathbf{r}; t) \\ &= -\frac{1}{m} \int \delta(\mathbf{r}-\mathbf{q}_1) \frac{\partial v(q_{12})}{\partial \mathbf{q}_1} \rho_2(x_1, x_2; t) dx_1 dx_2 \end{aligned} \quad (211)$$

Changing integration variables from \mathbf{p}_i to $\mathbf{p}'_i = \mathbf{p}_i - m\mathbf{v}(\mathbf{q}_i; t)$ and rearranging gives the exact balance equation

$$\begin{aligned} & \frac{\partial}{\partial t} \rho(\mathbf{r}; t) \mathbf{v}(\mathbf{r}; t) + \nabla \cdot \rho(\mathbf{r}; t) \mathbf{v}(\mathbf{r}; t) \mathbf{v}(\mathbf{r}; t) \\ &+ \nabla \cdot \int \frac{\mathbf{p}'_1 \mathbf{p}'_1}{m^2} \delta(\mathbf{r}-\mathbf{q}_1) \rho_1(x'_1; t) dx'_1 + \frac{1}{m} \int \delta(\mathbf{r}-\mathbf{q}_1) \frac{\partial v(q_{12})}{\partial \mathbf{q}_1} \rho_2(x_1, x_2; t) dx_1 dx_2 \\ &- \frac{1}{m} \mathbf{F}^{\text{ext}}(\mathbf{r}; t) \rho(\mathbf{r}; t) = 0 \end{aligned} \quad (212)$$

Separating out the trace and traceless part of the $\mathbf{p}'_1 \mathbf{p}'_1$ term, noting that the potential term does not involve momenta, and using the continuity equation gives

$$\begin{aligned} & \rho(\mathbf{r}; t) \frac{\partial}{\partial t} \mathbf{v}(\mathbf{r}; t) + \rho(\mathbf{r}; t) \mathbf{v}(\mathbf{r}; t) \cdot \nabla \mathbf{v}(\mathbf{r}; t) + \nabla \cdot \frac{1}{m} \rho(\mathbf{r}; t) k_B T(\mathbf{r}; t) \\ &+ \frac{1}{m} \int \delta(\mathbf{r}-\mathbf{q}_1) \frac{\partial v(q_{12})}{\partial \mathbf{q}_1} \rho_2(\mathbf{x}_1, \mathbf{x}_2; t) d\mathbf{x}_1 d\mathbf{x}_2 + \nabla \cdot \Pi^K - \frac{1}{m} \mathbf{F}^{\text{ext}}(\mathbf{r}; t) \rho(\mathbf{r}; t) = 0 \end{aligned} \quad (213)$$

with the local temperature defined as

$$\frac{D}{2} \rho(\mathbf{r}; t) k_B T(\mathbf{r}; t) = \int \frac{(p_1 - m\mathbf{v}(\mathbf{q}_1; t))^2}{2m} \delta(\mathbf{r}-\mathbf{q}_1) \rho_1(x_1; t) dx_1 \quad (214)$$

and where the kinetic part of the dissipative stress is

$$\Pi_{ij}^K = \int \frac{\mathbf{p}'_i \mathbf{p}'_j - \frac{1}{D} p_i'^2 \delta_{ij}}{m^2} \delta(\mathbf{r}-\mathbf{q}_1) \rho_1(x'_1; t) dx'_1 \quad (215)$$

Similarly, a balance equation for the temperature is obtained by multiplying the first BBGKY equation by $\frac{1}{2m}p_1^2\delta(\mathbf{r}-\mathbf{q}_1)$ and integrating over momenta. After some manipulations, the result is

$$\begin{aligned} & \frac{D}{2}\rho\frac{\partial}{\partial t}k_B T + \frac{D}{2}\rho\mathbf{v}\cdot\nabla k_B T + \Pi:\nabla\mathbf{v} \\ &= -\nabla\cdot\int\frac{p'_1}{m}\frac{1}{2m}p_1'^2\delta(\mathbf{r}-\mathbf{q}_1)\rho_1(x_1;t)dx_1 - \int\frac{p'_1}{m}\delta(\mathbf{r}-\mathbf{q}_1)\cdot\frac{\partial v(q_{12})}{\partial\mathbf{q}_1}\rho_2(x_1,x_2;t)dx_2 \end{aligned} \quad (216)$$

So far, these equations are exact and therefore quite formal, requiring the one and two body distributions for closure. However, for an *isothermal* system, the equations for the density and velocity decouple from the temperature equation. Following Archer and Rauscher [143] and introducing the local equilibrium hypothesis for the two-body term, Eq. (208), in the velocity equation then gives

$$\begin{aligned} & \frac{\partial}{\partial t}\rho(\mathbf{r};t) + \nabla\cdot\rho(\mathbf{r};t)\mathbf{v}(\mathbf{r};t) = 0 \\ & \frac{\partial}{\partial t}\mathbf{v}(\mathbf{r};t) + \mathbf{v}(\mathbf{r};t)\cdot\nabla\mathbf{v}(\mathbf{r};t) + \frac{1}{m}\nabla\frac{\delta F[\rho]}{\delta\rho(\mathbf{r};t)} + \rho(\mathbf{r};t)^{-1}\nabla\cdot\Pi - \frac{1}{m}\mathbf{F}^{\text{ext}}(\mathbf{r};t) = 0 \end{aligned} \quad (217)$$

To proceed further requires some sort of approximation for the dissipative stress. Most practical methods involve expressing it as an expansion in gradients of the density and velocity. One route is to use an approximate kinetic theory, such as the Boltzmann or Enskog equation, and the Chapman–Enskog expansion to obtain an analytic approximation to the gradient expansion of Π [142]. Alternatively, one can treat the term phenomenologically. In both cases, one could in principle keep the equation for the temperature as well, treating all difficult terms in the same way as Π . In all cases, the resulting equations have the interpretation of being the usual Navier–Stokes equations with a position-dependent pressure given by

$$m\rho(\mathbf{r};t)^{-1}\nabla p = \nabla\frac{\delta F[\rho]}{\delta\rho(\mathbf{r};t)} \quad (218)$$

which suggests another interpretation. The Gibbs–Duhem equation for a multi-component system is

$$\sum_i N_i d\mu_i = -SdT + Vdp \quad (219)$$

where N_i is the number of particles of species i and μ_i is the chemical potential for species i . Assuming local equilibrium, one finds for an isothermal,

single-component system

$$\begin{aligned}\rho(\mathbf{r}; t)d\boldsymbol{\mu}(\mathbf{r}; t) &= dp(\mathbf{r}; t) \Rightarrow \rho(\mathbf{r}; t)\nabla\boldsymbol{\mu}(\mathbf{r}; t) = \nabla p(\mathbf{r}; t) \\ &\Rightarrow \rho(\mathbf{r}; t)\nabla\frac{\delta F[\rho]}{\delta\rho(\mathbf{r}; t)} = \nabla p(\mathbf{r}; t)\end{aligned}\quad (220)$$

where the last line comes from the Euler–Lagrange equation and the assumption of local equilibrium. Thus, this generalized form of the Navier–Stokes equations can again be understood as the result of the use of an assumption of local equilibrium.

To make a connection to DDFT, which involves only the density, requires the additional approximation that the velocity responds much more quickly than does the density—that is, that the system is overdamped. In this case, for a given configuration of the density, the velocity quickly reaches a steady state driven by the gradient in the “pressure”. In this state, one imagines that the velocity will be proportional to the driving force,

$$\mathbf{v}(\mathbf{r}; t) = -\Gamma\left(\nabla\frac{\delta F[\rho]}{\delta\rho(\mathbf{r}; t)} + \mathbf{F}^{\text{ext}}(\mathbf{r}; t)\right)\quad (221)$$

where Γ is a constant. [This is equivalent to looking neglecting the convective term in the second line of Eq. (217) and assuming that $\nabla\cdot\Pi \sim \Gamma^{-1}\mathbf{v}$, the same assumptions leading to Darcy’s law. For example, this condition occurs naturally if the environment exerts a global friction as is the case in, e.g. Brownian dynamics [154]]. Then, the continuity equation gives

$$\frac{\partial}{\partial t}\rho(\mathbf{r}; t) = \Gamma\nabla\cdot\rho(\mathbf{r}; t)\left(\nabla\frac{\delta F[\rho]}{\delta\rho(\mathbf{r}; t)} + \mathbf{F}^{\text{ext}}(\mathbf{r}; t)\right)\quad (222)$$

which is the expected result.

Just as in the case of DDFT, a more systematic approach to the derivation of this “extended DDFT” is based on the projection operator techniques of Zwanzig [144] and Mori and co-workers [145, 146]. However, this more general model is much older than DDFT and is widely used in Kinetic Theory today (see, e.g., Ref. 47). For a one-component liquid, the result is a generalized Langevin equation of the form of Eq. (217) with the addition of fluctuating forces. The construction of this and related models is outlined in Ref. 148 and the case of the pure fluid is given explicitly in Refs. 149 and 150. In this mesoscopic picture, Eq. (217) is understood as the result of averaging over the noise, yielding the same dynamics but with renormalized transport coefficients, as discussed more fully below.

3. Brownian Dynamics

One case in which the velocities of the particles may often be ignored is when the particles are in some sort of solution. In the event that motion is damped by the bath, the dynamics can be approximated as that of a collection of particles moving under the effect of their mutual interactions as well as a friction proportional to their

velocities. Many derivations have been based on the ideas of Marconi and Tarazona [151] in which the starting point is a system described by this Brownian dynamics. The particles move according to the stochastic equations

$$m \frac{d^2 \mathbf{q}_i}{dt^2} + \Gamma^{-1} \frac{d\mathbf{q}_i}{dt} = - \frac{\partial}{\partial \mathbf{q}_i} \left[\sum_{j \neq i} v(\mathbf{q}_{ij}) + \phi(\mathbf{q}_i) \right] + \boldsymbol{\eta}_i(t) \quad (223)$$

where the first term on the right is the sum of the interparticle force and the force due to interaction with a one-body potential while $\boldsymbol{\eta}_i(t)$ is white noise representing interaction with the bath [152],

$$\begin{aligned} \langle \boldsymbol{\eta}_i(t) \rangle &= 0 \\ \langle \boldsymbol{\eta}_i(t) \boldsymbol{\eta}_j(t') \rangle &= 2k_B T \delta_{ij} \delta(t-t') \end{aligned} \quad (224)$$

The constant Γ is a measure of the friction due to the bath. In the limit of strong friction, $\Gamma^{-1} \gg 1$, the second-order time derivative can be ignored, giving a first-order equation of motion usually referred to as Brownian dynamics. Let $P(\mathbf{q}_1, \dots, \mathbf{q}_N; t)$ be the probability to find particle 1 at position \mathbf{q}_1 , and so on at time t . Then, the corresponding Fokker–Planck equation is [151, 152]

$$\frac{\partial}{\partial t} P(\mathbf{q}_1, \dots, \mathbf{q}_N; t) = \Gamma \sum_{i=1}^N \frac{\partial}{\partial \mathbf{q}_i} \cdot \left\{ k_B T \frac{\partial}{\partial \mathbf{q}_i} + \sum_{j \neq i} \frac{\partial v(\mathbf{q}_{ij})}{\partial \mathbf{q}_i} \right\} P(\mathbf{q}_1, \dots, \mathbf{q}_N; t) \quad (225)$$

Following Evans and Archer [153], we proceed as in the derivation of the BBGKY hierarchy above. The one-body density is

$$\begin{aligned} \rho(\mathbf{r}_1; t) &= \left\langle \sum_i \delta(\mathbf{r}_1 - \mathbf{q}_i); t \right\rangle \\ &= \int \sum_i \delta(\mathbf{r}_1 - \mathbf{q}_i) P(\mathbf{q}_1, \dots, \mathbf{q}_N; t) d\mathbf{q}_1 \dots d\mathbf{q}_N \\ &= N \int P(\mathbf{r}_1, \mathbf{q}_2, \dots, \mathbf{q}_N; t) d\mathbf{q}_2 \dots d\mathbf{q}_N \end{aligned} \quad (226)$$

So that an equation for its time evolution can be obtained by integrating the Fokker–Planck equation to get

$$\frac{\partial}{\partial t} \rho(\mathbf{r}_1; t) = \Gamma \frac{\partial}{\partial \mathbf{r}_1} \left\{ k_B T \frac{\partial}{\partial \mathbf{r}_1} \rho(\mathbf{r}_1; t) + \int \frac{\partial v(\mathbf{r}_{12})}{\partial \mathbf{r}_1} \rho(\mathbf{r}_1, \mathbf{r}_2; t) d\mathbf{r}_2 \right\} \quad (227)$$

where

$$\rho(\mathbf{r}_1, \mathbf{r}_2; t) = N(N-1) \int P(\mathbf{r}_1, \mathbf{r}_2, \mathbf{q}_3, \dots, \mathbf{q}_N; t) d\mathbf{q}_3 \dots d\mathbf{q}_N \quad (228)$$

Assuming that the equilibrium configuration of the colloidal particles under the influence of a field will be the same as that of the particles in the absence of a bath,

Eq. (208) holds for the *equilibrium* one-body distribution. Introducing this here as an assumption of local equilibrium gives

$$\begin{aligned} \frac{\partial}{\partial t} \rho(\mathbf{r}; t) &= \Gamma \nabla \cdot \left\{ k_B T \nabla \rho(\mathbf{r}; t) + \rho(\mathbf{r}; t) \nabla \frac{\delta F_{\text{ex}}[\rho]}{\delta \rho(\mathbf{r}; t)} \right\} \\ &= \Gamma \nabla \cdot \left\{ \rho(\mathbf{r}; t) \nabla \frac{\delta F[\rho]}{\delta \rho(\mathbf{r}; t)} \right\} \end{aligned} \quad (229)$$

which is the expected result.

4. A Note on Interpretation

There has been some discussion in the literature on whether or not a fluctuating force should be included in the DDFT equation [143, 151, 153, 155]. In fact, a careful examination of the derivations should give the answer in any particular case. The confusion is due to the fact that the same symbol is used by different workers for different objects leading, for example, to claims that some results make no sense [151]. The most fundamental level of description concerns the time evolution of the microscopic density, $\hat{\rho}(\mathbf{r}, t) = \sum_i \delta(\mathbf{r} - \mathbf{q}_i(t))$. This is just the Liouville equation. At a mesoscopic level, one projects out all except the slow variables associated with the local values of the conserved densities of number, momentum, and energy [142]. This results in the generalized Langevin equation, an exact equation, which certainly contains a noise term. Note that the density that occurs in this (exact) equation need not be the microscopic density $\hat{\rho}(\mathbf{r}, t)$ but is more commonly some coarse-grained mesoscopic density $\tilde{\rho}(\mathbf{r}, t)$. The presence of the noise term means that not all of the averaging has been done and so the local density appearing in the equations is not the fully ensemble-averaged quantity, $\rho(\mathbf{r}, t)$. The “free energy” appearing in these equations is also not, strictly speaking, the free energy functional of DFT. Typically, the “free energy functional” is actually a quantity of the form

$$\exp(-\beta \mathcal{F}([\tilde{\rho}], [\phi]; t)) = \int \delta(\tilde{\rho}(\mathbf{r}) - \hat{\rho}(\mathbf{r})) f_{\text{eq}}(q_1 \dots q_N; \phi) dx_1 \dots dx_N \quad (230)$$

where $\hat{\rho}$ is the microscopic density function, $f_{\text{eq}}(q_1 \dots q_N; \phi)$ is the *equilibrium* distribution and the external field is ϕ . (Note that the equilibrium distribution appears here, rather than the non-equilibrium distribution, because of the definition of projection operators for which one chooses the equilibrium distribution as the measure in phase space. This is therefore *not* the result of a local equilibrium approximation.) The definition of the delta function is actually delicate and is perhaps best thought of in a course-grained sense. For example, space could be divided into (arbitrarily) small cells, $C^{(m)}$, of volume $V^{(m)}$ with centers at the points

$\mathbf{r}^{(m)}$ for $m = 1, \dots, M$, and the mesoscopic variables can be taken to be the densities in each cell,

$$\hat{\rho}^{(m)} = \frac{1}{V^{(m)}} \int_{C^{(m)}} \hat{\rho}(\mathbf{r}) d\mathbf{r}. \quad (231)$$

In this case, the precise meaning of the delta function is that it fixes the density in the m th cell to be some specified value, $\tilde{\rho}^{(m)}$,

$$\delta(\tilde{\rho}(\mathbf{r}) - \hat{\rho}(\mathbf{r})) \Rightarrow \prod_{m=1}^M \delta(\hat{\rho}^{(m)} - \tilde{\rho}^{(m)}) \quad (232)$$

Thus, the collection of values $\{\tilde{\rho}^{(m)}\}$ constitutes the ‘‘function’’ $\tilde{\rho}(\mathbf{r})$. Then, the actual free energy would be obtained by means of a further average,

$$\exp(-\beta F[\phi]) = \int_0^\infty d\tilde{\rho}^{(1)} \dots \int_0^\infty d\tilde{\rho}^{(M)} \exp(-\beta \mathcal{F}([\tilde{\rho}], [\phi])) \delta\left(N - \sum_{m=1}^M \tilde{\rho}^{(m)} V^{(m)}\right) \quad (233)$$

and it is the quantity $F[\phi]$ with which contact is made with DFT. (Note that in this expression, it is assumed that the number of particles is fixed; the same arguments could be made in the grand canonical ensemble.) The constrained ‘‘free energy’’ $\mathcal{F}([\tilde{\rho}], [\phi])$ is the one that is discussed in field-theoretic approaches to statistical mechanics and is well-approximated via a mean-field model [156]. The true free energy $F[\phi]$ is a result of averaging over the coarse-grained density and includes renormalization effects as discussed by Reguerra and Reiss [157]. In terms of DDFT, the dynamical equations for the mesoscopic density $\tilde{\rho}(\mathbf{r}, t)$ would include a noise term,

$$\frac{\partial}{\partial t} \tilde{\rho}(\mathbf{r}; t) = \Gamma_0 \mathbf{V} \cdot \left\{ \tilde{\rho}(\mathbf{r}; t) \mathbf{V} \frac{\delta F([\tilde{\rho}], [\phi])}{\delta \tilde{\rho}(\mathbf{r}; t)} \right\} + \eta(\mathbf{r}; t) \quad (234)$$

The ensemble-averaged density is then the result of averaging this over the noise (i.e., the remaining degrees of freedom)

$$\frac{\partial}{\partial t} \langle \tilde{\rho}(\mathbf{r}; t) \rangle_\eta = \Gamma_0 \mathbf{V} \cdot \left\{ \left\langle \tilde{\rho}(\mathbf{r}; t) \mathbf{V} \frac{\delta F([\tilde{\rho}], [\phi])}{\delta \tilde{\rho}(\mathbf{r}; t)} \right\rangle_\eta \right\} \quad (235)$$

or

$$\frac{\partial}{\partial t} \rho(\mathbf{r}; t) \simeq \Gamma \mathbf{V} \cdot \left\{ \rho(\mathbf{r}; t) \mathbf{V} \frac{\delta F([\rho])}{\delta \rho(\mathbf{r}; t)} \right\} \quad (236)$$

where it is noted that typically, transport coefficients like Γ_0 are renormalized by the evaluated. (This supposes that the cells used in the coarse graining are

sufficiently small that the noise-averaged coarse grained density and ensemble averaged density are the same.)

In the case of Brownian dynamics, the situation is completely analogous. In the derivation given above, the starting point—the Brownian dynamical equations—are the result of projecting out the degrees of freedom of a bath and so are already (an approximation to) the generalized Langevin equation. Statistical averages are then evaluated with respect to the noise and the one-body distribution is in fact $\rho(\mathbf{r}; t)$, the noise-averaged one-body density $\langle \tilde{\rho}(\mathbf{r}; t) \rangle_\eta$. Thus, one derives the equivalent of Eq. (235) and not Eq. (234). It might seem that there is some advantage in this approach, rather than the projection operator derivation, because one avoids coarse-graining. However, this ignores the fact that the concept of local equilibrium is itself based on the idea that the system can be divided into small volumes, each of which is in an equilibrium state, but with thermodynamic variables varying from volume to volume [130, 158]. The main advantage of the systematic approach, such as that of Kawasaki [137], over the heuristic invocation of local equilibrium is to make such assumptions explicit. However, in practical applications, the use of local equilibrium, particularly Eq. (208), may be the shortest route to a DDFT-like description.

5. Applications of DDFT

There have been many interesting uses of DDFT and here a sampling of the literature is given to illustrate the range of applications. Evans and Archer used it to study the kinetics of spinodal decomposition [153]. Archer, Hopkins, and Schmidt [159] used DDFT to calculate the van Hove dynamic correlation function for a simple fluid (the generalization of the static PDF giving the probability to find a particle at time t at position r , given that there is a particle at the origin at time 0). The results compared well with simulations of Brownian dynamics. Fraaije has performed a number of studies using DDFT to model the dynamics of block copolymer melts [160–162]. Dzubiella and Likos have used DDFT to study squeezing and relaxation of soft, Brownian particles in a time-dependent external field [163]. Their comparisons to Brownian dynamical simulations are very good. Van Teefelen, Likos, and Löwen used DDFT to study 2-D solid nucleation of particles interacting with an inverse cube potential [164]. Rex and Löwen have extended the theory for Brownian dynamics to include hydrodynamic interactions between the colloidal particles [165].

B. Energy Surface Methods and the Problem of Nucleation

One problem not easily treated with DDFT is that of systems crossing large energy barriers. The prototypical example of such a problem is the nucleation of one phase from another. For example, consider the problem of the nucleation of a vapor bubble in a superheated liquid. The superheated liquid is metastable, and random

thermal fluctuations cause the formation of bubbles. These will either shrink and die if they are too small, or will grow without bound if they are large enough, thus converting the system from one phase to another. Such transitions are of interest in many important circumstances, and the question of nucleation has gained renewed interest due to the discovery of multistep processes involved in the nucleation of crystals from solution in the case of proteins [166]. However, even the physical picture just described for the nucleation of vapor bubbles has recently been called into question [167–169], thus contributing to the renewed interest in this subject. In the remainder of this subsection, a simple DFT for bubble nucleation will be presented and the classical nucleation theory will be reviewed. Various approaches to the description of nucleation within DFT will be described, concluding with a discussion of the current status of the subject.

As discussed previously, from any DFT—including exact DFT—a gradient expansion can be constructed. Let us parameterize the local density for the problem of bubble nucleation as a spherically symmetric, piecewise continuous function,

$$\begin{aligned} \rho(\mathbf{r}) = & \bar{\rho}_0 \Theta(R-w-r) \\ & + \left(\bar{\rho}_0 + \frac{\bar{\rho}_\infty - \bar{\rho}_0}{2w} (r-R+w) \right) \Theta(R+w-r) \Theta(r-R+w) \\ & + \bar{\rho}_\infty \Theta(r-R) \end{aligned} \quad (237)$$

which simply says that the density is ρ_0 for $r < R-w$ and ρ_∞ for $r > R+w$ and that it varies linearly in the intermediate region. The gradient model free energy will have the form

$$\Omega[\rho] = \int \left(f(\rho(\mathbf{r})) + g(\rho(\mathbf{r})) \left(\frac{\partial \rho(\mathbf{r})}{\partial \mathbf{r}} \right)^2 - \mu \rho(\mathbf{r}) \right) d\mathbf{r} \quad (238)$$

where $f(\rho)$ is the (Helmholtz) free energy per unit volume in the bulk fluid. Substituting the parameterization into this expression gives a function, $F(\bar{\rho}_0, \bar{\rho}_\infty, R, w)$. However, this is still rather complicated so two simplifications are made. The first is to take the coefficient of the gradient to be independent of density, $g(\rho(\mathbf{r})) = g$. The second is to take the capillary approximation in which the width of the interface goes to zero, $w \rightarrow 0$, while keeping the combination $\gamma = g/(2w)^2$ constant. This then gives

$$\Omega = V(R)(f(\bar{\rho}_0) - \mu \bar{\rho}_0) + (V - V(R))(f(\bar{\rho}_\infty) - \mu \bar{\rho}_\infty) + \gamma(\bar{\rho}_\infty - \bar{\rho}_0)^2 S(R) \quad (239)$$

where $V(R) = \frac{4\pi}{3} R^3$, $S(R) = 4\pi R^2$ and V_0 is the overall volume of the system (assumed eventually to be infinite). The first two terms on the right are the free energy contributions of the bulk phases, and the third term is the contribution due to surface tension. For a given chemical potential, it is assumed that there is an

equilibrium bulk vapor with density determined from $f'(\bar{\rho}_v) = \mu$ and an equilibrium liquid with density satisfying $f'(\bar{\rho}_l) = \mu$. [We will use the notation $\bar{\rho}_v(\mu)$ and $\bar{\rho}_l(\mu)$ to denote the solutions to these equations.] The Classical Nucleation Theory (CNT) uses this free energy function with $\bar{\rho}_0 = \bar{\rho}_v(\mu)$ and $\bar{\rho}_\infty = \bar{\rho}_l(\mu)$, so that the free energy is a function of a single parameter, R , the radius of the bubble. The function is cubic in the radius and has minima at zero radius (the metastable fluid), at some finite radius (the critical bubble) and at infinite radius (the uniform vapor). A slightly more general theory is to treat these densities as unknowns and to note that DFT tells us that the free energy function should be a minimized with respect to its parameters, giving

$$\begin{aligned} 0 &= (V - V(R))(f'(\bar{\rho}_\infty) - \mu) + 2\gamma(\bar{\rho}_\infty - \bar{\rho}_0)S(R) \\ 0 &= V(R)(f'(\bar{\rho}_0) - \bar{\rho}_0) - 2\gamma(\bar{\rho}_\infty - \bar{\rho}_0)S(R) \\ 0 &= R^2((f(\bar{\rho}_0) - \mu\bar{\rho}_0) - (f(\bar{\rho}_\infty) - \mu\bar{\rho}_\infty)) + 2\gamma(\bar{\rho}_\infty - \bar{\rho}_0)^2R \end{aligned} \quad (240)$$

For a very large system, $V \gg V(R)$, the first equation implies that $0 = f'(\bar{\rho}_\infty) - \mu$, so that the outer density must be either $\bar{\rho}_v(\mu)$ or $\bar{\rho}_l(\mu)$: One chooses the former to describe bubble nucleation. The second and third equations then determine the values of the inner density and the radius. Note that one solution is $R = 0$, in which case the inner density is irrelevant and the system is bulk liquid. The solution for finite R corresponds to the critical radius. So long as $(f(\bar{\rho}_0) - \mu\bar{\rho}_0) < (f(\bar{\rho}_\infty) - \mu\bar{\rho}_\infty)$ and with V large, there will also be an extremum at $V(R) = V$ corresponding to the bulk vapor.

One aspect of nucleation that has long been treated with DFT is the determination of the height of the barrier to nucleation. This is because the barrier is defined by the critical nucleus — the metastable state that corresponds to a maximum of the free energy functional. The determination of this state from something like DFT goes back to Cahn and Hilliard [170], and calculations using more sophisticated DFT include the early work by Oxtoby and Evans [171] and Teng and Oxtoby [172]. (It is worth noting, however, that even in this case one is stretching DFT beyond its theoretical foundations. As shown in Section II, the only density to which unambiguous physical meaning can be attached is one that minimizes the free energy functional. Since the critical cluster *maximizes* the free energy functional, one is assuming, analogously to DDFT, that the free energy functional governs the dynamics of the transition and does not just define the equilibrium states.)

The question is how one might describe the transition from the liquid to the vapor—that is, all the points on the path that are not extrema of the free energy. In terms of the density, one notes that a system with a small bubble has more atoms, on average, than does a system with a large bubble since the gas density is lower than the liquid density. One might therefore try to stabilize a noncritical system by “minimizing the free energy for a fixed number of atoms.” This means

minimizing the free energy subject to the constraint

$$\int \rho(\mathbf{r})d\mathbf{r} = N \quad (241)$$

for some specified value of N . The natural way to do this is through the method of Lagrange multipliers. One forms the Lagrangian,

$$L(\alpha, [\rho]) = \Omega[\rho] - \alpha \left(\int \rho(\mathbf{r})d\mathbf{r} - N \right) \quad (242)$$

and then solves for the constrained minimum via

$$\frac{\delta L(\alpha, [\rho])}{\delta \rho(\mathbf{r})} = 0, \quad \frac{\partial L(\alpha, [\rho])}{\partial \alpha} = 0 \quad (243)$$

giving

$$\begin{aligned} \frac{\delta F[\rho]}{\delta \rho(\mathbf{r})} - \mu - \alpha &= 0 \\ \int \rho(\mathbf{r}; \mu, \alpha)d\mathbf{r} &= N \end{aligned} \quad (244)$$

Thus, the effect of this procedure is first to shift the chemical potential from μ to $\mu + \alpha$, then to solve for the extremum for the shifted chemical potential, and then to adjust α until the system has the desired number of atoms. The result of this calculation is simply the critical cluster for the shifted chemical potential $\mu' = \mu + \alpha$. Note in particular that for the example of bubble nucleation, the density far from the bubble will not be $\bar{\rho}_l(\mu)$ but, rather, $\bar{\rho}_l(\mu')$. Away from the critical point, the vapor density is quite small, so that the difference between $\bar{\rho}_v(\mu)$ and $\bar{\rho}_v(\mu + \alpha)$ is quite small. Thus, for the problem of *liquid droplet* nucleation in a vapor, this shift of the background is probably not too important. However, for the problem of *bubble nucleation* in a fluid, the shift from $\bar{\rho}_l(\mu)$ to $\bar{\rho}_l(\mu + \alpha)$ can be quite substantial, potentially affecting the physics. For this reason, other methods have been developed.

One variation of the constraint approach is to fix the number of atoms within some volume V_0 which is smaller than the system volume V ,

$$\int_{V_0} \rho(\mathbf{r})d\mathbf{r} = N \quad (245)$$

In this case, there are two parameters, the radius of the constrained volume, R_0 , and the number N . The Euler–Lagrange equation now takes the form

$$\frac{\delta F[\rho]}{\delta \rho(\mathbf{r})} - \mu - \alpha \Theta(R_0 - r) = 0 \quad (246)$$

so that in effect one has a discontinuous chemical potential. This necessarily leads to discontinuous density profiles unless $\alpha = 0$, which only happens for the critical cluster for the chemical potential μ : All subcritical and supercritical clusters will exhibit discontinuous profiles. Talanquer and Oxtoby [173] used this method to study droplet nucleation. However, rather than solve the Euler–Lagrange equation, Eq. (246), for $r > R_0$, they took V_0 to be much larger than the droplet and approximated the outer density as a constant that was adjusted so as to give a continuous density profile. This would appear to essentially be the same as the calculation described above with a shifted chemical potential everywhere. Uline and Corti used Eq. (246) as it stands, thereby obtaining discontinuous profiles [167]. Their results are particularly interesting because they report that supercritical bubbles become unstable so that no solution to the equations exists above some critical size. Their conclusion is that the assumption that the outer density is $\bar{\rho}_l(\mu)$ is no longer true, thus indicating something like a spinodal breakdown of the fluid. However, it is hard to see, physically, how a bubble of finite size can destabilize the fluid far away from the bubble. In fact, it was subsequently shown that using this constraint with the toy DFT given above, similar instabilities occur [168, 169]. This is disturbing because Eq. (239) is a smooth, continuous function of its arguments, so any such instability must be due to the constraint. Furthermore, another physically reasonable constraint was shown not to give such instabilities, so that the robustness of the constraint method must be questioned.

An alternative method has recently been proposed which appears to circumvent such problems [168, 169]. Just as classical DFT was inspired by methods developed in the context of ab initio quantum mechanical calculations, so the new technique is borrowed from the quantum chemistry community. In quantum chemistry, a subject of great interest is the determination of reaction pathways—that is, a description of how a complicated, many-body system transforms from one metastable configuration into another. What is known is the free energy surface governing the transition. Many methods have been developed, primarily within the last 20 years, for finding the most probable path for such transitions (see, e.g., Wales [174] and references therein). The problem of nucleation in classical systems is quite similar in that it is formulated as the desire to trace the path in density space by which the system transforms from a metastable uniform state to another, stable, uniform state. If one accepts the functional $\Omega[\rho]$ as governing the dynamics of the transition—as is done, for example, in DDFT—then the same energy surface methods can be used.

One approach is to consider a collection of $M + 1$ density functions, $\{\rho^{(m)}(\mathbf{r})\}_{m=0}^M$, where $\rho^{(0)}(\mathbf{r})$ is the initial metastable state, $\rho^{(M)}(\mathbf{r})$ is the final stable state, and the remaining states define a path between these two. For example, in the bubble nucleation problem, one has that $\rho^{(0)}(\mathbf{r}) = \bar{\rho}_l(\mu)$ and $\rho^{(M)}(\mathbf{r}) = \bar{\rho}_v(\mu)$. In between, in the toy model, one can choose the parameters

for the m th density, $\bar{\rho}_0^{(m)}$ and $R^{(m)}$, in a convenient way, say as $\bar{\rho}_0^{(m)} = \bar{\rho}_v(\mu)$ and $R^{(m)} = \frac{m}{M}R_V$ where R_V is the radius of the overall volume V . The goal is to adjust this chain of images, as they are called, so as to map out the most likely path between the endpoints in density space. As discussed in Wales [174], there are several ways to do this and here, a particularly simple one called the Nudged Elastic Band (NEB) [175] method is described.

Clearly, if one tried to minimize the total energy of the path, $E = \sum_{m=1}^{M-1} \Omega[\rho^{(m)}]$, the densities would all end up in one of the metastable states because these are, by definition, local minima. To map out the desired path, it is necessary to force the densities to remain evenly spaced, in some sense, along the path. In the NEB, this is done by adding fictitious elastic forces between neighboring images. However, simply adding the couplings is too crude because the elastic forces alter the effective free energy landscape. Instead, one wants to apply the elastic forces only *along* the path and to minimize the total energy in directions perpendicular to the path, with no elastic forces. The key then is to define, for each image, the direction in density space of the tangent to the current path. First, one defines an inner product and distance in density space,

$$\begin{aligned} \langle \rho^{(m)}, \rho^{(m')} \rangle &= \int \rho^{(m)}(\mathbf{r}) \rho^{(m')}(\mathbf{r}) d\mathbf{r} \\ d[\rho^{(m)}, \rho^{(m')}] &= \langle \rho^{(m)} - \rho^{(m')}, \rho^{(m)} - \rho^{(m')} \rangle^{1/2} \\ &= \left(\int (\rho^{(m)}(\mathbf{r}) - \rho^{(m')}(\mathbf{r}))^2 d\mathbf{r} \right)^{1/2} \end{aligned} \quad (247)$$

The tangent at image m is defined in terms of its neighbors, images $m-1$ and $m+1$, based on the local energy landscape. For example, if the energy is monotonically increasing, $\Omega[\rho^{(m-1)}] < \Omega[\rho^{(m)}] < \Omega[\rho^{(m+1)}]$, then the tangent at the image ρ_m , called t_m , is

$$t^{(m)}(\mathbf{r}) = \rho^{(m+1)}(\mathbf{r}) - \rho^{(m)}(\mathbf{r}) \quad (248)$$

and the normalized tangent, $\hat{t}^{(m)}(\mathbf{r}) = t^{(m)}(\mathbf{r}) / \langle t^{(m)}, t^{(m)} \rangle$. If the energy is monotonically decreasing, the tangent is based on $\rho^{(m)} - \rho^{(m-1)}$. For nonmonotonic neighbors, the heuristic is given in Ref. 175. The NEB method then consists of finding a configuration that gives zero NEB force. Let the “force” due to the actual free-energy surface be $\mathcal{F}^{(m)}(\mathbf{r}) = -\frac{\partial \beta \Omega[\rho^{(m)}]}{\partial \rho(\mathbf{r})}$. Then the NEB method consists of solving

$$0 = \mathcal{F}^{\perp(m)}(\mathbf{r}) + k \hat{t}^{(m)}(\mathbf{r}) (d[\rho^{(m+1)}, \rho^{(m)}] - d[\rho^{(m)}, \rho^{(m-1)}]) \quad (249)$$

where $\mathcal{F}^{\perp(m)}(\mathbf{r}) = \mathcal{F}^{(m)}(\mathbf{r}) - \hat{t}^{(m)}(\mathbf{r}) (\hat{t}^{(m)} * \mathcal{F}^{(m)})$ is the component of the thermodynamic force orthogonal to the tangent vector and k is the spring constant. Further details can be found in Refs. 168 and 169, where the NEB method is applied to the problems of bubble and droplet nucleation. For droplet nucleation, where a

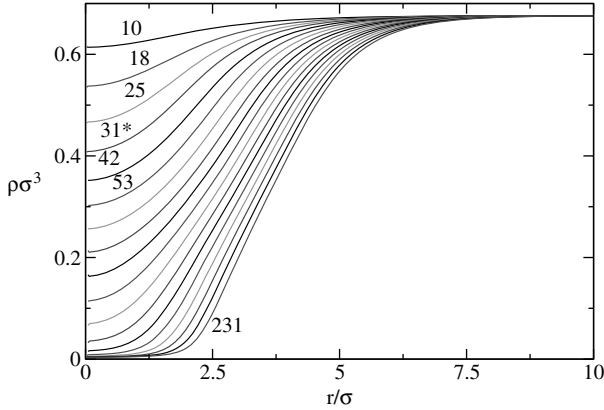


Figure 9. The process of bubble formation as calculated using the NEB and DFT for a Lennard-Jones fluid with $k_B T = 0.8\epsilon$ and supersaturation $\frac{\mu - \mu_{\text{coex}}}{\mu_{\text{coex}}} = -0.20$, where μ_{coex} is the value of the chemical potential at coexistence. The potential is truncated and shifted at a distance $r_c = 4\sigma$. The figure shows the density profile, $\rho(r)$, for the various images along the optimal path between the uniform liquid and the uniform gas. The size, in terms of the number of missing atoms relative to the background liquid, is given for several profiles and the critical profile is marked with an asterisk. From Lutsko [169].

significant amount of detailed simulation data is available, the method proves to be very accurate in locating and describing the critical cluster as well as in computing the shape of nucleation barrier. No sign of instabilities is found in these calculations. As shown in Fig. 9, the picture of bubble formation that emerges from these calculations is very different than that of CNT. Rather than forming as a gas-containing void with initially small radius that slowly grows, the bubble forms as a finite-sized region in which the density gradually decreases until it reaches something approaching the gas density. Only then does it begin to grow in radius; in the example shown, the growth occurs only long after the bubble has passed criticality. Very recently, a similar technique (but based on the String method [176], rather than the NEB) has been applied to the problem of capillary condensation [177].

VII. CONCLUSIONS

The main points to be drawn from the survey of the current state of DFT are as follows:

1. Classical DFT is based on a collection of exact theorems regarding the behavior of systems in the grand canonical ensemble. In some cases, such as the ideal gas, the quasi-zero-dimensional system, and one-dimensional hard rods, the exact excess free energy functional can be constructed.

2. Effective liquid theories and liquid-state-based perturbation theory continue to be used in many calculations because of their simplicity.
3. For realistic, three-dimensional, inhomogeneous systems, the best theory currently available is probably the Fundamental Measure Theory for hard spheres.
4. Most calculations for potentials other than hard spheres are performed using a sum of the hard-sphere excess free energy and a perturbative and/or mean-field treatment of the attractive part of the potential.
5. DFT is increasingly used to study non-equilibrium systems. Many models dating back to the 1970s include something like a local pressure expressed as a functional derivative of the free energy. More recently, Dynamic DFT, a generalization of the diffusion equation, is used to model overdamped systems. Other methods for exploring the energy surface are also being used to study problems involving large barriers such as homogeneous nucleation.

Acknowledgments

This work was supported in part by the European Space Agency under contract number ESA AO-2004-070.

APPENDIX A: DFT FOR HARD RODS

The statistical mechanics of hard rods can be completely solved as discussed, for example, in Ref. 70. Surprisingly, it was only in 1976 that Percus first explicitly worked out the structure of DFT for hard rods [9]. The presentation here follows his work closely.

The great simplification of hard spheres in one dimension is that (a) they only interact with their two nearest neighbors and (b) they cannot move past one another. The second property means that we can, without loss of generality, label a finite collection of hard rods such that $q_1 < q_2 < \dots < q_n$. Hence, if the system is subject to a one-body potential, $\phi(r)$, the grand partition function is

$$\Xi(\beta, \mu; [\phi]) = 1 + \int_{-\infty}^{\infty} \exp(-\beta\tilde{\phi}(q_1))dq_1 + \sum_{n=2}^{\infty} \int_{-\infty}^{\infty} \exp\left(-\beta\sum_{i=1}^n \tilde{\phi}(q_i)\right) W(q_1, \dots, q_n) dq_1, \dots, dq_n \quad (\text{A1})$$

where $\tilde{\phi}(r) \equiv \phi(r) - \mu$ and

$$W(q_1, \dots, q_n) \equiv \Theta(q_2 - q_1 - d) \dots \Theta(q_n - q_{n-1} - d) \quad (\text{A2})$$

The one-body density is

$$\rho(r) = \langle \hat{\rho}(r) \rangle = -k_B T \frac{\delta \ln \Xi}{\delta \phi(r)} \quad (\text{A3})$$

$$\begin{aligned} &= \Xi^{-1} \exp(-\beta \tilde{\phi}(r)) \\ &+ \Xi^{-1} \sum_{n=2}^{\infty} \sum_{k=1}^n \left\{ \int_{-\infty}^{\infty} \exp\left(-\beta \sum_{i=1}^{k-1} \tilde{\phi}(q_i)\right) \right. \\ &\quad \left. \times W(q_1, \dots, q_{k-1}, r) dq_1, \dots, dq_{k-1} \right\}^{(k=1)} \end{aligned} \quad (\text{A4})$$

$$\begin{aligned} &\times \exp(-\beta \tilde{\phi}(r)) \left\{ \int_{-\infty}^{\infty} \exp\left(-\beta \sum_{i=k+1}^n \tilde{\phi}(q_i)\right) \right. \\ &\quad \left. \times W(r, q_{k+1}, \dots, q_n) dq_{k+1}, \dots, dq_n \right\}^{(k=n)} \end{aligned} \quad (\text{A5})$$

where the notation $\{\dots\}^{(k=r)}$ means that the bracket should be set equal to 1 if $k=r$. Relabeling the dummy integration variables q_{k+1}, \dots, q_n allows the last term in brackets to be written as

$$\begin{aligned} &\int_{-\infty}^{\infty} \exp\left(-\beta \sum_{i=k+1}^n \tilde{\phi}(q_i)\right) W(r, q_{k+1}, \dots, q_n) dq_{k+1}, \dots, dq_n \\ &= \int_{-\infty}^{\infty} \exp\left(-\beta \sum_{i=1}^{n-k} \tilde{\phi}(q_i)\right) W(r, q_1, \dots, q_{n-k}) dq_1 \dots dq_{n-k} \end{aligned} \quad (\text{A6})$$

Then, noting that

$$\sum_{n=1}^{\infty} \sum_{k=1}^n X(k, n) = \sum_{k=1}^{\infty} \sum_{n=k}^{\infty} X(k, n) = \sum_{k=1}^{\infty} \sum_{m=1}^{\infty} X(k, m+k-1) \quad (\text{A7})$$

allows this to be written as

$$\begin{aligned} \rho(r) &= \Xi^{-1} \sum_{k=1}^{\infty} \sum_{m=1}^{\infty} \exp(-\beta \mu(m+k-1)) \\ &\quad \times \left\{ \int_{-\infty}^{\infty} \exp\left(-\beta \sum_{i=1}^{k-1} \tilde{\phi}(q_i)\right) W(q_1, \dots, q_{k-1}, r) dq_1 \dots dq_{k-1} \right\}^{(k=1)} \\ &\quad \times \exp(-\beta \phi(r)) \left\{ \int_{-\infty}^{\infty} \exp\left(-\beta \sum_{i=1}^{m-1} \tilde{\phi}(q_i)\right) \right. \\ &\quad \left. \times W(r, q_1, \dots, q_{m-1}) dq_1 \dots dq_{m-1} \right\}^{(m=1)} \end{aligned} \quad (\text{A8})$$

which clearly factorizes into the product of terms that resemble the grand partition function. It is convenient to define a more general function of two variables as

$$\begin{aligned}
 & \Xi(x, y; \beta, \mu; [\phi]) \\
 &= \Theta(y - (x + d)) \sum_{n=1}^{\infty} \left\{ \int_{-\infty}^{\infty} \exp\left(-\beta \sum_{i=1}^{n-1} \tilde{\phi}(q_i)\right) \right. \\
 & \quad \times W(x, q_1, \dots, q_{n-1}, y) dq_1, \dots, dq_{n-1} \left. \right\}^{(n=1)} \\
 &= \Theta(y - (x + d)) + \Theta(y - (x + d)) \sum_{k=1}^{\infty} \int_{-\infty}^{\infty} \exp\left(-\beta \sum_{i=1}^k \tilde{\phi}(q_i)\right) \\
 & \quad \times W(x, q_1, \dots, q_k, y) dq_1 \dots dq_k
 \end{aligned} \tag{A9}$$

so that $\Xi(\beta, \mu; [\phi]) = \Xi(-\infty, \infty; \beta, \mu; [\phi])$. Then, one has that

$$\rho(r) = \exp(-\beta \tilde{\phi}(r)) \Xi(-\infty, r; \beta, \mu; [\phi]) \Xi(r, \infty; \beta, \mu; [\phi]) \Xi^{-1}(-\infty, \infty; \beta, \mu; [\phi]) \tag{A10}$$

Now, simple differentiation gives

$$\begin{aligned}
 \frac{\partial}{\partial x} \Xi(x, y) &= -\delta(y - (x + d)) - \exp(-\beta \tilde{\phi}(x + d)) \Xi(x + d, y) \\
 \frac{\partial}{\partial y} \Xi(x, y) &= \delta(y - (x + d)) + \exp(-\beta \tilde{\phi}(y - d)) \Xi(x, y - d)
 \end{aligned} \tag{A11}$$

and, in particular,

$$\begin{aligned}
 \frac{\partial}{\partial r} \Xi(r, \infty) &= -\exp(-\beta \tilde{\phi}(r + d)) \Xi(r + d, \infty) \\
 &= -\rho(r + d) \Xi(-\infty, \infty) / \Xi(-\infty, r + d) \\
 \frac{\partial}{\partial r} \Xi(-\infty, r) &= \exp(-\beta \tilde{\phi}(r - d)) \Xi(-\infty, r - d) \\
 &= \rho(r - d) \Xi(-\infty, \infty) / \Xi(r - d, \infty)
 \end{aligned} \tag{A12}$$

Note that the second equation implies

$$\frac{\partial}{\partial r} \Xi(-\infty, r + d) = \rho(r) \Xi(-\infty, \infty) / \Xi(r, \infty) \tag{A13}$$

Combined with the first line of Eq. (A13), one has that

$$\frac{\partial}{\partial r} \Xi(r, \infty) \Xi(-\infty, r + d) = (\rho(r) - \rho(r + d)) \Xi(-\infty, \infty) \tag{A14}$$

so

$$\Xi(x, \infty)\Xi(-\infty, x+d) = \Xi(-\infty, \infty) - \Xi(-\infty, \infty) \int_x^{x+d} \rho(r) dr \quad (\text{A15})$$

where the integration constant is fixed by assuming that the density vanishes sufficiently fast as $r \rightarrow \infty$, the limit $x \rightarrow \infty$. With this result, Eq. (A13) can now be written as

$$\begin{aligned} \frac{\partial}{\partial r} \Xi(r, \infty) &= \frac{-\rho(r+d)\Xi(r, \infty)}{1 - \int_r^{r+d} \rho(y) dy} \\ \frac{\partial}{\partial r} \Xi(-\infty, r) &= \frac{\rho(r-d)\Xi(-\infty, r)}{1 - \int_{r-d}^r \rho(y) dy} \end{aligned} \quad (\text{A16})$$

giving

$$\begin{aligned} \ln \Xi(x, \infty) &= \ln \Xi(-\infty, \infty) - \int_{-\infty}^x \frac{\rho(r+d)}{1 - \int_r^{r+d} \rho(y) dy} dr \\ \ln \Xi(-\infty, x) &= \ln \Xi(-\infty, \infty) - \int_x^{\infty} \frac{\rho(r-d)}{1 - \int_{r-d}^r \rho(y) dy} dr \end{aligned} \quad (\text{A17})$$

where, again, the integration constants are fixed by taking the limit $x \rightarrow \mp \infty$. The opposite limits, $x \rightarrow \pm \infty$, then give

$$\begin{aligned} \ln \Xi(-\infty, \infty) &= \int_{-\infty}^{\infty} \frac{\rho(r+d)}{1 - \int_r^{r+d} \rho(y) dy} dr = \int_{-\infty}^{\infty} \frac{\rho(r+d/2)}{1 - \int_{-d/2}^{d/2} \rho(r+y) dy} dr \\ \ln \Xi(-\infty, \infty) &= \int_{-\infty}^{\infty} \frac{\rho(r-d)}{1 - \int_{r-d}^r \rho(y) dy} dr = \int_{-\infty}^{\infty} \frac{\rho(r-d/2)}{1 - \int_{-d/2}^{d/2} \rho(r+y) dy} dr \end{aligned} \quad (\text{A18})$$

These can be combined to give the symmetric form:

$$\ln \Xi(-\infty, \infty) = \int_{-\infty}^{\infty} \frac{\frac{1}{2}(\rho(r+d/2) + \rho(r-d/2))}{1 - \int_{-d/2}^{d/2} \rho(r+y) dy} dr \quad (\text{A19})$$

Extensions to sticky hard spheres and to mixtures of hard spheres have also been given [71, 178].

To make contact with the density functional formalism, note that the field does not occur in this expression: It is the equivalent of Eq. (23) giving the grand potential at equilibrium, after the field has been eliminated. To get $F[n]$, we use

Eq. (A15) in Eq. (A10) and take the log to get

$$\begin{aligned}
\frac{\delta\beta F[\rho]}{\delta\rho(\mathbf{r})} &= -\beta\tilde{\phi}(r) = \ln\rho(r) - \ln\Xi(-\infty, r) - \ln\Xi(r, \infty) + \ln\Xi(-\infty, \infty) \\
&= \ln\rho(r) + \int_{-\infty}^r \left(-\frac{\rho(x-d)}{1 - \int_{x-d}^x \rho(y)dy} + \frac{\rho(x+d)}{1 - \int_x^{x+d} \rho(y)dy} \right) dr \\
&= \ln\rho(r) - \int_{-\infty}^{r-d/2} \left(\frac{\rho(x-d/2)}{1 - \int_{-d/2}^{d/2} \rho(x+y)dy} \right) dr \\
&\quad + \int_{-\infty}^{r+d/2} \left(\frac{\rho(x+d/2)}{1 - \int_{-d/2}^{d/2} \rho(x+y)dy} \right) dr \\
&= \ln\rho(r) - \frac{1}{2} \ln \left(1 - \int_{r-d}^r \rho(y)dy \right) - \frac{1}{2} \ln \left(1 - \int_r^{r+d} \rho(y)dy \right) \\
&\quad + \frac{1}{2} \int_{-r-d/2}^{r+d/2} \left(\frac{\rho(x+d/2) + \rho(x-d/2)}{1 - \int_{-d/2}^{d/2} \rho(x+y)dy} \right) dr \tag{A20}
\end{aligned}$$

Performing the functional integration gives

$$\beta F[\rho] = \beta F_{\text{id}}[\rho] - \int \frac{1}{2} (\rho(x+d/2) + \rho(x-d/2)) \ln \left(1 - \int_{-d/2}^{d/2} \rho(x+y)dy \right) dr \tag{A21}$$

In principle, there could be a density-independent integration constant, but this is of no relevance.

APPENDIX B: FMT TWO-BODY TERM

The FMT two-body contribution is

$$F_2 = - \int d\mathbf{r} \psi(\eta(\mathbf{r})) \int d\mathbf{s}_1 d\mathbf{s}_2 \rho(\mathbf{r} + \mathbf{s}_1) w(s_1) \rho(\mathbf{r} + \mathbf{s}_2) w(s_2) P(\mathbf{s}_1, \mathbf{s}_2) \tag{B1}$$

The effect of the kernel $P(\mathbf{s}_1, \mathbf{s}_2)$ is to couple what would otherwise be two factors of $s(\mathbf{r})$. To see what kind of contribution this gives when the density is a sum of delta functions, consider the integral

$$\begin{aligned}
&\int d\mathbf{s}_1 d\mathbf{s}_2 \delta(\mathbf{r} + \mathbf{s}_1) w(s_1) \delta(\mathbf{r} + \mathbf{s}_2 - \mathbf{R}) w(s_2) P(\mathbf{s}_1, \mathbf{s}_2) \\
&= \left(\frac{1}{4\pi(d/2)^2} \right)^2 \delta \left(r - \frac{d}{2} \right) \delta \left(|\mathbf{R} - \mathbf{r}| - \frac{d}{2} \right) P(-\mathbf{r}, \mathbf{R} - \mathbf{r}) \tag{B2}
\end{aligned}$$

Since the kernel is a scalar, assume it is a function of the scalar product of its arguments, $P(\mathbf{s}_1, \mathbf{s}_2) = P(\mathbf{s}_1 \cdot \mathbf{s}_2)$. Let \mathbf{R} define the z -direction in the r integral so that $\mathbf{R} \cdot \mathbf{r} = Rr\cos x$ where x is the azimuthal variable. Using the fact that the first delta function fixes the value of r and using the usual rules for change of variable in the second delta function gives

$$\begin{aligned} & \int d\mathbf{s}_1 d\mathbf{s}_2 \delta(\mathbf{r} + \mathbf{s}_1) w(s_1) \delta(\mathbf{r} + \mathbf{s}_2 - \mathbf{R}) w(s_2) P(\mathbf{s}_1, \mathbf{s}_2) \\ &= \left(\frac{1}{4\pi(d/2)^2} \right)^2 \delta\left(r - \frac{d}{2}\right) \frac{\delta(x - R/d)}{R} P\left(\left(\frac{d}{2}\right)^2 - \left(\frac{R^2}{2}\right)\right) \end{aligned} \quad (\text{B3})$$

Assuming that $\lim_{R \rightarrow 0} P\left(\left(\frac{d}{2}\right)^2 - \left(\frac{R^2}{2}\right)\right)/R = 0$, one immediately finds

$$\begin{aligned} F_2 &= -2N_1 N_2 \left(\frac{1}{4\pi(d/2)^2} \right)^2 R^{-1} P\left(\left(\frac{d}{2}\right)^2 - \left(\frac{R^2}{2}\right)\right) \\ &\quad \times \int d\mathbf{r} \psi(\boldsymbol{\eta}(\mathbf{r})) \delta\left(r - \frac{d}{2}\right) \delta(x - R/d) \\ &= -2N_1 N_2 \left(\frac{1}{4\pi(d/2)^2} \right)^2 P\left(\left(\frac{d}{2}\right)^2 - \left(\frac{R^2}{2}\right)\right) \\ &\quad \times \int d\mathbf{r} \psi(\boldsymbol{\eta}(\mathbf{r})) \delta\left(r - \frac{d}{2}\right) \delta\left(|\mathbf{R} - \mathbf{r}| - \frac{d}{2}\right) \end{aligned} \quad (\text{B4})$$

This integral is easily evaluated as a limit of the case that the cavities have different diameters, d_1 and d_2 . Writing $\psi(\boldsymbol{\eta}) = \frac{\partial^2}{\partial \boldsymbol{\eta}^2} \psi_0(\boldsymbol{\eta})$ gives

$$\begin{aligned} F_2 &= -2 \left(\frac{1}{4\pi(d/2)^2} \right)^2 P\left(\left(\frac{d}{2}\right)^2 - \left(\frac{R^2}{2}\right)\right) \\ &\quad \times \lim_{d_1, d_2 \rightarrow d} \frac{\partial^2}{\partial(d_1/2) \partial(d_2/2)} \int d\mathbf{r} \psi_0(\boldsymbol{\eta}(\mathbf{r})) \\ &= -2 \left(\frac{1}{4\pi(d/2)^2} \right)^2 P\left(\left(\frac{d}{2}\right)^2 - \left(\frac{R^2}{2}\right)\right) \\ &\quad \times \lim_{d_1, d_2 \rightarrow d} 4 \frac{\partial^2}{\partial d_1 \partial d_2} (|V_1 - V_{12}| \psi_0(N_1) + |V_2 - V_{12}| \psi_0(N_2) + |V_{12}| \psi_0(N)) \\ &= -2 \left(\frac{1}{4\pi(d/2)^2} \right)^2 P\left(\left(\frac{d}{2}\right)^2 - \left(\frac{R^2}{2}\right)\right) \frac{\pi d^2}{2R} (\psi_0(N) - \psi_0(N_1) - \psi_0(N_2)) \end{aligned} \quad (\text{B5})$$

The sum gives the exact result, provided that $\psi_0(\eta) = \Phi_0(\eta)$ and

$$-2 \left(\frac{1}{4\pi(d/2)^2} \right)^2 P \left(\left(\frac{d}{2} \right)^2 - \frac{R^2}{2} \right) \frac{\pi d^2}{2R} = \frac{R}{d} \quad (\text{B6})$$

Simplification gives

$$P \left(\frac{d^2}{4} - \frac{R^2}{2} \right) = -\pi d R^2 \quad (\text{B7})$$

or

$$P(y) = -\pi d \left(\frac{d^2}{2} - 2y \right) = -4\pi \frac{d}{2} \left(\frac{d^2}{4} - y \right) \quad (\text{B8})$$

Putting this together gives the two-body contribution

$$\begin{aligned} F_2 &= 4\pi \frac{d}{2} \left(\frac{1}{4\pi(d/2)^2} \right)^2 \int d\mathbf{r} \psi''_0(\eta(\mathbf{r})) \\ &\quad \times \int d\mathbf{s}_1 d\mathbf{s}_2 \rho(\mathbf{r} + \mathbf{s}_1) w(\mathbf{s}_1) \rho(\mathbf{r} + \mathbf{s}_2) w(\mathbf{s}_2) \left(\frac{d^2}{4} - \mathbf{s}_1 \cdot \mathbf{s}_2 \right) \\ &= \frac{1}{2\pi d} \int d\mathbf{r} \psi''_0(\eta(\mathbf{r})) (s^2(\mathbf{r}) - v^2(\mathbf{r})) \end{aligned} \quad (\text{B9})$$

which is the same as the second contribution to the Rosenfeld functional.

APPENDIX C: PROOF OF THE WALL THEOREM FOR THE VDW MODEL

Here, the proof of the wall theorem is given for VdW models such as given in Eqs. (190)–(193). The location of the wall is taken to be $z = 0$, and the system is uniform in the other directions. It therefore follows that the potential and the FMT weights can be integrated over the directions parallel to the wall and all quantities become one-dimensional functions of z [see, e.g., Eq. (163)]. Restricting attention to the region $z > 0$, the Euler–Lagrange equation is

$$0 = \ln \rho(z_1) + \int dz_2 \frac{\partial \Phi(z_2; [\rho])}{\partial n_\alpha(z_2)} w_\alpha(z_{21}) - \mu + \int_{-\infty}^{\infty} w(z_{12}) \rho(z_2) dz_2 \quad (\text{C1})$$

Differentiating with respect to z_1 and multiplying through by $\rho(z_1)$ gives

$$0 = \frac{d\rho(z_1)}{dz_1} + \int_{-\infty}^{\infty} dz_2 \frac{\partial\Phi(z_2; [\rho])}{\partial n_\alpha(z_2)} \rho(z_1) \frac{d}{dz_1} w_\alpha(z_{21}) + \int_{-\infty}^{\infty} \rho(z_1) \left(\frac{d}{dz_1} w(z_{12}) \right) \rho(z_2) dz_2 \quad (\text{C2})$$

Now, we make two important assumptions. First is that there is some point $z_B > 0$ such that for $z > z_B$, the density is indistinguishable from the bulk: $\rho(z) = \rho_l(\mu)$, where the bulk density is determined by the imposed chemical potential. Second, we assume that the potential tail has a finite range r_c . We now integrate Eq. (C2) from an initial point at the wall, 0_+ , to a point z_b that is sufficiently far in the bulk region that $z_b > z_B + z_c$ and $z_b > z_B + d$. This gives

$$0 = \rho(z_b) - \rho(0_+) + \int_{-\infty}^{\infty} dz_2 \frac{\partial\Phi(z_2; [\rho])}{\partial n_\alpha(z_2)} \int_{0_+}^{z_b} \rho(z_1) \frac{d}{dz_1} w_\alpha(z_{21}) dz_1 + \int_{0_+}^{z_b} dz_1 \int_0^{\infty} \rho(z_1) \left(\frac{d}{dz_1} w(z_{12}) \right) \rho(z_2) dz_2 \quad (\text{C3})$$

where the fact that $\rho(z) = 0$ for $z < 0$ has been used. Now, by assumption, $\rho(z_b) = \rho_l(\mu)$, so this can be rearranged to give

$$\rho(0_+) = \rho_l(\mu) + I_{\text{FMT}} + I_{\text{MF}} \quad (\text{C4})$$

The mean field contribution is

$$I_{\text{MF}} = \int_{0_+}^{z_b} dz_1 \int_{0_+}^{\infty} \rho(z_1) \left(\frac{d}{dz_1} w(z_{12}) \right) \rho(z_2) dz_2 = \int_{0_+}^{z_b} dz_1 \int_{0_+}^{z_b} \rho(z_1) \left(\frac{d}{dz_1} w(z_{12}) \right) \rho(z_2) dz_2 + \int_{0_+}^{z_b} dz_1 \int_{z_b}^{\infty} \rho(z_1) \left(\frac{d}{dz_1} w(z_{12}) \right) \rho(z_2) dz_2 \quad (\text{C5})$$

The first term on the right vanishes since it is odd under a relabeling $z_1 \leftrightarrow z_2$. Thus

$$I_{\text{MF}} = \int_{0_+}^{z_b} dz_1 \int_{z_b}^{\infty} \rho(z_1) \left(\frac{d}{dz_1} w(z_{12}) \right) \rho(z_2) dz_2 = \rho_l(\mu) \int_{0_+}^{z_b} dz_1 \int_{z_b}^{\infty} \rho(z_1) \left(\frac{d}{dz_1} w(z_{12}) \right) dz_2 = \rho_l(\mu) \int_{0_+}^{z_b} \rho(z_1) w(z_1 - z_b) dz_1 \quad (\text{C6})$$

Making use of the finite range of the potential

$$I_{\text{MF}} = \rho_l(\mu) \int_{z_b-r_c}^{z_b} \rho(z_1) w(z_1-z_b) dz_1 \quad (\text{C7})$$

and since, by hypothesis, z_b-r_c is still in the bulk region, this gives

$$\begin{aligned} I_{\text{MF}} &= \rho_l(\mu)^2 \int_{z_b-r_c}^{z_b} w(z_1-z_b) dz_1 \\ &= \rho_l(\mu)^2 \int_0^{r_c} w(z_1) dz_1 \end{aligned} \quad (\text{C8})$$

The FMT contribution is

$$\begin{aligned} I_{\text{FMT}} &= \int_{-\infty}^{\infty} dz_2 \frac{\partial \Phi(z_2; [\rho])}{\partial n_\alpha(z_2)} \int_{0_+}^{z_b} \rho(z_1) \frac{d}{dz_1} w_\alpha(z_{21}) dz_1 \\ &= - \int_{-\infty}^{\infty} dz_2 \frac{\partial \Phi(z_2; [\rho])}{\partial n_\alpha(z_2)} \int_{0_+}^{\infty} \rho(z_1) \frac{d}{dz_2} w_\alpha(z_{21}) dz_1 \\ &\quad + \int_{-\infty}^{\infty} dz_2 \frac{\partial \Phi(z_2; [\rho])}{\partial n_\alpha(z_2)} \int_{z_b}^{\infty} \rho(z_1) \frac{d}{dz_2} w_\alpha(z_{21}) dz_1 \\ &= - \int_{-\infty}^{\infty} dz_2 \frac{\partial \Phi(z_2; [\rho])}{\partial n_\alpha(z_2)} \frac{dn_\alpha(z_2)}{dz_2} \\ &\quad + \rho_l(\mu) \int_{-\infty}^{\infty} dz_2 \frac{\partial \Phi(z_2; [\rho])}{\partial n_\alpha(z_2)} \int_{z_b}^{\infty} \frac{d}{dz_2} w_\alpha(z_{21}) dz_1 \end{aligned} \quad (\text{C9})$$

The first term is an exact differential

$$\int_{-\infty}^{\infty} dz_2 \frac{\partial \Phi(z_2; [\rho])}{\partial n_\alpha(z_2)} \int_{0_+}^{\infty} \rho(z_1) \frac{d}{dz_2} w_\alpha(z_{21}) dz_1 = f_{\text{ex}}^{\text{HS}}(\rho_\infty d^3) - f_{\text{ex}}^{\text{HS}}(\rho_{-\infty} d^3) \quad (\text{C10})$$

where $f_{\text{ex}}^{\text{HS}}(\rho d^3)$ is the excess free energy per unit volume in the hard-sphere fluid. The second term is

$$\begin{aligned} &\rho_l(\mu) \int_{-\infty}^{\infty} dz_2 \frac{\partial \Phi(z_2; [\rho])}{\partial n_\alpha(z_2)} \int_{z_b}^{\infty} \frac{d}{dz_2} w_\alpha(z_{21}) dz_1 \\ &= \rho_l(\mu) \int_{-\infty}^{\infty} dz_2 \frac{\partial \Phi(z_2; [\rho])}{\partial n_\alpha(z_2)} w_\alpha(z_2-z_b) \end{aligned} \quad (\text{C11})$$

Now, the function $w_\alpha(z_{21})$ is only nonzero in the range $-d/2 < z_{21} < d/2$; so as long as $z_b - d/2$ is in the bulk region, one has that

$$\rho_l(\mu) \int_{-\infty}^{\infty} dz_2 \frac{\partial \Phi(z_2; [\rho])}{\partial n_\alpha(z_2)} \int_{z_b}^{\infty} \frac{d}{dz_2} w_\alpha(z_{21}) dz_1 = \rho_l(\mu) \frac{\partial f_{\text{HS}}(\rho_b d^3)}{\partial \rho_b} \quad (\text{C12})$$

Thus

$$I_{\text{FMT}} = -f_{\text{ex}}^{\text{HS}}(\rho_l(\mu) d^3) + \rho_l(\mu) \frac{\partial f_{\text{ex}}^{\text{HS}}(\rho_l(\mu) d^3)}{\partial \rho_l(\mu)} = \beta P_{\text{ex}}^{\text{HS}}(\rho_l(\mu) d^3) \quad (\text{C13})$$

The final result is

$$\rho(0_+) = \rho_l(\mu) + \beta P_{\text{ex}}^{\text{HS}}(\rho_l(\mu) d^3) + \rho_l(\mu)^2 \int_0^{r_c} w(z_1) dz_1 = \beta P(\rho_l(\mu)) \quad (\text{C14})$$

References

1. J. S. Rowlinson, *J. Stat. Phys.* **20**, 197 (1979).
2. J. D. van der Waals, *Z. Phys. Chem.* **13**, 657 (1894).
3. V. Ginzburg and L. Landau, *Zh. Eksp. Teor. Fiz.* **20**, 1064 (1950).
4. J. W. Cahn and J. E. Hilliard, *J. Chem. Phys.* **28**, 258 (1958).
5. N. D. Mermin, *Phys. Rev.* **137**, A1441 (1965).
6. T. V. Ramakrishnan and M. Yussouff, *Phys. Rev. B* **19**, 2775 (1979).
7. C. Ebner, W. F. Saam, and D. Stroud, *Phys. Rev. A* **14**, 2264 (1976).
8. W. F. Saam and C. Ebner, *Phys. Rev. A* **15**, 2566 (1977).
9. J. K. Percus, *J. Stat. Phys.* **15**, 505 (1976).
10. H. Reiss, H. L. Frisch, and J. L. Lebowitz, *J. Chem. Phys.* **31**, 369 (1959).
11. E. Helfand, H. Reiss, H. L. Frisch, and J. L. Lebowitz, *J. Chem. Phys.* **33**, 1379 (1960).
12. H. Reiss and R. V. Casberg, *J. Chem. Phys.* **61**, 1107 (1974).
13. R. Evans, *Adv. Phys.* **28**, 143 (1979).
14. R. Evans, in *Fundamentals of Inhomogeneous Fluids*, D. Henderson, editor, Marcel Dekker, New York, 1992.
15. M. Baus and J. F. Lutsko, *Physica A* **176**, 28 (1991).
16. H. Löwen, *Phys. Rep.* **237**, 249 (1994).
17. J. Wu, *AIChE J.* **52**, 1169 (2006).
18. S. L. Singh and Y. Singh, *Euro. Phys. Lett.* **88**, 16005 (2009).
19. P. Chaudhuri, S. Karmakar, C. Dasgupta, H. R. Krishnamurthy, and A. K. Sood, *Phys. Rev. Lett.* **95**, 248301 (2005).
20. S. van Teeffelen, C. N. Likos, N. Hoffmann, and H. Löwen, *Europhys. Lett.* **75**, 583 (2006).
21. J.-P. Hansen and I. McDonald, *Theory of Simple Liquids*, Academic Press, San Diego, CA, 1986.
22. T. Frankel, *The Geometry of Physics*, Cambridge University Press, Cambridge, UK, 1997.
23. J. K. Percus, in *The Equilibrium Theory of Classical Fluids*, H. L. Frisch and H. L. Lebowitz, editors, Benjamin, New York, 1964.

24. J. K. Percus, *Phys. Rev. Lett.* **8**, 462 (1962).
25. J. F. Lutsko and M. Baus, *Phys. Rev. A* **41**, 6647 (1990).
26. M. Baus and J. L. Colot, *Mol. Phys.* **56**, 804 (1985).
27. M. Baus, J. L. Colot, and H. Xu, *Mol. Phys.* **57**, 809 (1986).
28. B. Groh and B. Mulder, *Phys. Rev. E* **61**, 3811 (2000).
29. J. F. Lutsko, *Physica A* **366**, 229 (2006).
30. A. D. J. Haymet and D. W. Oxtoby, *J. Chem. Phys.* **74**, 2559 (1981).
31. D. W. Oxtoby and A. D. J. Haymet, *J. Chem. Phys.* **76**, 6262 (1982).
32. H. Löwen, T. Beier, and H. Wagner, *Europhys. Lett.* **9**, 791 (1989).
33. H. Löwen, T. Beier, and H. Wagner, *Z. Phys. B* **79**, 109 (1990).
34. P. Tarazona, *Phys. Rev. E* **47**, 4284 (1993).
35. J.-J. Weis, *Mol. Phys.* **28**, 187 (1974).
36. W. A. Curtin, *J. Chem. Phys.* **88**, 7050 (1988).
37. M. Baus and J. L. Colot, *Mol. Phys.* **55**, 653 (1985).
38. M. Baus, *J. Phys.: Cond. Matt.* **1**, 3131 (1989).
39. J. F. Lutsko and M. Baus, *Phys. Rev. Lett.* **64**, 761 (1990).
40. W. A. Curtin and N. W. Ashcroft, *Phys. Rev. A* **32**, 2909 (1985).
41. A. R. Denton and N. W. Ashcroft, *Phys. Rev. A* **39**, 4701 (1985).
42. J. F. Lutsko, *J. Chem. Phys.* **128**, 184711 (2008).
43. P. Tarazona, *Phys. Rev. A* **31**, 2672 (1985).
44. D. Hendersen and E. W. Grundke, *J. Chem. Phys.* **63**, 601 (1975).
45. M. Baus and J. L. Colot, *Phys. Rev. A* **36**, 3912 (1987).
46. W. A. Curtin and K. Runge, *Phys. Rev. A* **35**, 4755 (1987).
47. C. F. Tejero, *Phys. Rev. E* **55**, 3720 (1997).
48. C. N. Likos and N. W. Ashcroft, *Phys. Rev. E* **52**, 5714 (1995).
49. J. L. Barrat, J. P. Hansen, G. Pastore, and F. M. Waisman, *J. Chem. Phys.* **86**, 6360 (1987).
50. F. J. Rogers and D. A. Young, *Phys. Rev. A* **30**, 999 (1984).
51. Y. Rosenfeld and N. W. Ashcroft, *Phys. Rev. A* **20**, 1208 (1979).
52. W. G. Hoover, D. A. Young, and R. Grover, *J. Chem. Phys.* **56**, 2207 (1972).
53. B. B. Laird and D. M. Kroll, *Phys. Rev. A* **42**, 4810 (1990).
54. A. de Kuijper, W. L. Vos, J.-L. Barrat, J.-P. Hansen, and J. A. Schouten, *J. Chem. Phys.* **93**, 5187 (1990).
55. A. D. J. Haymet, in *Fundamentals of Inhomogeneous Fluids*, D. Henderson, ed., Marcel Dekker, New York, 1992.
56. D. C. Wang and A. P. Gast, *J. Chem. Phys.* **110**, 2522 (1999).
57. W. G. Hoover and F. M. Ree, *J. Chem. Phys.* **49**, 3609 (1968).
58. W. A. Curtin, *Phys. Rev. B* **39**, 6775 (1989).
59. R. Ohnesorge, H. Löwen, and H. Wagner, *Phys. Rev. A* **43**, 2870 (1991).
60. R. Ohnesorge, H. Löwen, and H. Wagner, *Phys. Rev. E* **50**, 4801 (1994).
61. D. W. Marr and A. P. Gast, *Phys. Rev. E* **47**, 1212 (1993).
62. A. Kyralidis and R. A. Brown, *Phys. Rev. E* **51**, 5832 (1995).
63. W. A. Curtin and N. W. Ashcroft, *Phys. Rev. Lett.* **59**, 2385 (1987).

64. A. R. Denton and N. W. Ashcroft, *Phys. Rev. A* **39**, 426 (1989).
65. S.-C. Kim and G. L. Jones, *Phys. Rev. A* **41**, 2222 (1990).
66. J. A. White and R. Evans, *J. Phys. Condens. Matter* **2**, 2435 (1990).
67. A. R. Denton and N. W. Ashcroft, *Phys. Rev. A* **44**, 1219 (1991).
68. A. R. Denton and N. W. Ashcroft, *Phys. Rev. A* **41**, 2224 (1990).
69. J. L. Barrat, J. P. Hansen, and G. Pastore, *Mol. Phys.* **63**, 747 (1988).
70. Z. W. Salsburg, R. W. Zwanzig, and J. G. Kirkwood, *J. Chem. Phys.* **21**, 1098 (1953).
71. T. K. Vanderlick, H. T. Davis, and J. K. Percus, *J. Chem. Phys.* **91**, 7136 (1989).
72. T. K. Vanderlick, H. T. Davis, and J. K. Percus, *J. Chem. Phys.* **91**, 7136 (1989).
73. J. K. Percus, *J. Chem. Phys.* **75**, 1316 (1981).
74. R. Roth, R. Evans, A. Lang, and G. Kahl, *J. Phys. Condens. Matter* **14**, 12063 (2002).
75. Y. Rosenfeld, *Phys. Rev. Lett.* **63**, 980 (1989).
76. Y. Rosenfeld, D. Levesque, and J.-J. Weis, *J. Chem. Phys.* **92**, 6818 (1990).
77. E. Kierlik and M. L. Rosinberg, *Phys. Rev. A* **42**, 3382 (1990).
78. S. Phan, E. Kierlik, M. L. Rosinberg, B. Bildstein, and G. Kahl, *Phys. Rev. E* **48**, 618 (1993).
79. E. Kierlik and M. L. Rosinberg, *Phys. Rev. A* **44**, 5025 (1991).
80. Y. Rosenfeld, M. Schmidt, H. Löwen, and P. Tarazona, *Phys. Rev. E* **55**, 4245 (1997).
81. J. F. Lutsko, *Phys. Rev. E* **74**, 021121 (2006).
82. P. Tarazona, *Physica A* **306**, 243 (2002).
83. P. Tarazona, *Phys. Rev. Lett.* **84**, 694 (2000).
84. J. A. Cuesta, Y. Martínez-Raton, and P. Tarazona, *J. Phys. Condens. Matter* **14**, 11965 (2002).
85. G. A. Mansoori, N. F. Carnahan, K. E. Starling, and T. W. Leland, Jr., *J. Chem. Phys.* **54**, 1523 (1971).
86. V. B. Warshavsky and X. Song, *Phys. Rev. E* **73**, 031110 (2006).
87. J. F. Lutsko, *Phys. Rev. E* **74**, 021603 (2006).
88. Y. Rosenfeld, *Phys. Rev. E* **50**, R3318 (1994).
89. J. A. Cuesta, *Phys. Rev. Lett.* **76**, 3742 (1996).
90. J. A. Cuesta and Y. Martínez-Ratón, *Phys. Rev. Lett.* **78**, 3681 (1997).
91. L. Lafuente and J. A. Cuesta, *Phys. Rev. Lett.* **93**, 130603 (2004).
92. Y. Martínez-Raton, J. A. Capitan, and J. A. Cuesta, *Phys. Rev. E* **77**, 051205 (2008).
93. M. Schmidt, *Phys. Rev. E* **60**, R6291 (1999).
94. M. Schmidt, *Phys. Rev. E* **62**, 4976 (2000).
95. C. N. Likos, A. Lang, M. Watzlawek, and H. Löwen, *Phys. Rev. E* **63**, 031206 (2001).
96. J. A. Barker, and D. Henderson, *J. Chem. Phys.* **47**, 4714 (1967).
97. D. Chandler and J. D. Weeks, *Phys. Rev. Lett.* **25**, 149 (1970).
98. D. Chandler, J. D. Weeks, and H. C. Andersen, *J. Chem. Phys.* **54**, 5237 (1971).
99. H. C. Andersen, D. Chandler, and J. D. Weeks, *Phys. Rev. A* **4**, 1597 (1971).
100. F. Lado, *Mol. Phys.* **52**, 871 (1984).
101. J. M. Kincaid and J. J. Weis, *Mol. Phys.* **34**, 931 (1977).
102. C. Rascón, L. Mederos, and G. Navascués, *Phys. Rev. E* **54**, 1261 (1996).
103. C. Rascón, L. Mederos, and G. Navascués, *J. Chem. Phys.* **105**, 10527 (1996).
104. V. B. Warshavsky and X. Song, *Phys. Rev. E* **69**, 061113 (2004).

105. P. Paricaud, *J. Chem. Phys.* **124**, 154505 (2006).
106. Y. Rosenfeld, *J. Chem. Phys.* **98**, 8126 (1993).
107. Y. Tang and J. Wu, *Phys. Rev. E* **70**, 011201 (2004).
108. S. Sokolowski and J. Fischer, *J. Chem. Phys.* **96**, 5441 (1992).
109. T. Wadewitz and J. Winkelmann, *J. Chem. Phys.* **113**, 2447 (2000).
110. Z. Tang, L. E. Scriven, and H. T. Davis, *J. Chem. Phys.* **95**, 2659 (1991).
111. G. Stell and O. Penrose, *Phys. Rev. Lett.* **51**, 1397 (1983).
112. W. A. Curtin and N. W. Ashcroft, *Phys. Rev. Lett.* **56**, 2775 (1986).
113. L. Verlet and D. Levesque, *Physica* **36**, 245 (1967).
114. J. P. Hansen and L. Verlet, *Phys. Rev.* **184**, 151 (1969).
115. F. H. Ree, *J. Chem. Phys.* **64**, 4601 (1976).
116. H. S. Kang, C. S. Lee, T. Ree, and F. H. Ree, *J. Chem. Phys.* **82**, 414 (1985).
117. B. Q. Lu, R. Evans, and M. M. Telo da Gamma, *Mol. Phys.* **55**, 1319 (1985).
118. J. F. Lutsko and G. Nocolis, *Phys. Rev. Lett.* **96**, 046102 (2006).
119. Y. Tang, *J. Chem. Phys.* **118**, 4140 (2003).
120. J. F. Lutsko, *J. Chem. Phys.* **127**, 054701 (2007).
121. M. Llano-Restrepo and W. G. Chapman, *J. Chem. Phys.* **97**, 2046 (1992).
122. P. Grosfils and J. F. Lutsko, *J. Chem. Phys.* **130**, 054703 (2009).
123. P. R. ten Wolde and D. Frenkel, *Science* **77**, 1975 (1997).
124. P. Grosfils and J. F. Lutsko, unpublished (2009).
125. F. van Swol and J. R. Henderson, *Phys. Rev. A* **40**, 2567 (1989).
126. D. Henderson, ed., *Fundamentals of Inhomogeneous Fluids*, Marcel Dekker, New York, 1992.
127. W. A. Steele, *Surf. Sci.* **36**, 317 (1973).
128. W. A. Steele, *The Interaction of Gases with Solid Surfaces*, Pergamon, Oxford, 1974.
129. A. J. Archer, D. Pini, R. Evans, and L. Reatto, *J. Chem. Phys.* **126**, 014104 (2007).
130. S. R. de Groot and P. Mazur, *Non-Equilibrium Thermodynamics*, Dover, New York, 1984.
131. J. W. Cahn, *J. Chem. Phys.* **42**, 93 (1965).
132. P. C. Hohenberg and B. I. Halperin, *Rev. Mod. Phys.* **49**, 435 (1977).
133. T. Munakata, *J. Phys. Soc. Japan* **43**, 1723 (1977).
134. T. Munakata, *J. Phys. Soc. Japan* **45**, 749 (1978).
135. B. Bagchi, *Physica A* **145**, 273 (1987).
136. W. Dieterich, H. L. Frisch, and A. Majhofer, *Z. Phys. B* **78**, 317 (1990).
137. K. Kawasaki, *J. Stat. Phys.* **93**, 527 (1998).
138. U. M. B. Marconi and P. Tarazona, *J. Chem. Phys.* **110**, 8032 (1999).
139. S. P. Das, *Rev. Mod. Phys.* **76**, 785 (2004).
140. T. R. Kirkpatrick and P. G. Wolynes, *Phys. Rev. A* **35**, 3072 (1987).
141. G.K.-L. Chan and R. Finken, *Phys. Rev. Lett.* **94**, 183001 (2005).
142. J. A. McLennan, *Introduction to Nonequilibrium Statistical Mechanics*, Prentice-Hall, Englewood Cliffs, NJ, 1989.
143. A. J. Archer and M. Rauscher, *J. Phys. A Math. Gen.* **37**, 9325 (2004).
144. R. Zwanzig, *Phys. Rev.* **124**, 983 (1961).
145. H. Mori and H. Fujisaka, *Prog. Theor. Phys.* **49**, 764 (1973).

146. H. Mori, H. Fujisaka, and H. Shigematsu, *Prog. Theor. Phys.* **51**, 109 (1974).
147. S. Sinha and M. C. Marchetti, *Phys. Rev. A* **46**, 4942 (1992).
148. S.-K. Ma and G. F. Mazenko, *Phys. Rev. B* **11**, 4077 (1975).
149. T. R. Kirkpatrick and J. C. Nieuwoudt, *Phys. Rev. A* **33**, 2651 (1986).
150. T. R. Kirkpatrick and J. C. Nieuwoudt, *Phys. Rev. A* **33**, 2658 (1986).
151. U. M. B. Marconi and P. Tarazona, *J. Chem. Phys.* **110**, 8032 (1999).
152. C. W. Gardiner, *Handbook of Stochastic Methods*, Springer-Verlag, Berlin, 2004.
153. A. J. Archer and R. Evans, *J. Chem. Phys.* **121**, 4246 (2004).
154. A. J. Archer *J. Chem. Phys.* **130**, 014509 (2009).
155. H. Löwen, *J. Phys. Cond. Matter* **15**, V1 (2003).
156. H. Löwen, *J. Phys. Cond. Matter* **15**, V1 (2003).
157. J. Zinn-Justin, *Quantum Field Theory and Critical Phenomena*, Clarendon Press, Oxford, 2002.
158. D. Reguera and H. Reiss, *J. Chem. Phys.* **120**, 2558 (2004).
159. D. N. Zubarev, ed., *Nonequilibrium Statistical Thermodynamics*, Consultants Bureau, New York, 1974.
160. A. J. Archer, P. Hopkins, and M. Schmidt, *Phys. Rev. E* **75**, 040501 (2007).
161. J.G.E.M. Fraaije, *J. Chem. Phys.* **99**, 9202 (1993).
162. J.G.E.M. Fraaije, *J. Chem. Phys.* **100**, 6984 (1994).
163. J.G.E.M. Fraaije, B. A. C. van Vlimmeren, N. M. Maurits, M. Postma, O. A. Evers, C. Hoffmann, P. Altevogt, and G. Goldbeck-Wood *J. Chem. Phys.* **106**, 4260 (1997).
164. J. Dzubiella and C. N. Likos, *J. Phys. Cond. Matter* **15**, L147 (2003).
165. S. van Teeffelen, C. N. Likos, and H. Löwen, *Phys. Rev. Lett.* **100**, 108302 (2008).
166. M. Rex and H. Löwen, *Phys. Rev. Lett.* **101**, 148302 (2008).
167. P. G. Vekilov, *Cryst. Growth Des.* **4**, 671 (2004).
168. M. J. Uline and D. S. Corti, *Phys. Rev. Lett.* **99**, 076102 (2007).
169. J. F. Lutsko, *Europhys. Lett.* **83**, 46007 (2008).
170. J. F. Lutsko, *J. Chem. Phys.* **129**, 244501 (2008).
171. J. W. Cahn and J. E. Hilliard, *J. Chem. Phys.* **31**, 688 (1959).
172. D. W. Oxtoby and R. Evans, *J. Chem. Phys.* **89**, 7521 (1988).
173. X. C. Zeng and D. W. Oxtoby, *J. Chem. Phys.* **94**, 4472 (1991).
174. V. Talanquer and D. W. Oxtoby, *J. Chem. Phys.* **100**, 5190 (1994).
175. D. Wales, *Energy Landscapes*, Cambridge University Press, Cambridge, 2003.
176. G. Henkelman and H. Jónsson, *J. Chem. Phys.* **113**, 9978 (2000).
177. E. Weinan, W. Ren, and E. V. Eijnden, *J. Chem. Phys.* **126**, (2007).
178. C. Qiu, T. Qian, and W. Ren, *J. Chem. Phys.* **129**, 154711 (2008).
179. J. K. Percus, *J. Stat. Phys.* **28**, 67 (1981).